



Bergvesenet

Postboks 3021, N-7441 Trondheim

BÆRBAR MASKIN

Rapportarkivet

Bergvesenet rapport nr	Intern Journal nr	Internt arkiv nr	Rapport lokalisering	Gradering
6823				

Kommer fra arkiv	Ekstern rapport nr	Oversendt fra	Fortrolig pga	Fortrolig fra dato:
Grong Gruber AS		Grong Gruber a.s.		

Tittel

The geology of the Gjersvik area, Central Norway, and a study of the chemistry and occurrence of Stilpnomelane and Biotite in thr eruptive rocks in this region

Forfatter	Dato	Ar	Bedrift (Oppdragsgiver og/eller oppdragstaker)
Mellin, Adrian . C			Norsulfid Grong Gruber AS
	Mai 1979		

Kommune	Fylke	Bergdistrikt	1: 50 000 kartblad	1: 250 000 kartblad
Røyrvik	Nord-Trøndelag		19244	Grong

Fagområde	Dokument type	Forekomster (forekomst, gruvefelt, undersøkelsesfelt)
Geologi Litogeokjemi		Gjersvik Lillefjellet

Råstoffgruppe	Råstofftype
Malm/metall	Cu, py,po

Sammendrag, innholdsfortegnelse eller innholdsbeskrivelse

B. Sc. Thesis fra Royal School of Mines.

Beskriver geologi med bergarts sammensetning og strukturer i Gjersvikfeltet og i Lillefjellet lenger nord. Mineraliseringen i Gjersvik gjennomgås og det foreslås en strukturmodell for malmen. Malmen har en begrenset fortsettelse langs sin søndre foldeflanke ut under Limingen.

SHELL SOUTH AFRICA LTD (METALS
DIV.)

BRAANFONTEIN

2017 JOHANNESBURG

SOUTH AFRICA

27th October 1979

Dear Ave.

As you can see I have accepted a job in South Africa with Billton. It was a hard choice between Billton and Western Mining in Western Australia but chose Billton mainly because I'm on a tin-tungsten prospect as opposed to greenstones in Australia. I fancied a broadening of geological experience and also Billton have a very impressive set up. I fly out on November 1st and am working near Uitenhage in northern Cape Province. When I know my address there I will write and let you know. I enclose a copy of my report from Ljersvik. One thing I must stress is that in Sect B some of the interpretations were made on flimsy evidence ~~due to~~ in order to give a little 'meat' for my degree assessment. The chemical analyses (whole rock) are not reliable in many cases (as you can see from the totals) and this tends to give high uncertainty on interpretations. The probe analyses are very good though. I have asked to send you copies of our maps from this year and I will try and manage the Ljersvik maps. Hope you had a good time in Canada and can recover at work. All best wishes for your latest addition.

Adrian

The area has undergone 3 major recognizable phases of Deformation D_1-D_3 often with associated brittle fracturing in the more competent lithologies.

* the structure is more easily elucidated in the sedimentary rocks exposed to east of eruptive sequence.

tectonic
style
in
eruptive

The development of a heterogeneously strained fold system is probably primarily due to the differential absorption of strain by lithologies of different competence.

* most competent units become dominant, — hence development of a heterogeneous style

D_1 The style of folding and metamorphic reconstitution occurring during this first phase of tectonic deformation suggests that it was largely responsible for the major textural reconstitution of the rocks in producing the early penetrative schistosity.

* F_1 probably parasitic isoclinal F_1 folds. with wavelength 15-30m. schistosity is approx parallel to bedding also reflecting the isoclinal style.

— D_1 orientation not easy but bedding + S_1 intersection indicate F_1 structure lies (sedimentary) now plunging $10^\circ - 20^\circ$ to the North — with axial plane S_1 , modified by D_2 and D_3 structures

— intense flattening during D_1 has resulted in the reorientation of highly flattened clasts parallel to S_1 . Pressure solution between clasts and redistribution of quartz and ferromagnesian calcite in pressure shadows. and tectonic segregation also occurred during D_1 .

* These features have been folded during subsequent deformation

Structures produced from folds of S_1 schists are common. These formed by D_1 folding of bedding. The very tight fold produced during D_1 deformation is competent masses during subsequent deformation and due to the orientation of D_1 folds is especially influenced by the orientation of the D_2 folds in the immediate vicinity!

— Reflected in the spread of orientations of F_2 fold axes seen

* Some major ~~large~~ fractures are axial planar to D_2 folds at least. Likelihood movement has occurred along the axial planes of the D_2 fold structures (S_2)

* In the sedimentary rocks the D_2 folds are characterized by their tight form and steeply dipping axial planes. Locally possible to see parallel F_1 isoclinal

— Roughly cylindrical forms for F_2 in the redwells, with fold axis plunging approx 35° to 250°

For: Asymmetrical folds show variation $10-20^\circ$ to $230-270^\circ$.

* Small scale F_2 structures are also seen in the more phyllitic metabeds.

* F_2 style of folding in the amphibolite is ~~not~~ noticeably different.

* Folding from lower S_2 schists developed in amphibolite close to the sediment / amphibolite contact suggests there may have been some tectonic adjustment along the plane during D_2

Sed. Volcanic contact. testified by F_2 axial plane faulting?

Nature of fractures related to D_2 folds

- ① Fractures developed along axial plane of D_2 folds.
- ② Potential fractures developed in response to couples induced by D_2 folding. — in appropriate component of flow (which)

D_3 Deformation D_3 fol

D_3 - folding best seen in pediments.

— the upward dip of D_3 seen in uplift

— D_3 fold in fact distinguished from D_2 by their foliation axial planes

Orientation of F_3 fold axis is strongly influenced by earlier structures.

But generally dip to 20° SW. to SW. and also can angular discordance

at 20-30° with F_2 fold axis.

— concordant crystalline with D_3 often have a flat lying axial plane (concordant ~~crystalline~~)

— D_3 folds Tend to have an open style, especially long small scale features.

THE GEOLOGY OF THE GJERSVIK AREA, CENTRAL NORWAY
AND A STUDY OF THE CHEMISTRY AND
OCCURRENCE OF STILPNOMELANE
AND BIOTITE IN THE ERUPTIVE
ROCKS IN THIS REGION

A. C. MELLIN

A Thesis
submitted in partial fulfillment of the requirements
for the degree of
B.Sc. (Mining Geology)
at the
University of London
and the
Associateship of the Royal School of Mines

Mining Geology Section,
Royal School of Mines,
Imperial College of
Science and Technology,
London.

May, 1979

CONTENTS

	Page
ABSTRACT	(iii)
SECTION A FIELD REPORT	
CHAPTER 1. INTRODUCTION	1
CHAPTER 2. REGIONAL SETTING	2
CHAPTER 3. LITHOLOGICAL UNITS	6
3.1 Basic and mafic intermediate volcanics 'greenstones'.	6
3.2 Acid to intermediate eruptives	13
3.3 Intrusive basic rocks	19
3.4 Intermediate intrusive rocks	21
3.5 Sedimentary rocks	21
CHAPTER 4. STRUCTURE	25
4.1 D ₁ Deformation	28
4.2 D ₂ Deformation	34
4.3 D ₃ Deformation	45
4.4 Brittle Fracturing	47
CHAPTER 5. MINERALISATION	50
5.1 Massive sulphide mineralisation - The 'Gjersvik Orebody'	50
5.2 Disseminated mineralisation	59
5.3 Peripheral exhalitive mineralisation	60
5.4 Relationships between individual styles of mineralisation	66
CHAPTER 6. CONCLUSIONS	70
REFERENCES	71

SECTION B. A CHEMICAL AND MINERALOGICAL STUDY
OF THE ERUPTIVE ROCKS IN THE GJERSVIK
REGION

INTRODUCTION	73
CHAPTER 7. CHEMISTRY AND PETROGRAPHY OF THE GJERSVIK ERUPTIVES	75
7.1 Basic eruptives	75
7.2 Acidic eruptives	80
CHAPTER 8. THE OCCURRENCE OF STILPNOMELANE AND BIOTITE IN THE GJERSVIK REGION	84
8.1 Field occurrence	84
8.2 Relationships between ferro and ferri - stilpnomelane	86
8.3 Textural and crystallographic features	86
8.4 Whole rock chemistry of stilpnomelane and biotite bearing rocks	96
8.5 Chemistry of stilpnomelane and biotite	97
8.6 Genesis of stilpnomelane and biotite	103
CHAPTER 9. CONCLUSIONS AND FURTHER WORK	106
ACKNOWLEDGEMENTS	107
REFERENCES	108
APPENDIX	110

ABSTRACT

The original basaltic, basaltic andesite and dacitic eruptives of the Gjersvik area provide evidence of having undergone a period of ocean floor metamorphism prior to tectonic deformation. This involved chemical alteration producing rocks of spilitic affinity showing a greenschist facies metamorphic assemblage. The area then underwent three major episodes of tectonic deformation. The first phase of tectonic deformation is believed to have been the most intense and responsible for most of the pervasive textural modification and the lower greenschist facies metamorphic mineral assemblage now observed. The mineralisation in the Gjersvik area is believed to have crystallised as a consequence of metasomatic activity of hydrothermal solutions discharged onto the sea floor. These solutions then precipitated metal sulphides in structural traps in the sea floor, or as thin exhalite bands away from these traps. The emission of the mineralising solutions immediately post dates extrusion of rhyo dacitic pyroclastics and is considered to be linked with the intrusion of acidic feeder dykes.

The eruptive rocks are believed to have developed within an ensimatic island arc environment of tholeiitic affinity, as suggested by major and trace element compositions of both basic and acidic rocks. Stilpnomelane and biotite are believed to have crystallised as a consequence of metasomatic action by hydrothermal solutions during the late stages of mineralisation and then later mimetically recrystallised during regional metamorphism.

The present study was undertaken as part of an exploration program to evaluate the economic potential of the Lillefjell area approximately 5 km north of Gjersvik, Nord Trøndelag, Norway. An electromagnetic "Turam" /over the Lillefjell prospect revealed /survey significant near surface conductors. These anomalies were further investigated by blasting nine trenches, which were sampled by geologists Halls and Mellin.

The main aim of the study was to establish a geological connection, if any, between the disseminated sulphide mineralisation of the Lillefjell area, and the massive sulphide mineralisation of the 'Gjersvik Orebody'.

Detailed geological mapping of the area was carried out at a scale of 1:5000, together with measured sections of the road cuttings around the outcrop of the 'Gjersvik Orebody' at a scale of 1:200.

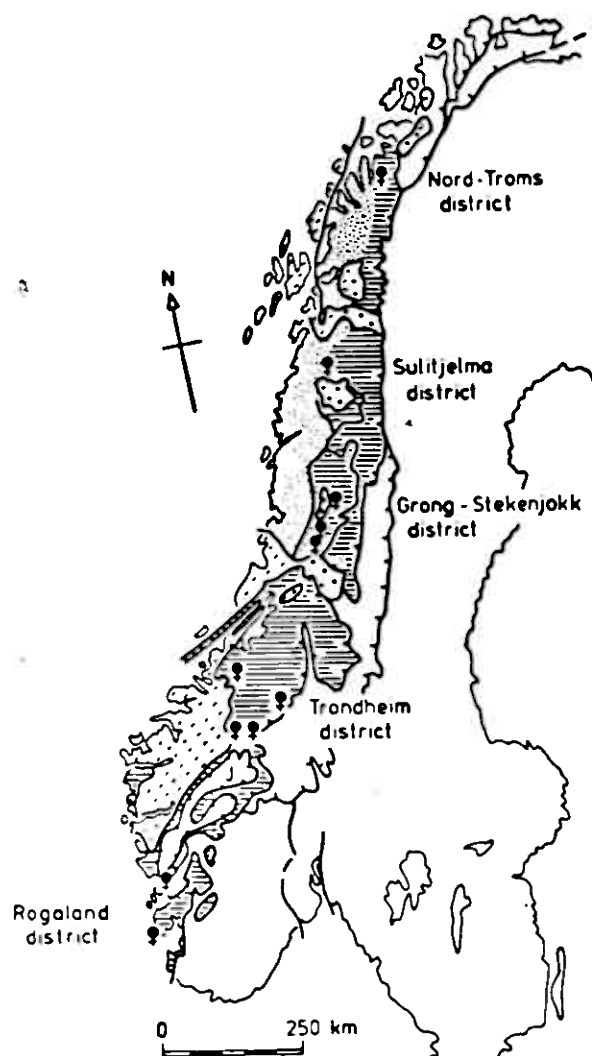
A strip of ground approximately 1-1.5 km wide, extending northwards approximately 4 km from the northern shore of Limingen Lake towards the Lillefjell area was mapped. Complete coverage was not possible in some areas due to the structural and lithological complexity of the area, which require systematic detailed observations to determine their nature.

The Caledonian orogenic belt which extends over most of Northern, Central and South-Western Norway and the metamorphosed Lower Paleozoic rocks which lie within it, contain a series of stratiform pyritic massive sulphide deposits distributed along its length (Fig. 2.1). The Gjersvik deposit lies in the Grong Stekenjokk region of Nord Trondelag and is one of a series of deposits associated with the eruptive suites in this region.

The allochthonous volcanics, intrusives and clastics in the Grong-Stekenjokk area can be divided into several major structural and stratigraphic units⁵ (Fig. 2.2). The 'Gjersvik Orebody' lies within the eruptive "greenstones" of the Gjersvik Nappe in a similar structural and probably stratigraphic position to the currently mined Skorovass orebody 40 km to the south.

No fossil remains of chronographic significance have so far been recorded in the Gjersvik Nappe, and thus no precise dating of the sequence has been possible. Halls et. al. (1976)⁵ attempted a correlation with similar sequences in the Stekenjokk area and it seems likely that the Gjersvik Nappe sequence is approximately Lower to Middle Ordovician in age.

The essentially tholeiitic to "calc-alkaline" eruptive rocks have been interpreted as part of an ensimatic island arc, which then underwent rapid uplift and erosion prior to allochthonous transportation during the climax of the Caledonian orogeny. Halls et. al.⁵ referred to this period of regional tectonic uplift as the 'Gjersvik Disturbance', which gave rise to the polymict conglomerates exposed to the east of the eruptive sequence. Similar periods of regional uplift have





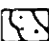

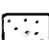


-  Eastern thrust boundary of the Caledonian allochthon
-  Eastern thrust boundary of Seve-Koli nappe or equivalent with metamorphosed sediments and eruptives of Cambrian-Silurian age
-  Basement inliers and culminations, Pre-Cambrian
-  Jotun nappes and related structures with allochthonous Pre-Cambrian rocks
-  Pre-Cambrian basement re-worked during the Caledonian orogeny
-  Helgeland, Rødingstjøll, Beiar and equivalent nappes with L Palaeozoic rocks at higher metamorphic grades overlying the Seve-Koli nappe in N Norway
-  Principal stratiform pyritic orebodies of volcanic affinity at the Koli structural level

Fig.2.1. Regional geological map of Norway showing setting of stratiform massive sulphide deposits at Koli structural level.
(after Halls et. al. ⁵)

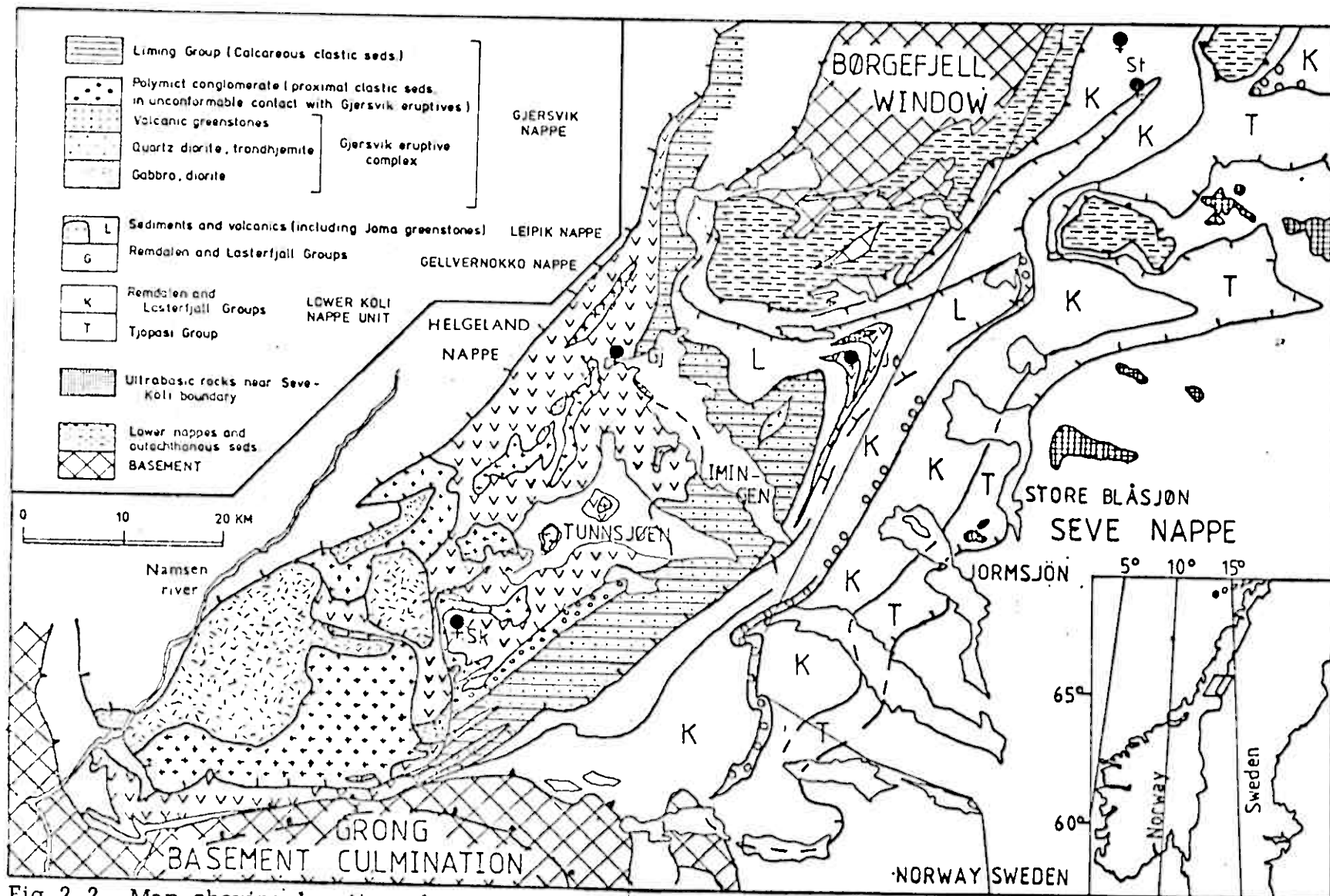


Fig.2.2. Map showing location of main massive sulphide ore deposits in the Grong - Stekeniokk district and main structural and stratigraphic units distinguished within the Koli Nappe (after Halls et. al.⁵)

been recorded in the Trenchheim region, which have been named the "Trenchheim Disturbance",⁷ though this probably occurs at a different stratigraphic level.⁵

In general terms the area can be considered as a series of basic to intermediate lavas, with occasional acidic pyroclastics, which have been intruded by a series of acidic, gabbro/dolerite and porphyritic andesite dykes. This eruptive sequence is then unconformably overlain by a series of calcareous polymict conglomerates and phyllites.

The area has been modified by intense plastic and brittle deformation (Ch 4), and by low grade greenschist facies metamorphism. The chemistry, petrology and mineralogy of the volcanic rocks is the subject of a more detailed study which accompanies this report. As such the sections below will concentrate on the field relations of the mapped lithological units.

The area is cut by a major N.N.E-S.S.W. trending fault e.g. Y10 760, X765 000, which is effectively downthrown to the west. This fault divides the area into two distinct regions. The region to the east appears to have a noticeably more sub-volcanic character as regards the acidic rocks, whereas some of the acidic rocks of the westerly region have extrusive affinities (Ch 3.2). Thus the easterly region is interpreted as being stratigraphically lower in the volcanic sequence.

3.1 BASIC AND INTERMEDIATE VOLCANICS (GREENSTONES)

The basic and more mafic intermediate volcanic rocks account for <70% of the total rock volume in the mapped area. They also provide the most instructive insight into the tectonic and metamorphic history of the area.

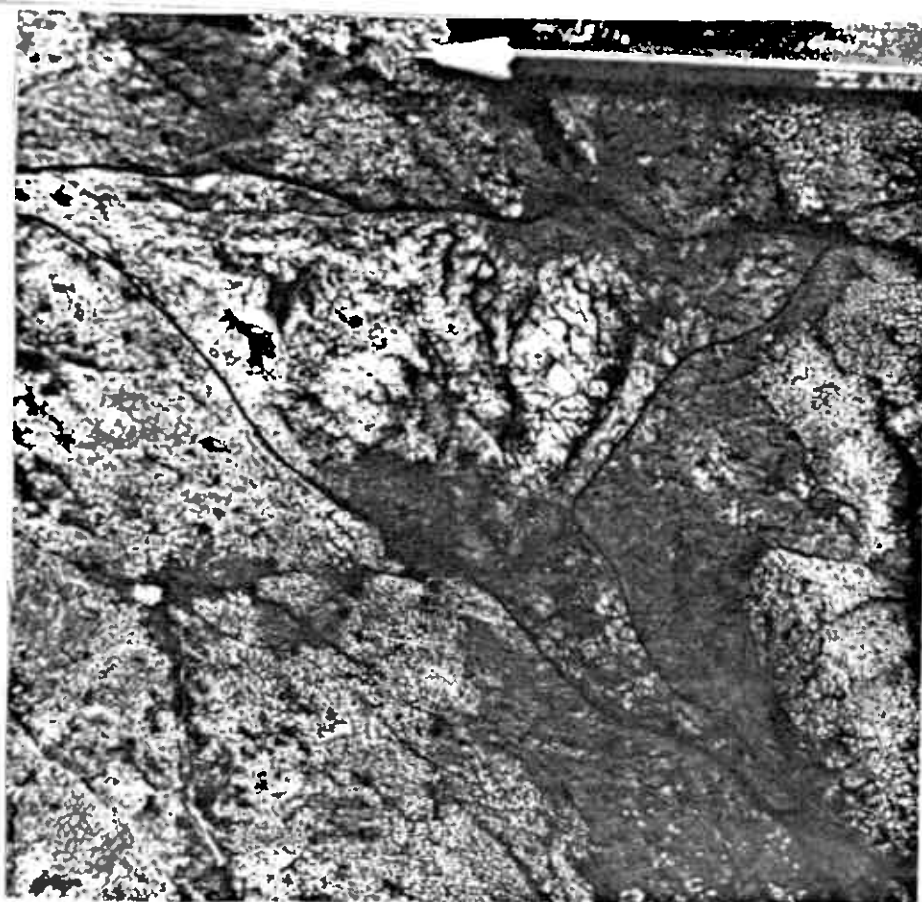
The intense tectonic deformation and often complete metamorphic reconstitution of these rocks makes it difficult to erect a meaningful volcano - stratigraphy. It seems probable, due to repetition by both D_1 and D_2 folding (Ch 4.1, 4.2) that in the area to the west of the main N.N.E.-S.S.W. fracture less than 250 m of the original volcanic pile are exposed at surface. It is not possible to map individual flow units, due to the reasons given above, though it is possible in some exposures to define probable contacts between the vesicular top of one flow unit and the massive base of the overlying unit. Unfortunately the inability to trace such contacts over any appreciable distance complicates the use of facing criteria provided by such features, due to the effects of small scale folding.

The basic lavas often show pillow structures which show varying degrees of preservation and flattening, (Fig. 3.1-1a). The flattened pillows vary in size from approximately 20 cm x 8 cm to 6 m x 2 m (Y10 765, X764 015). They often show chilled chloritic margins with occasionally preserved flattened tricusate cherty inter-pillow infilling, (Fig. 3.1-1b). sometimes containing magnetite). A probable pillow breccia was recognised at Y10 995, X764 660, underlying an acidic pyroclastic horizon (see Ch 3.2). A highly flattened lapilli crystal tuff was recognised at Y10 195, X766 415 with flattened chloritic lapilli approximately 5 mm in maximum dimension.

The lavas are very often vesicular in both recognisable pillowed and unpillowed sequences. The vesicles vary in size from a few millimetres to approximately 1.5 cm in maximum dimension. They have been flattened and infilled by a variety



A.

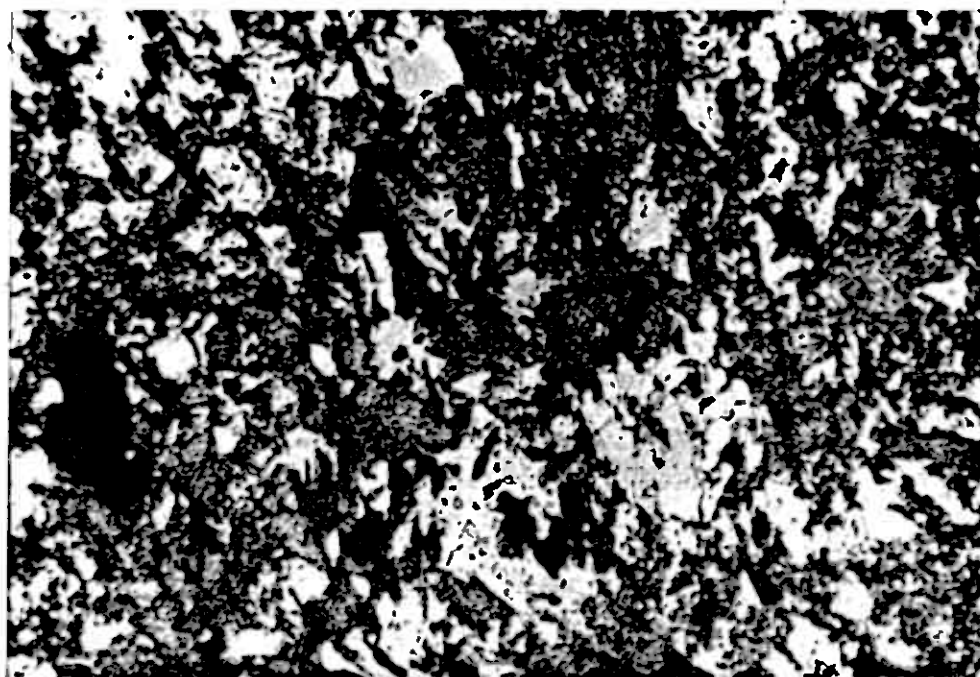


B.

Fig 3.1-1A.Flattened pillow structures developed in basic lavas
 B.Flattened tri-cusate, chert + magnetite, inter-pillow infilling.

of secondary minerals, notably quartz, epidote, ferroan calcite and occasionally chlorite, either singularly or in combination. Pyrite is a common accessory mineral in amygdalites in the vicinity of mineralised horizons.

Thus it is apparent that the majority, if not all of the basic and mafic intermediate lavas were extruded in a submarine environment. The presence of large amygdalites suggest the lavas were extruded at shallow depths, probably between 100 and 500m^{8, 12}.



PPL

250 μm

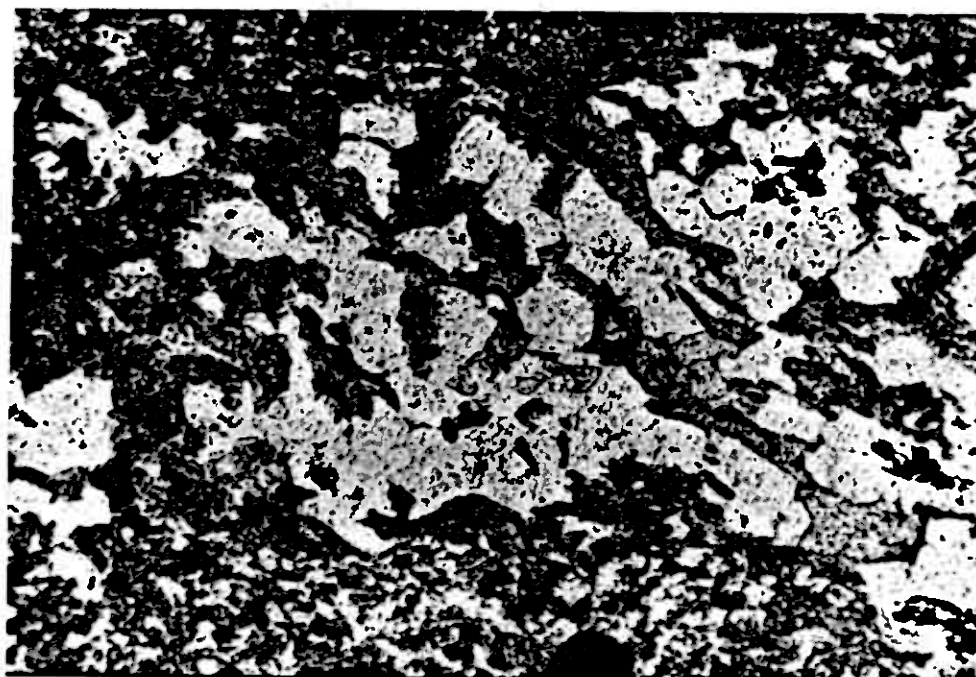
Fig.3.1-2. Typical epidote(yellow-green) - chlorite(green) - albite - quartz(colourless), secondary magnetite(opaque) assemblage of meta basalts in the Gjersvik area.

The extrusive "greenstones" are generally dark green, fine grained (approximately 0.1mm), rarely visibly porphyritic, equigranular, holocrystalline meta-basalts or meta-basaltic andesites. The essentially chlorite-epidote-albite-quartz-calcite assemblage is the result of retrograde lower greenschist facies metamorphism (see below). Magnetite, probably titaniferous, is a common fine grained anhedral accessory mineral, with less abundant pyrite apatite and sphene (probably from the breakdown of iron titanium oxides) as anhedral or euhedral approximately 10 μ m in size. The presence of larger pyrite and magnetite euhedral 0.5-2mm in size, in the vicinity of mineralised horizons are almost certainly introduced by secondary processes, probably metasomatic.

The relative proportions of the essential minerals varies considerably, with some lavas being very chloritic with only minor amounts of epidote, whereas others are very epidote rich with lesser chlorite. Similarly the quartz content is very variable, though this partially reflects secondary processes, which are discussed below. It is possible to recognise a noticeably calcareous unit which is rich in ferroan calcite and probably reflects a stratigraphic unit. This unit lies 10-20m structurally beneath the level of the "Gjersvik Orebody" on the Gjersvik road section. A similar probably stratigraphic unit containing abundant accessory magnetite can be recognised lying structurally beneath the more calcareous unit in the Gjersvik road section (see 1:200 sections). Unfortunately contacts are now often indistinct and these units can only be consistently defined where exposure is very good e.g. road cuttings.

The mineral assemblage described above is a typical low to intermediate pressure metamorphic assemblage produced from regional metamorphism of basaltic and basaltic andesite composition rocks under conditions of the greenschist facies¹¹. Evidence for a period of retrograde, probably greenschist facies metamorphism, prior to the first phase of tectonic deformation is seen in these basic rocks. Epidote concentrations in the form of irregular "knots", usually in the centre of recognisable flattened pillows can be seen to be flattened consistently with the pillow margins, and are often cut by the penetrative S_1 shistosity. This probably reflects a period of ocean floor metamorphism¹⁰, occurring soon after the deposition of the volcanic pile, while still in an area of very high heat flow and water saturated, allowing extensive chemical mobility which gave rise to allochemical metamorphism. This selective mobilisation is partially reflected in the variable content of the main mineral phases, e.g. the variable quartz, epidote and carbonate content of many of the basic lavas. Cann (1969)², described the differential mineralogy between the chilled margins of pillows and their cores seen on the deep ocean floor. During conditions of ocean floor metamorphism of the greenschist facies the palagonitic glassy pillow margins develop a dominantly chloritic assemblage - "hyalospilite", while the more crystalline core develops an albite-epidote-quartz assemblage with lesser chlorite - "orthospilite". This may explain some of the local mineralogical variations seen in the Gjersvik lavas, even when they show no conspicuous pillow structures. The reactions producing the above mineral assemblage involve a volume reduction of approximately 10%². This probably gives rise to the abundance of fine quartz, carbonate, epidote (\pm chlorite, pyrite) veinlets,

in varying combinations, which cut the basic rocks Fig. 3.1.3.



PPL

1mm

Fig. 3.1-3. Granular quartz (colourless) - epidote (high relief) - minor chlorite (green) veinlet cutting meta basalt.

They may also reflect the path taken by circulating metasomatic solutions within the volcanic pile.

During the first phase of tectonic deformation (D_1) the area underwent a subsequent period of regional metamorphism of lower greenschist facies which is probably for many of the textural features observed. Most of the basic eruptives are completely recrystallised and only rarely can retrograde metamorphic reactions between grains be observed (e.g. HM 113 (c)). This indicates that the system reached equilibrium under the prevailing temperature and pressure conditions during this phase of regional metamorphism. Many tectonic segregations of quartz and ferroan calcite formed perpendicular

to the maximum principle stress, due to pressure solution along grain boundaries. These segregations tend to be more abundant in the vicinity of fold closures in these more basic rocks. The tectonic segregations can be seen to be folded during D_2 , indicating they were formed during D_1 .

Stilpnomelane (and/or biotite) is a common porphyroblastic mineral phase in both basic and acidic rocks in this region. Its occurrence will be discussed in some detail in Section B of this report and as such will not be described here.

3.2 ACID TO INTERMEDIATE ERUPTIVES

The more acidic rocks of the Gjersvik area can be recognised in the field by their light grey leucocratic appearance, together with recognisable free quartz. These more acidic rocks of dacitic or rhyodacitic composition⁶ (locally referred to as keratophyre) can be subdivided into lithologies of intrusive and of extrusive character.

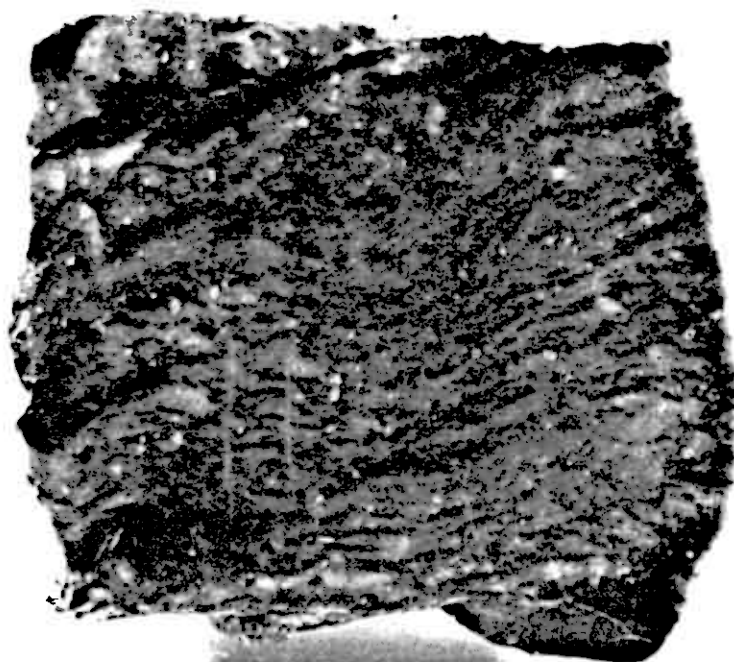
EXTRUSIVE, PYROCLASTIC ROCKS

It was possible to recognise rocks of probable pyroclastic origin e.g. Y10 543, X764 000. Due to the intense deformation and mineralogical reconstitution of these rocks it was not possible to conclusively demonstrate this affinity.

The pyroclastic textures show well on weathered surfaces, Fig. 3.2-1(a). The angular or lensoid 'fragments', vary in size from 1-5cm in maximum dimension and consist of very fine grained (approximately 5-10 μ m) equigranular, now holocrystalline quartz and albite, with lesser epidote and some chlorite. Magnetite and



A.



1mm

B.

Fig. 3.2-1. Fragmentary pyroclastic textures in acidic rocks near outcrop of the Gjersvik Orebody:

A. On weathered surface.

B. On polished face.

pyrite, up to 2% by volume, are nearly always present as very fine grained (2-3 μ m) subhedral to anhedral accessories, within the 'fragments'. Apatite and sphene are less abundant euhedral accessories. The 'fragments' are now enclosed by a matrix of subhedral granular quartz, with ferroan calcite and some epidote, grain size approximately 250 μ m, which has probably replaced an original ashy matrix.

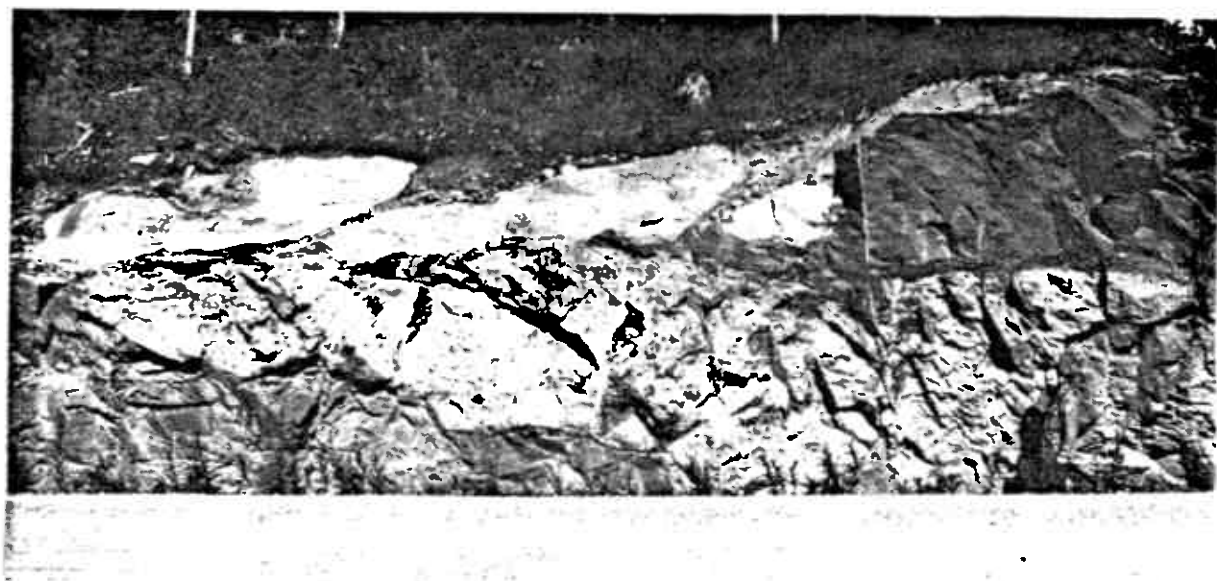
The observed quartz-albite-epidote-minor chlorite mineral assemblage is probably a retrograde lower greenschist metamorphic assemblage, as described in Ch 3.2. Despite the intense deformation, and probably allochemical metamorphism, the large percentage of quartz and albite (presumably after plagioclase feldspar), together with no recognisable potash feldspar indicates a dacitic or rhyo-dacitic composition⁶.

INTRUSIVE ROCKS

The intrusive rocks are split into two distinct regions bounded by the major N.N.E.-S.S.W. trending fault. To the west of the fault the acidic intrusives occur in dykes or sills 1-2m wide Fig. 3.2.-2. Usually it is not possible to trace individual bodies continuously over more than 50-100m, mainly due to folding, shearing and boudinage produced during tectonism. As in the pyroclastic material, the essential mineralogy is a retrograde lower greenschist metamorphic assemblage of quartz-albite-epidote-chlorite with a grain size of 10-30 μ m. Some relict plagioclase feldspar phenocrysts (C.AN₃₀ - oligoclase - andesine) 0.5 - 1.5 mm in size are often preserved, though they are often partially or totally saussuritised. As in the basic rocks stilpnomelane occurs as large



A.

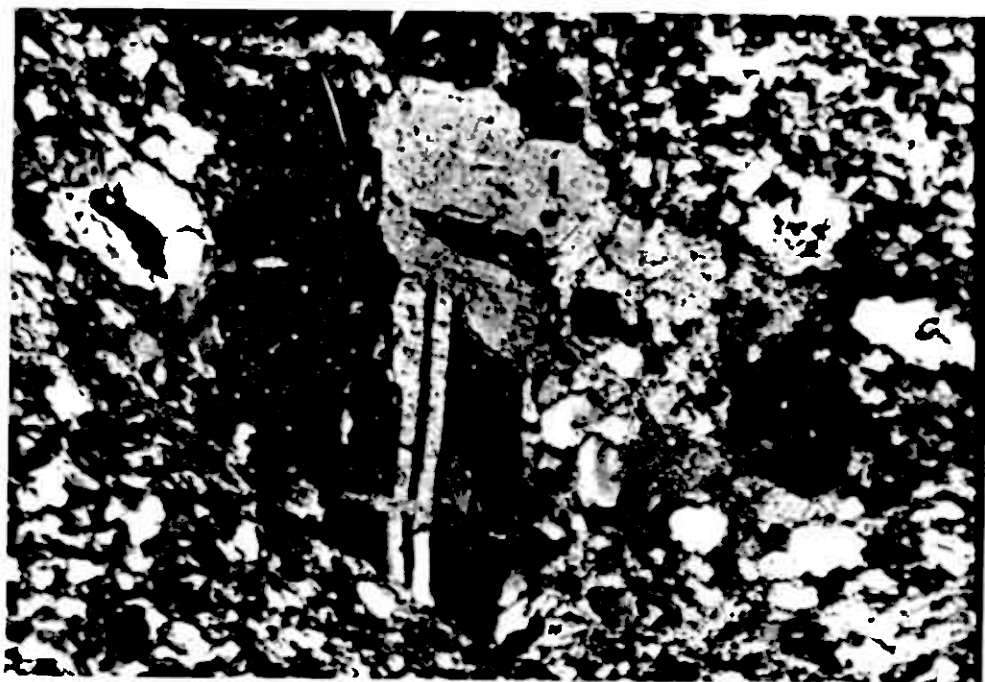


B.

Fig. 3.2-2. A. Folded meta rhyo dacite dyke - sill transition.
B. Flattened meta rhyo dacite sill, with underlying feeder dyke.

needle like porphyroblasts 0.5 - 1.5 mm in size e.g. Y 10 740, X764 345. Its occurrence is not as extensive as in the basic rocks, but it displays the same textural and morphological features (see Section B). Magnetite and pyrite occur as very fine grained (10 - 20 μ m) anhedral accessories in the groundmass, and also as larger euhedral porphyroblasts 0.5 - 2 mm in size near mineralised horizons, which is also seen in the pyroclastic material. Tetrahedral crystals of arsenopyrite 2-3 mm in size were observed in the more porphyritic rhyo-dacite, 20 m structurally beneath the outcrop of the 'Gjersvik Orebody' (HM102). Apatite and sphene occur as very fine grained euhedral accessories.

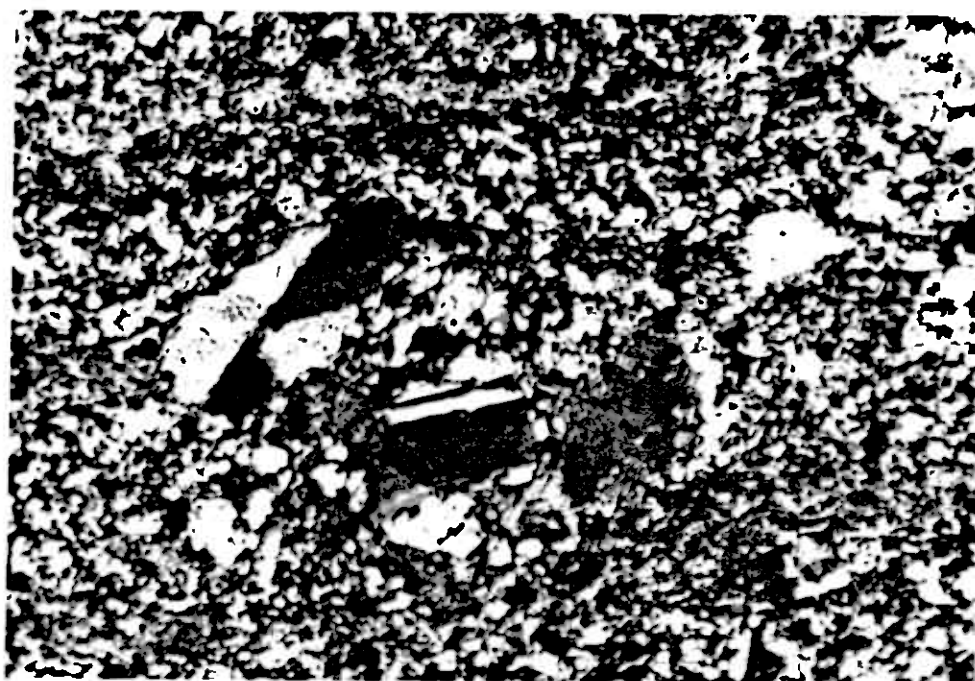
To the east of the main fracture the relative volume of acidic material is much greater (up to 60%). Again it occurs as dykes and possibly sills up to 5 m wide. However the mineralogy is significantly different; the relict plagioclase feldspar phenocrysts are generally larger, grainsize 0.5 - 1.5 mm and more abundant than in the acidic rocks to the West. Large irregular quartz grains are also present which appear to have undergone pressure solution along their boundaries and are probably original phenocrysts. Biotite porphyroblasts are nearly always present to a greater or lesser degree, as opposed to staurolite to the West. It forms large platy crystals 0.5 - 1.0 mm in size often partially completely or pseudomorphed by chlorite along 001. Specimen HM 152, Y11 285, X765 085, contains a large amount of a fine sericitic mineral with a very small axial angle, probably paragonite. The above assemblage appears to represent a slightly higher grade metamorphic mineral assemblage than is found to the West of the fracture.



X N

250 μ

A.



X N

1mm

B.

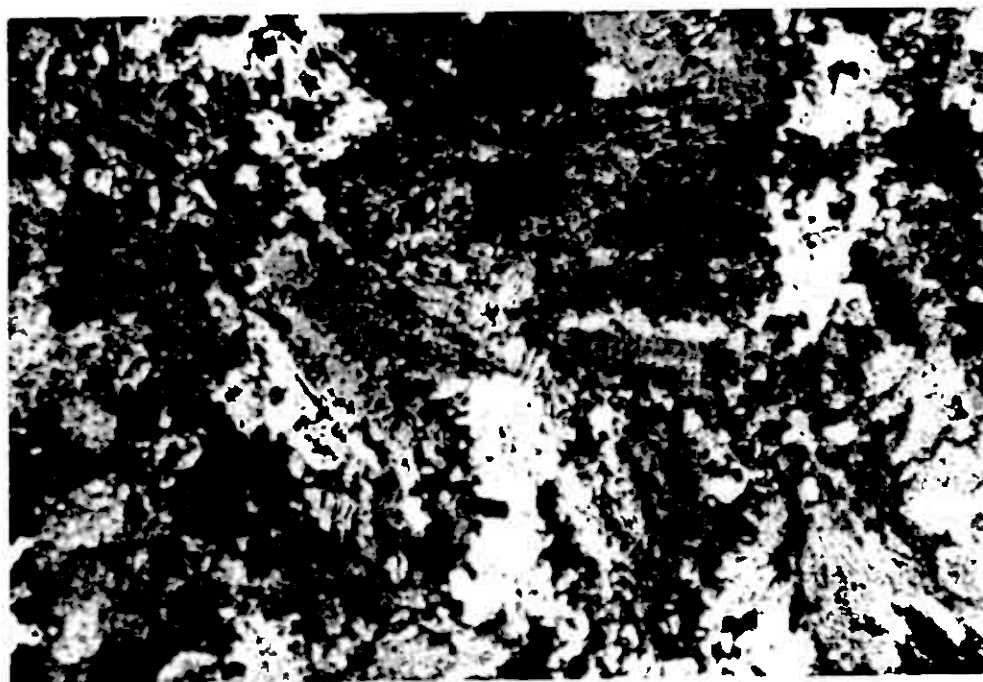
Fig 3.2-3. A. Sausuritised plagioclase feldspar porphyritic meta rhyodacite - West of main fracture (see text).
B. Coarser grained more porphyritic meta dacite - East of main fracture (see text).

It seems reasonable to suppose that the porphyritic intrusive dykes acted as feeders for the extrusive pyroclastic flows? and are thus sub-volcanic. The area to the East of the fracture appears to represent a deeper level in the volcanic pile due to its apparently higher grade metamorphic mineral assemblage, more porphyritic texture and the larger proportion of acidic dykes suggesting the area is closer to the magma source. This crude indication of volcano-stratigraphic level is useful in determining structural 'facing'.

3.3 Intrusive Basic Rocks

Dykes and/or sills of medium-coarse grained mafic 'greenstone' showing relict ophitic textures are found in restricted areas of the Gjersvik volcanics. The dykes/sills are typically 1-3 m wide occasionally showing a preserved chilled margin 1 - 3 cm wide. There is no visible evidence of thermal metamorphism of the country rocks, which if originally present, has since been obscured by metamorphic reconstitution.

The original plagioclase feldspar phenocrysts show relatively little breakdown to albite and epidote consistent with the retrograde chlorite-epidote-albite + minor quartz greenschist metamorphic assemblage seen in the groundmass, but are often partially saussuritised. Plagioclase phenocrysts 0.2 - 0.5 mm in size, lying in the Andesine composition range (An_{32}) are intergrown in an ophitic manner with chlorite masses, presumably pseudomorphs after original ferromagnesian minerals. Epidote is often intimately associated with chlorite and also occurs as small dispersed euhedra 25-50 μ m in size. Chlorite contributes 30 - 40% of the rock by volume. Some fine grained pyrite approximately



XN

250µm

Fig. 3.3-1. Ophitically intergrown epidote - chlorite masses (lower first and second order interference colours) and corroded relict plagioclase feldspar phenocrysts (showing simple twins)

25µm in size and sphene (probably after iron-titanium oxides) are found in the groundmass.

The main area of dolerite intrusions lies to the north and south of Lillefjell Varde (Y10 945, X765 750). In this area much of the relatively extensive outcrop is due to repetition by folds produced during D1 and D2 in the plane of the hillside of relatively few original dykes/sills. A tectonic facies of the dolerite containing large needle like porphyroblasts of actinolite up to 2 cm in length is seen on Lillefjell Varde (Y10 981, X765 715). This marks a texturally reconstructive episode of the regional metamorphism under the influence of relatively high local stress

in the greenschist facies.

The chronology of the intrusive rocks is difficult to establish. They have all deformed during the three major phases of deformation recognised in the area ($D_1 - D_3$). In some exposures (e.g. Y11 060, X765 360) the acidic dykes appear to cut the basic dykes, suggesting the basic dykes pre-date the more acidic ones. Unfortunately it is not possible to prove this conclusively.

3.4 Intermediate Intrusive Rocks

Isolated dykes/sills of feldspar porphyritic fine-medium grained, mesocratic, intermediate "andesite" occur within the Gjersvik volcanics (e.g. Y11 015, X764 920). These dyles/sills are 1-1.5 m wide with no apparent chilled margins or visibly altered country rock. It is difficult to trace these bodies over more than approximately 30 - 50 m and it is not possible to unequivocally establish their position within the chronology of the intrusive rocks. However, their composition would suggest their emplacement was intermediate between the doleritic and dacitic lithologies described above.

3.5 Sedimentary Rocks

The rocks exposed to the east of the eruptive suite described above are a clastic sedimentary sequence. These sediments comprise the lower portion of the Limingen group⁵ of phyllites, graded wackestones and polymict conglomerates, probably flysch type deposits formed during the "Gjersvik Disturbance"⁵.

The eruptive/sediment/is not exposed at outcrop, though it /contact often forms a distinct break in slope and there is a sharp change in flora across it. The strong penetrative shistosity which cuts S1 and several shear zones within the eruptives close to the contact, together with large concentrations of veins and pods of tectonic quartz and ferroan calcite in the sediments in the vicinity of the contact, suggest it is largely tectonic. It seems likely that the contact dips at a moderate angle to the west, the clast assemblage described below and observed field relations suggesting the sediments stratigraphically overlie the eruptives. The contact has been folded during D2, as it can be seen to mimic the folding of the S1 shistosity in the adjacent eruptives e.g. Y10 900, X764 400. Regional evidence of the lateral continuation of the Limingen group⁵, and the clast assemblage described below, suggest it to be laterally related to the Gjersvik eruptives. Thus the amount of movement on the thrust is probably not great.

F₂ fold
thrust

Immediately adjacent to the contact is approximately 50 - 60 m structurally, of very coarse to fine sand grade calcareous graded wackestone. Individual graded units are typically 0.3 - 0.7m thick. Finer grained pelitic beds often occur between the graded horizons. To the south-east of the graded wackestone lies a unit of fine grained, very calcareous Phyllite which supports a species rich and abundant calcareous flora. This unit is probably 150 - 250 m thick structurally. Further to the east the sediments become conglomeratic.

microcline
thick
grainy
15-20cm
thick
on

The conglomerates vary widely in their grain size and the relative proportions of the components clasts. In general terms they form very poorly sorted, sub-angular to sub-rounded, highly flattened, polymict conglomerates, with a maximum grain size between 0.5 and 10.0 cm. Large pebbles or quartzite ferroan calcite - limestone, trondhjemite, meta dacite, and occasionally 'greenstone' are the major clastic constituents Fig. 3.5-1. The matrix is dominantly fine grained, shistose: chlorite, sericite, quartz and lesser euhedral pyrite. Fuchsite was observed in the matrix in one exposure.

The volcanic 'greenstone' meta-dacite and carbonate clasts, together with the very chloritic matrix, would seem to indicate a local Westerly origin for these sediments. However, a source for the abundant mature quartzite clasts is difficult to envisage within an immature island arc environment. Thus one must assume a source within the shield area to the East for a large proportion of the sediment. Thus the provenance of the sediment is obviously complex and a greater or lesser proportion of the observed clast assemblage may originate from other than these two more obvious sources.

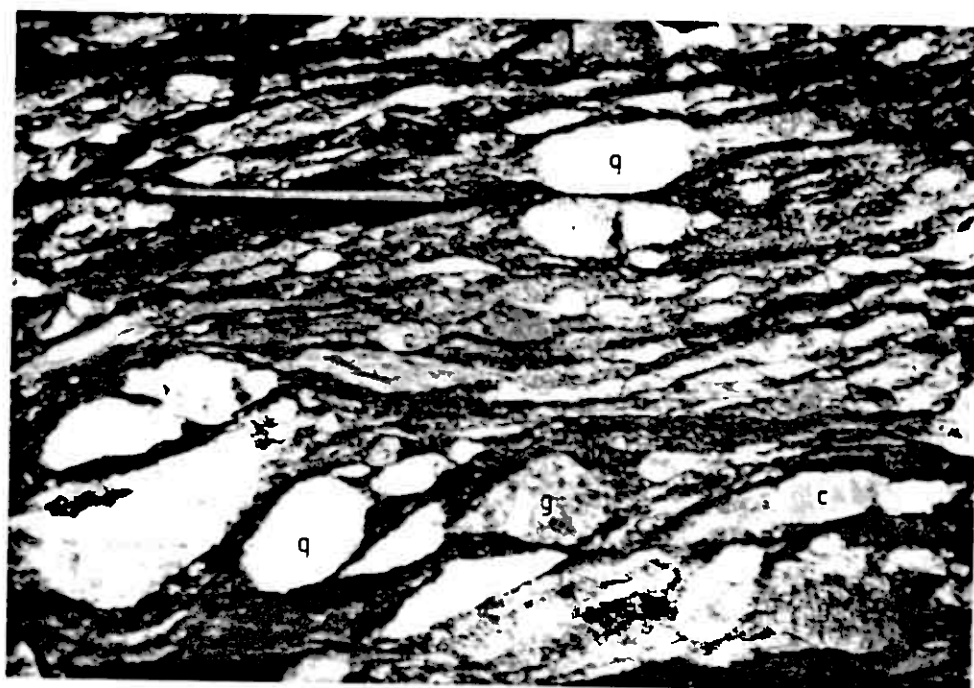


Fig 3.5-1. Typical clast assemblage of deformed polymict conglomerates in the Gjersvik area.

- q - quartzite
- c - ferroan calcite-'limestone'
- g - granodiorite, trondhiemite
- v - chloritic, highly flattened 'greenstone'

The area has undergone three major recognisable phases of deformation ($D_1 - D_3$) Fig. 4-1, often with associated brittle fracturing in the more competent lithologies. The structure is more easily elucidated in the sedimentary rocks exposed to the east of the eruptive sequence. The presence of original stratigraphy and sedimentary structures within the sediments together with their being relatively incompetent and thus deforming more homogeneously than the eruptive rocks, allows a more complete insight into the history of deformation within the area on a more local scale, than is possible in the eruptive rocks.

The very intense deformation during both D_1 and D_2 is characteristically heterogeneous, which is reflected in the variable attitudes of fold axes and axial planes. The development of a heterogeneously strained fold system is probably primarily due to the differential absorption of strain by lithologies of different competence. In the eruptive rocks, observations of the mechanical behaviour of the various lithologies after deformation suggest a classification on the basis of competence:

Dolerite \approx dacite $>$ basic volcanics \gg sulphides, e.g. Fig.4-2

Thus the relative proportion of the more competent lithologies present in a particular area will affect the amount of strain absorbed by the less competent lithology (usually basic greenstones). In absolute terms the basic greenstones are very competent rocks and thus they tend to deform along planes of weakness within the rock when they are subjected to large strains, and probably strain rates, giving rise to heterogeneous folding and shearing e.g. Lillefjell Varde area.



Fig. 4-1. Three superimposed phases of folding seen in schists exposed on Rörvik road section.



Fig.4-2. Mullion structures developed in more competent rhyo dacitic dyke cutting basic lavas.

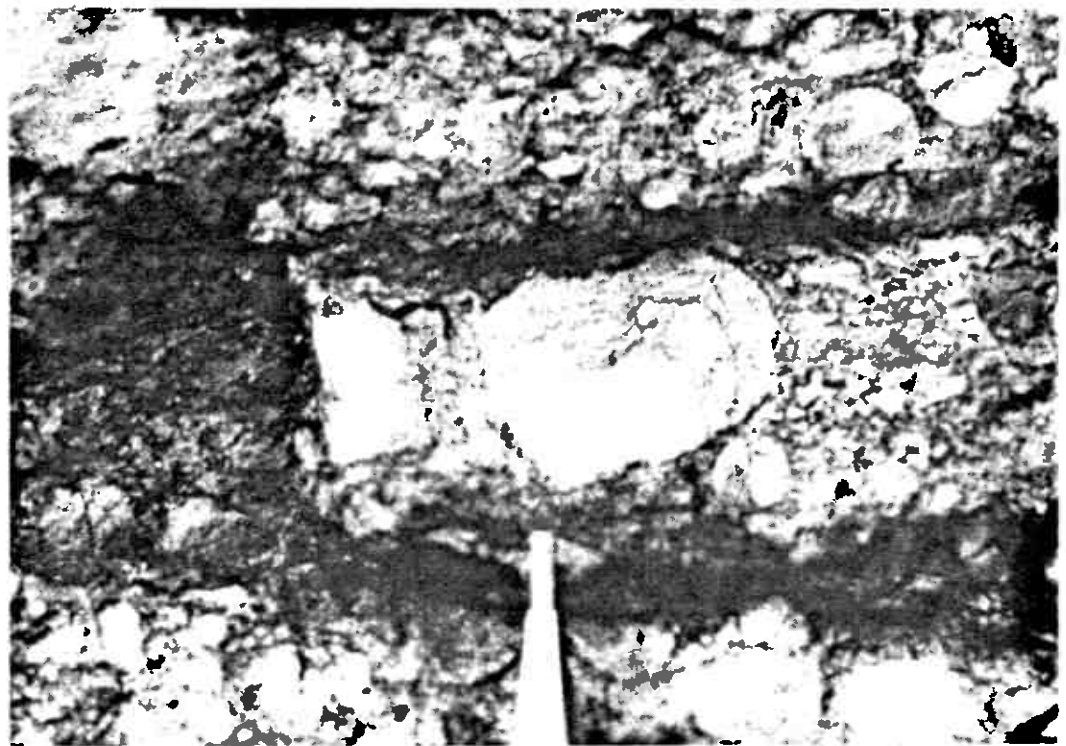
4.1 D₁ DEFORMATION

The style of folding and metamorphic reconstitution occurring during the first phase of tectonic deformation suggest that it was largely responsible for the major textural reconstitution of the rocks in producing the early penetrative shistosity. Intense flattening and tectonic segregations by pressure solution perpendicular to the maximum principle stress (σ_1) also occurred during this first phase of deformation.

Reversals in the direction of grading within the clastic beds, e.g. Y11 530, X764 560 indicate the presence of probably parasitic, isoclinal, F_1 folds with a wavelength of 15-30 m. Shistosity is approximately parallel to bedding also reflecting the isoclinal style. The orientation of D_1 structures is not easily determined due to their being obscured by subsequent deformation. However, limited information suggests that the D_1 structures in the sediments now plunge between 10° and 20° to the North, with the axial plane shistosity (S_1) modified by D_2 and D_3 fold structures Fig. 4.2-1. The intense flattening during D_1 has resulted in the orientation of highly flattened clasts parallel to S_1 . Pressure solution between clasts and redistribution of quartz and ferroan calcite in pressure shadows Fig. 4.1-1 and tectonic segregations Fig. 4.1-2, where the calcite is often spathic, also occurred during D_1 . These features have been folded during subsequent deformation Fig. 4.1-2. An interesting feature of these rocks is the occasional preferential mobilisation of quartz against calcite by pressure solution. It is often possible to see carbonate clasts penetrating quartz clasts, with quartz being preferentially deposited in pressure shadows Fig. 3.5-1, though the reverse is more common.



A.



1 cm

B.

Fig.4.1-1. A. Dilational fracturing in trondhjemite clast and redistribution of quartz and ferroan calcite in pressure shadows.
B. Dilational fracturing and rotation of carbonate clast by D_1 .

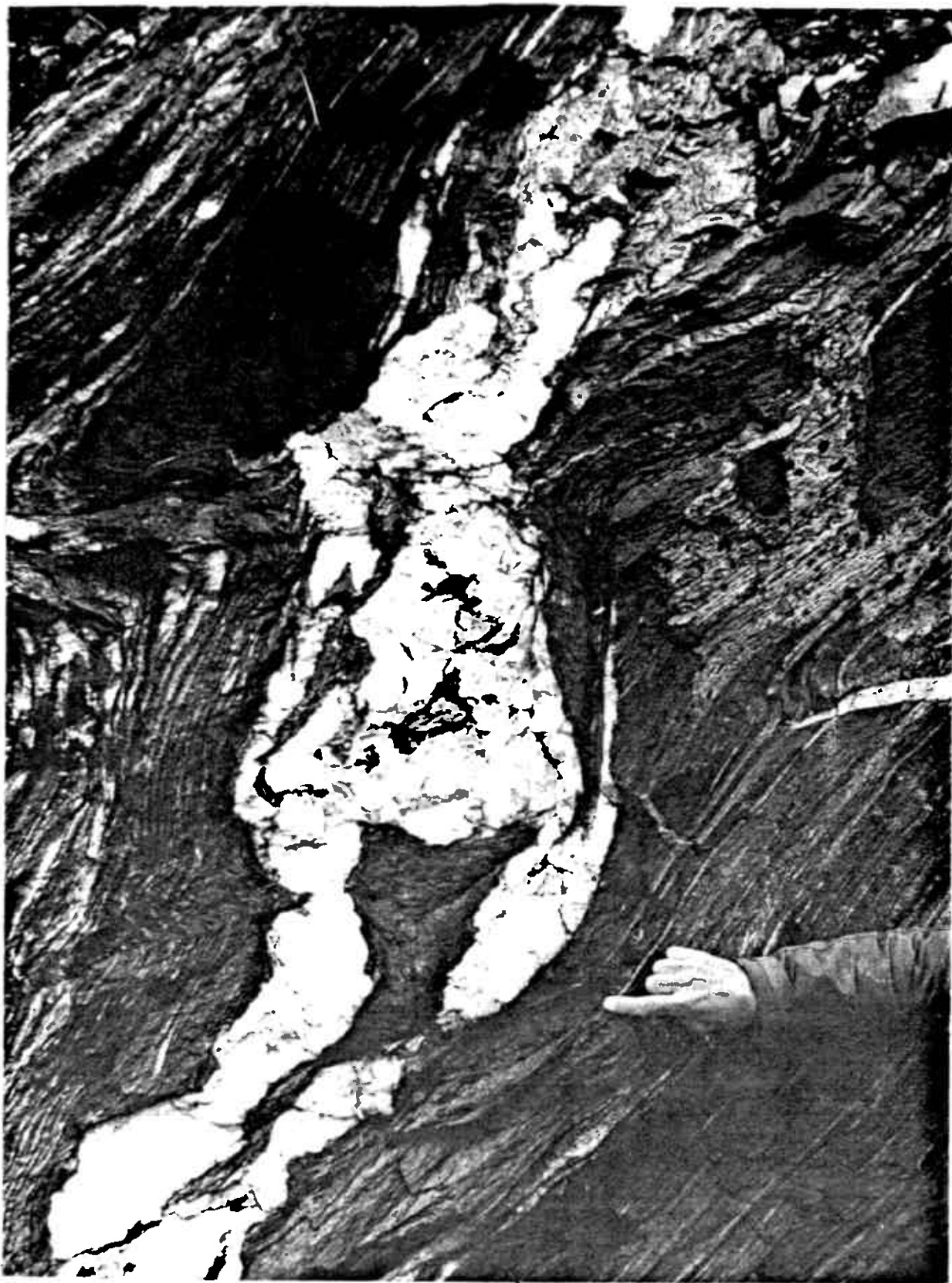


Fig. 4.1-2. Tectonic segregations of ferroan calcite and quartz parallel to S_1 , refolded and boudinaged by D_2 and D_3 folding.

In the eruptive rocks, the general lack of recognisable stratigraphy makes it very difficult to ascertain the location and form of D_1 folds. Minor isoclinal D_1 folding can be seen producing repetition of the intrusive dacitic and doleritic dykes, with easily recognisable axial plane schistosity (S_1) Fig. 4.1-3 now refolded into D_2 structures. These D_1 folds generally plunge between 10 and 20° north to north-east or south to south-east, though precise measurements are difficult to obtain. The presence of the massive sulphide mineralisation of the Gjersvik Orebody e.g. Y10 550, X764 010 and its probable stratigraphic continuation as pyritic and sideritic exhalites to the north (Ch 5.3) e.g. Y11 017, X764 755 together with recognisable pyroclastic dacites associated with these horizons and the position of sub-volcanic, dacite dykes immediately to the north of the pyroclastics, structurally overlying the Gjersvik orebody and to the west of the pyroclastics at Y11 017, X764 755, suggest the major structure in this southern area is a large D_1 isoclinal synformal anticline. This structure with probably an originally flat lying axial plane, has a wavelength of at least 500 m and an amplitude of similar magnitude. It has a closure truncated by the major N.N.E-S.S.W. fault in the area Y10 700-900, X764 250-500 Fig. 4.1-4 and has been folded by subsequent deformation (Ch 4.2), probably from an originally antiformal closure to the synformal style now seen, Fig. 4.1-4.

The inferred tectonic contact between the eruptive and the sedimentary rocks, is folded congruent with S_1 into F_2 closures e.g. Y11 920, X764 890 and is thus a structure of pre D_2 age, produced almost certainly during D_1 . This together



Fig.4.1-3. D_1 isoclinal fold closure (looking up plunge), developed in possibly extrusive meta dacite against basic lavas.

GEOLOGICAL SECTION THROUGH THE GJERSVIK AREA

NO VERTICAL EXAGGERATION

LEGEND

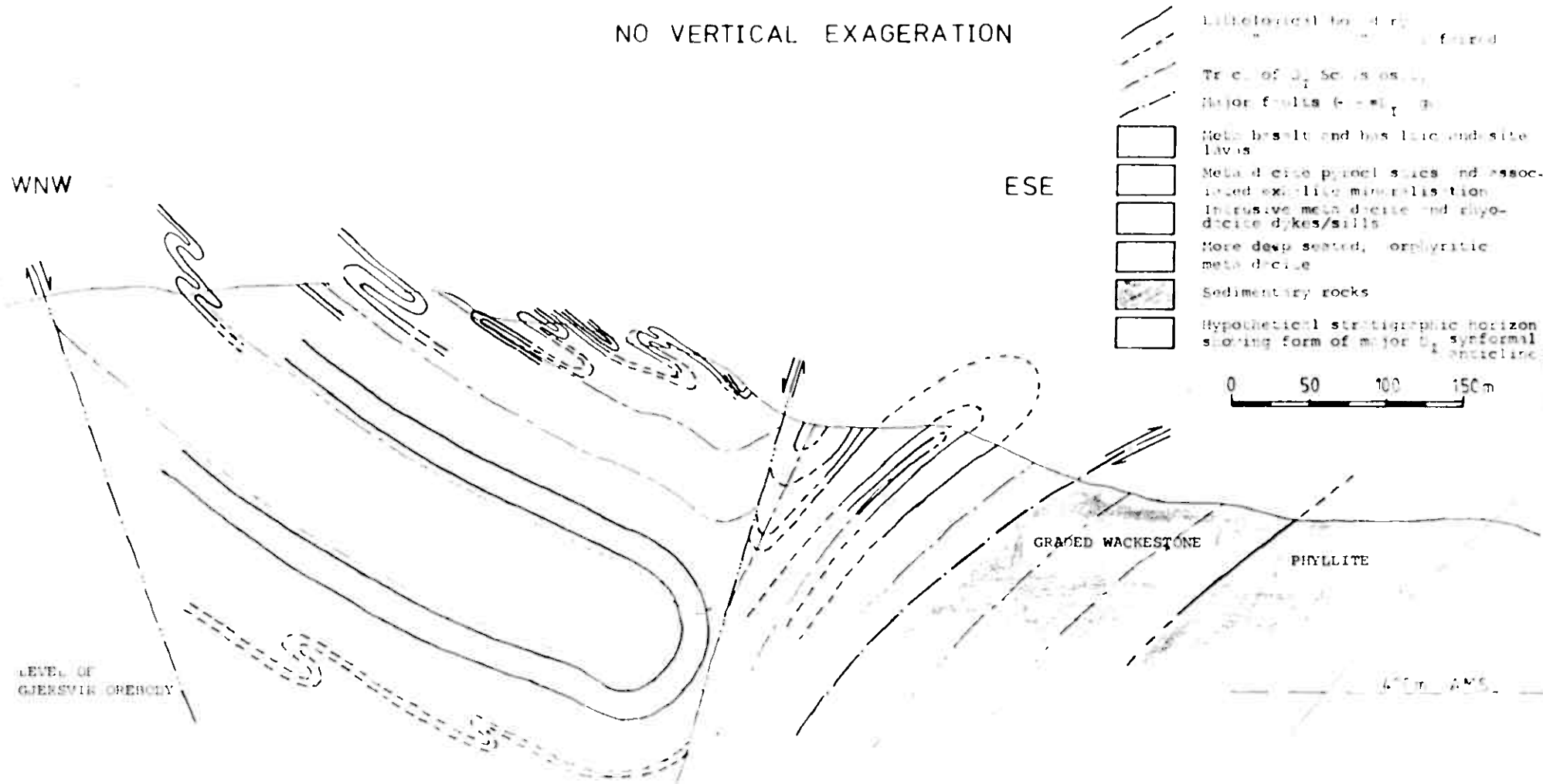


Fig 4.1-4.

with regional evidence⁵ suggests that large scale thrusting of allochthonous nappes from the West along shallow westerly dipping thrust planes occurred during D_1 . Due to allochthonous transportation the true orientation of the stress system is unknown. However, the flat lying axial plane and large sub-horizontal shear stress indicates the maximum principle stress (σ_1) to have been sub-horizontal, probably trending approximately east-west, with the least principle stress (σ_3) sub-vertical i.e. overburden pressure.

4.2 D_2 DEFORMATION

The second phase of deformation is very easily recognised in the field as folding of the penetrative S_1 shistosity, veinlets and flattened pebbles produced during D_1 and by repetition of intrusive dykes within the volcanic sequence. As D_1 folding formed isoclinal structures, S_1 shistosity is approximately parallel to bedding i.e. the dihedral angle between bedding and shistosity is approximately zero, except around fold closures. Thus, structures produced from the folding of S_1 shistosity will mimic those formed by the refolding of bedding. The very tight folds produced during D_1 deform as competent masses during subsequent deformation and thus the orientation of D_2 folds is strongly influenced by the orientation of the D_1 folds in the immediate vicinity. The heterogeneous style of D_1 affects the directional stability of the F_2 fold axes (Ramsay¹³, p.p. 540). This is reflected in the spread of orientations of F_2 fold axes seen e.g. 40-50° in Fig. 4.2-1.

- S1 SHISTOSITY - π POLES
- ▲ F1 FOLD AXES - PLUNGE
- S2 SHISTOSITY - π POLES
- ▲ F2 FOLD AXES - PLUNGE
- C F2 CRENULATIONS - PLUNGE
- △ F2 FOLD AXIS - π POLE TO π CIRCLE

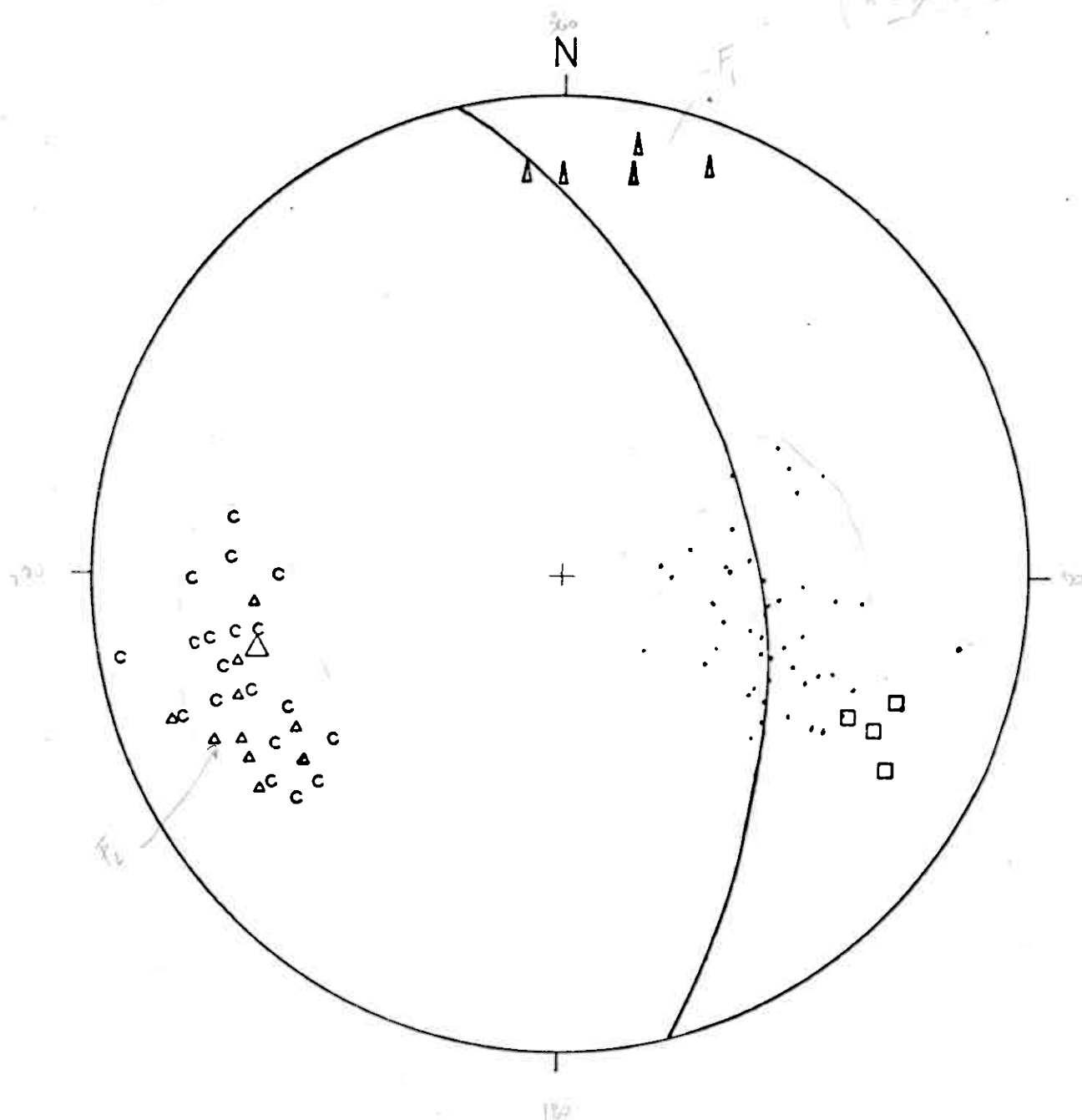


Fig4.2-1.F1 & F2 Structures from Sediments.
lower hemisphere, equal area projection

in orientation, though in the area south of Lillefjell Varde they plunge $10-20^{\circ}$ north to north-east or south to south-west. Part of this variation is due to the distinctly periclinal nature of the D_2 fold structures Fig. 4.2-5, 4.2-6. From Fig. 4.2-5 and observations in the field, the D_2 periclinal folds have an aspect ratio in plan view of approximately 6-9:1. The area around the major F_1 closure at Y10 700-900, X764 250-500 appears to have acted as a rigid block during D_2 , undergoing body rotation only, resulting in the discordant trend of S_1 seen in Fig. 4.2-5.

Several unfolded post D_1 fractures are seen to cut the area e.g. Y10 650, X764 850 - Y10 875, X765 315. They vary widely in orientation, though very generally they trend north east - south west, with probably a moderate to steep dip, though this was never accurately measured due to poor exposure. In some cases these fractures are axial planar to D_2 folds e.g. Y10 500, X765 290 - Y10 795, X765 500 and it seems likely movement has occurred along the axial plane of the D_2 fold structure (S_2) Fig. 4.2-8. Elsewhere this is not the case and the fracture movements have a distinctly rotational character about a central axis where there is apparently little movement and the fracture plane has no apparent correlation with S_2 . This is substantiated by the variation in the orientation of F_2 fold axes and S_2 adjacent to the fault Y10 650, X764 850 - Y10 875, X765 315 to the north and south, Fig. 4.2-7 which indicates a rotation of approximately 40° . In the area Y11 100, X765 140 acid dykes show little evidence of displacement across the fracture and the axis of rotation probably lies in this region.

MAJOR POST D_1 STRUCTURES ELUCIDATED BY TRACE OF S_1 SCHISTOSITY

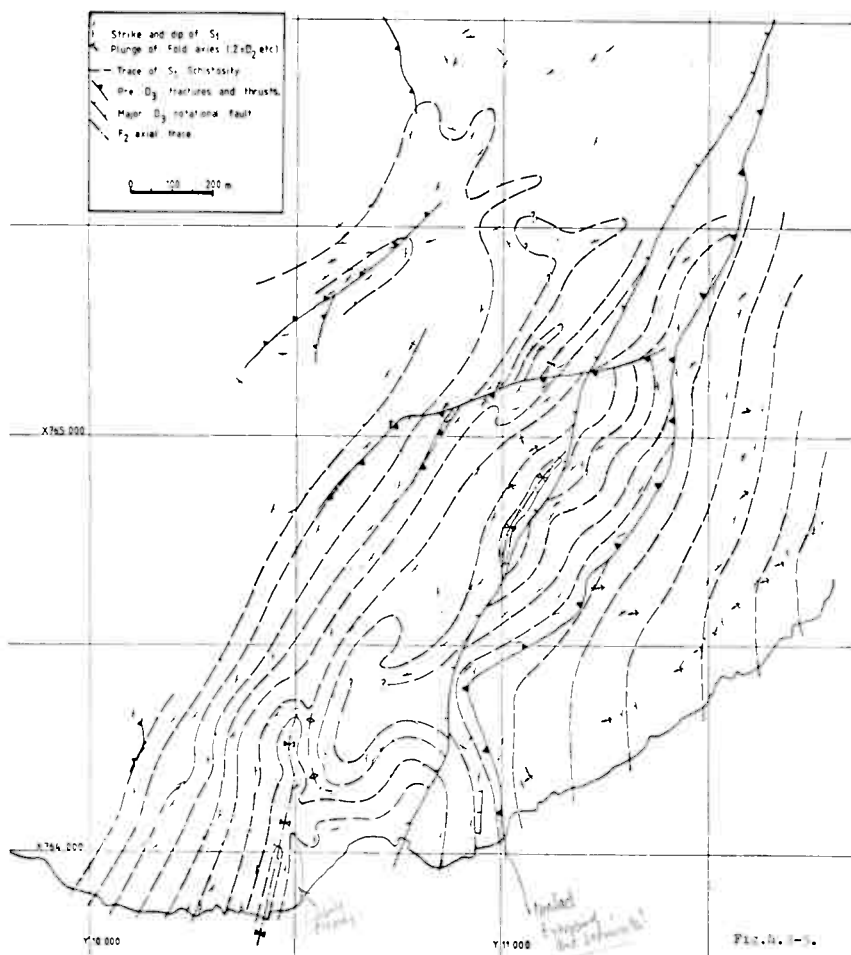


FIG. 4. 1-3.

In the sedimentary rocks the D_2 folds are characterised by
their tight form and steeply dipping axial planes, Fig. 4.2-2.
Locally it is possible to see refolded F_1 isoclines e.g. Fig. 4-1,
though usually the structure is elucidated from the folding of
 S_1 . The plot of π poles to S_1 lie approximately on a great
circle, indicating a roughly cylindrical form for F_2 in the
sediments, with a fold axis plunging approximately 35° to 250° , F_2
Fig. 4.2-1. Actual plunges of measured fold axes tend to vary
about this value, generally in the range $10-30^\circ$ to $230 - 270^\circ$.
The axial planes also show some variation in orientation, though
always steeply dipping. Small scale F_2 crenulations are also
seen in the more phyllitic interbands, with wavelengths of
2-5 cm and amplitudes of approximately 1 cm. Again these have
steeply dipping axial planes and the orientation of their fold
axes is consistent with that of the larger scale folds, Fig. 4.2-1.

The style of D_2 folding in the eruptive rocks is noticeably different
either side of the major N.N.E.-S.S.W. fault. To the east of the
fault the style of deformation is very similar to that seen in
the adjacent sediments. The D_2 structures seen are large scale,
fairly open, approximately cylindrical structures with a moderate
plunge to the N.N.W. Fig. 4.2-3. The sediment/eruptive contact is
folded consistently with S_1 in this area, as mentioned above. A
strong penetrative S_2 schistosity developed in the eruptives close
to the sediment/eruptive contact suggests there may have been
some tectonic adjustment along this plane during D_2 . To the
west of the fracture the D_2 folds are usually closed or tight,
asymmetric, generally with a steep axial plane, though this is
very variable, Fig. 4.2-4. The F_2 fold axes show a wide variation



Fig. 4.2-2. D_2 folds with characteristic steep axial plane, refolding isoclinaly folded (D_1) quartzose horizons in deformed conglomerate, coupled with boudinage on the limbs. Note accommodation structures around fold colures.

• S1 SHISTOSITY - π POLES

Δ F2 FOLD AXIS - π POLE TO π CIRCLE

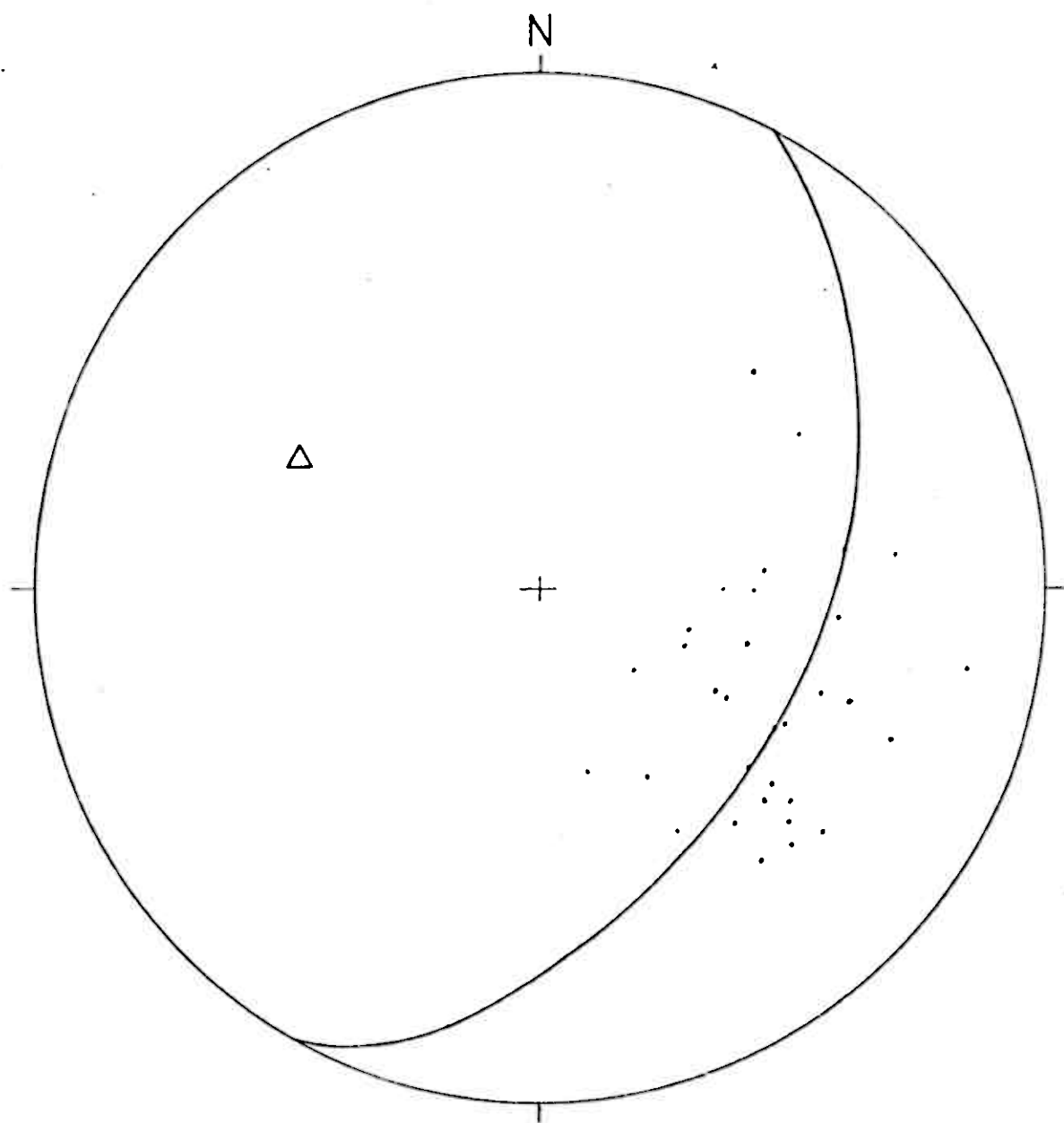


Fig.4.2-3. Structural data from eruptives
East of main fracture (see text)
lower hemisphere, equal area projection.



Fig.4.2-4. Tight - open style of D_2 folds seen in fallen block of basic 'greenstone'.

- S_1 SHISTOSITY - π POLES
- S_2 " " "
- △ F_2 FOLD AXES - PLUNGE
- △ " " " - π POLE TO π CIRCLE
- c " CRENULATIONS - PLUNGE

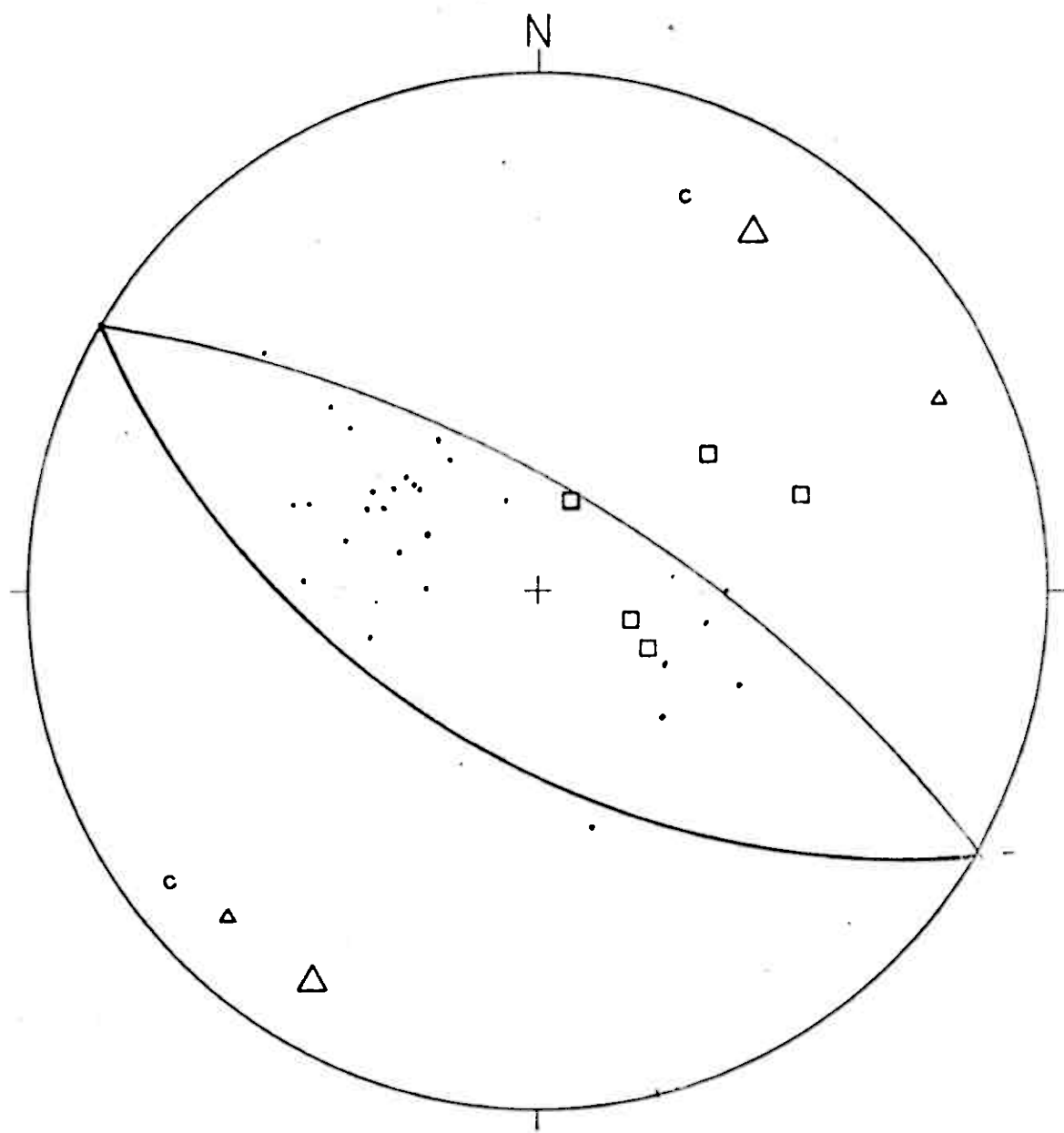


Fig.4.2-6. Periclinal F_2 Folding immediately
North of the 'Gjersvik Orebody'
Lower hemisphere equal area projection

- S1- π POLES
- S2- π POLES
- c F2 CRENULATIONS - PLUNGE
- △ F2 FOLD AXES - PLUNGE
- △ F2 FOLD AXIS- π POLE TO π CIRCLE
- OPEN SYMBOLS - NORTH OF FRACTURE
- SOLID " " SOUTH " " "

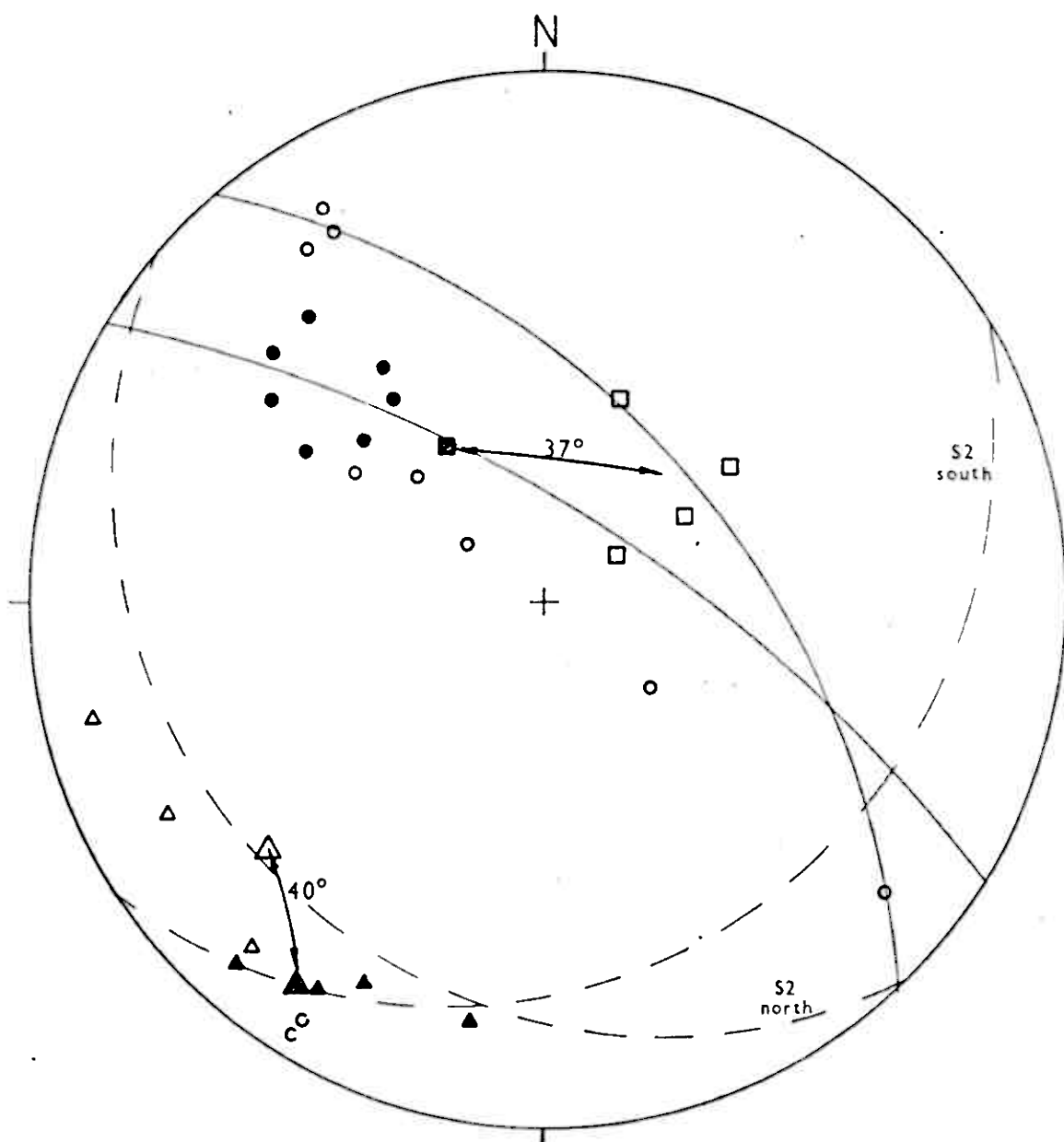
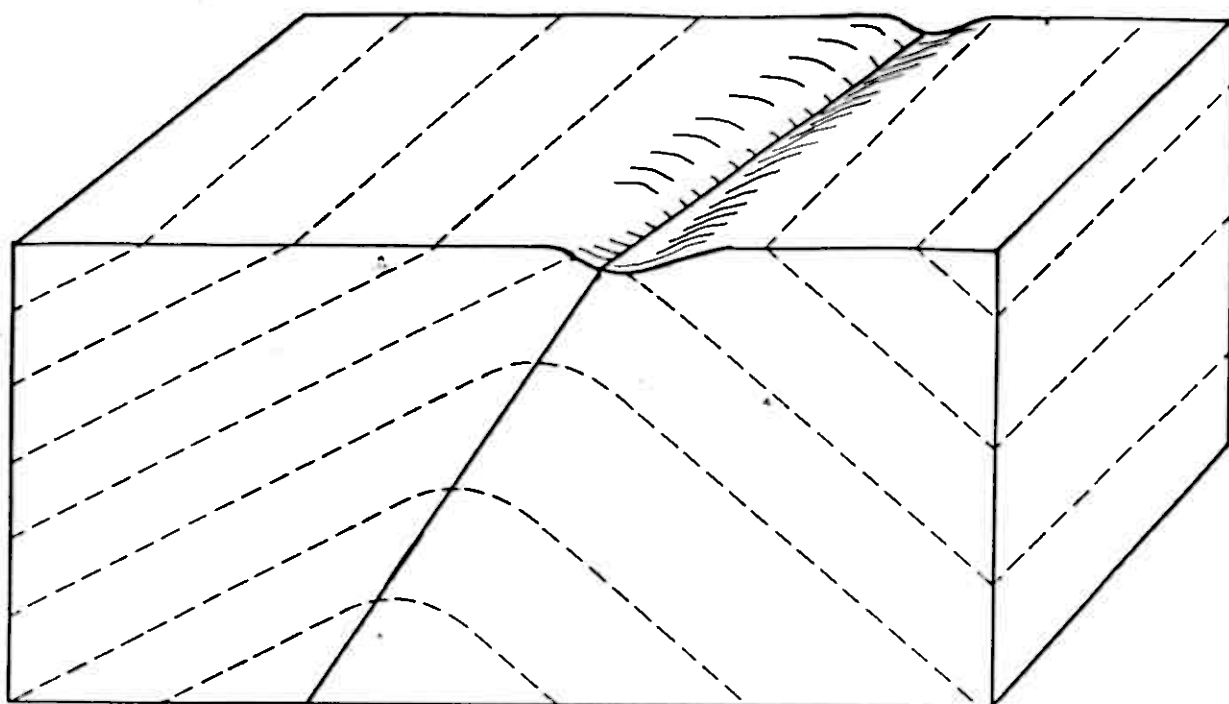
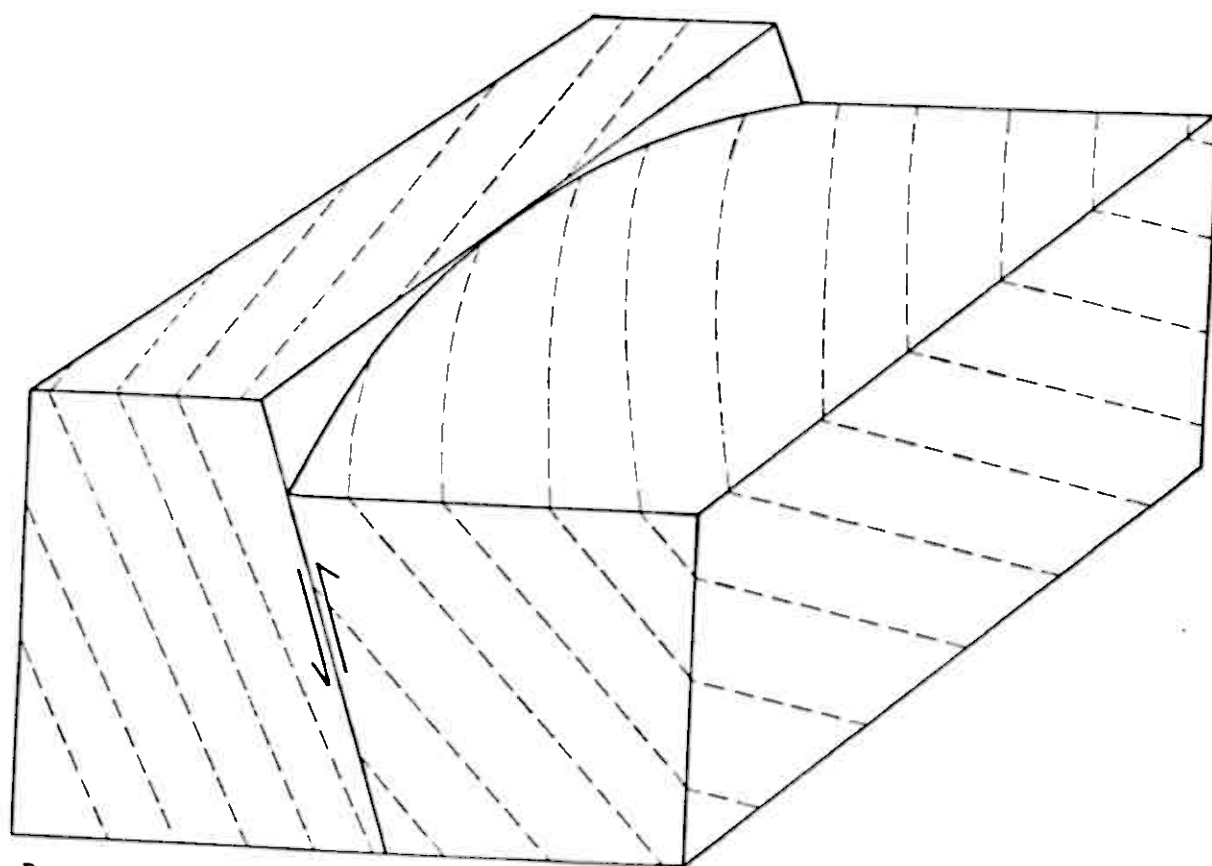


Fig4.2-7. Illustration of rotation about F2
 East-West fracture (Y10 650,X764 850 to
 Y10 875,X765 315)
 lower hemisphere, equal area projection

--- S₁ Planes



A.



B.

Fig 4.2-8. Schematic diagram showing nature of fractures related to D₂ folds:
 A. Fractures developed along axial plane of D₂ folds
 B. Rotational fractures developed in response to couples induced by D₂ folding

These rotational faults probably developed as a result of rotational shear stresses induced by refolding (with an appreciable component of flexural slip) of D_1 structures, with a dihedral angle between limbs greater than zero, during D_2 (see Ramsay¹³ p.p. 541-547).

The orientation of the principle stresses during D_2 is difficult to ascertain due to the low directional stability of D_2 structures. In general it would appear that the maximum principle stress (σ_1) was horizontal, trending north west - south east, with the least principle stress (σ_3) approximately vertical. The dominant mechanism of folding is difficult to assess from structures preserved in these rocks. Components of flexural slip, simple shear and tangential longitudinal strain can all be seen, though the relative important of individual mechanisms is unknown.

4.3 D_3 DEFORMATION

A third phase of folding is seen in the sedimentary rocks Fig. 4-1, though conclusive evidence of D_3 folding is not so evident in the eruptive suite.

D_3 folds in the sediments are distinguished from D_2 structures by their flat lying axial planes, which trend approximately north-south with a dip of $10-20^\circ$ west. The orientation of F_3 fold axes is strongly influenced by earlier structures, but generally plunge $10-20^\circ$ south west to south south west and show an angular discordance of $20-30^\circ$ with F_2 fold axes Fig. 4.3-1. The plunge of small scale crenulations plot around the F_3 fold axis Fig. 4.3-1 and often have a flat lying axial plane (crenulation cleavage) and are thus probably D_3 in age. D_3 folds tend to have an open style, generally

- △ F2 FOLD AXES - PLUNGE
- ▲ F3 FOLD AXES - "
- S2 SHISTOSITY - π POLES
- S3 SHISTOSITY - " "
- c POST S1 CRENUATIONS - PLUNGE

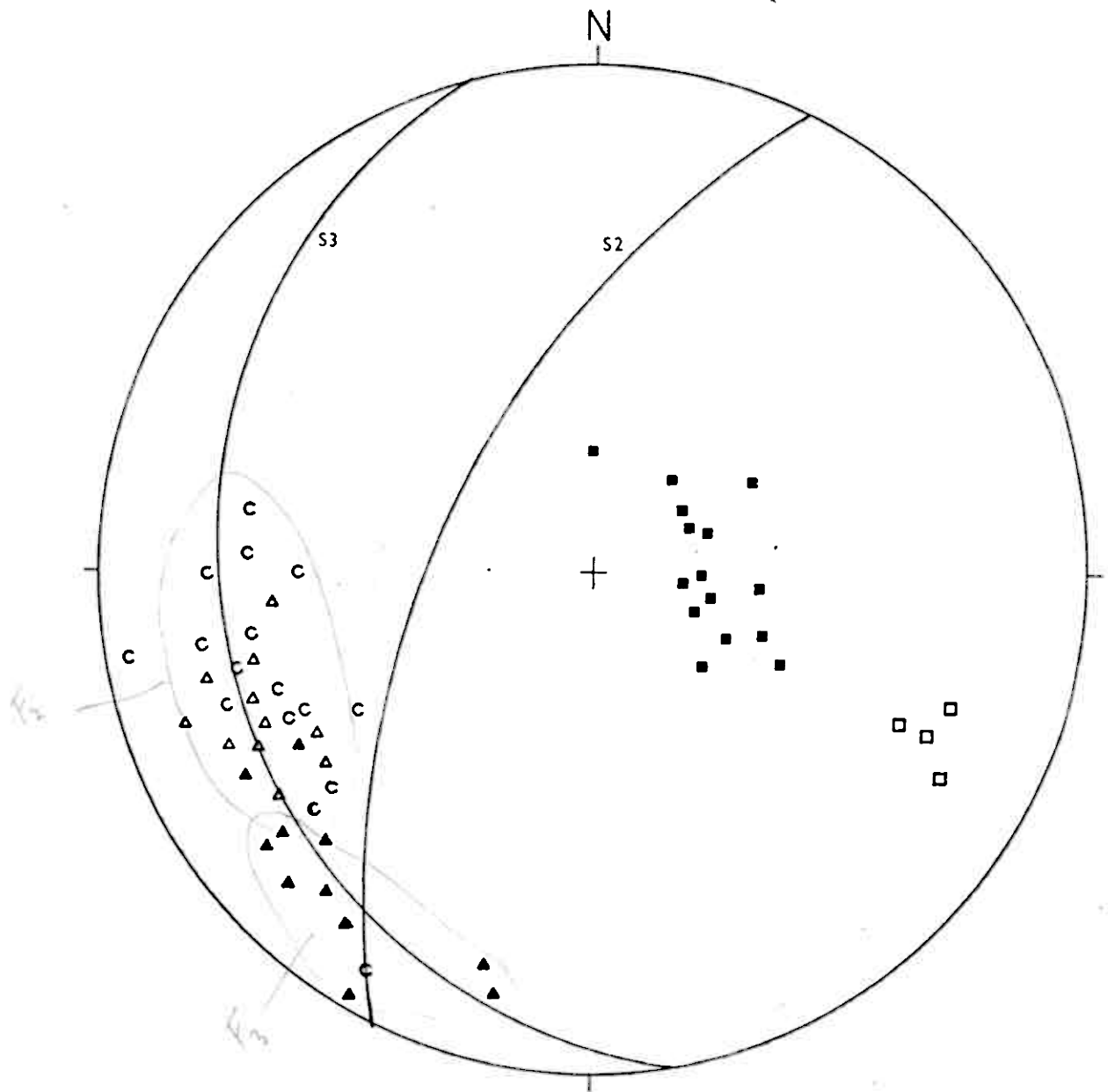


Fig. 4.3-1. Orientation of F2 & F3 Structures from the Sediments.

Lower hemisphere, equal area projection.

forming small scale features and are thus not a major influence on the overall structure.

In the eruptive rocks no unequivocal D_3 folds were observed and the cause of this is discussed in the next section.

It would appear that the maximum principle stress (σ_1) was approximately vertical, with the minimum principle stress (σ_3) trending approximately N.N.W.-E.S.E. As σ_1 is the overburden pressure it would suggest that the area had become deeply buried, or that the high horizontal compressive stresses present during D_1 and D_2 were relaxed.

4.4 BRITTLE FRACTURING

Apart from the small scale fracturing associated with D_2 folding and the tectonic sedimentary/eruptive contact discussed above, the major brittle fracture is the approximately N.N.W.-S.S.E. trending fault at e.g. Y11 010 X764 035 to Y11 385, X765 500. This fault dips steeply to the west and separates higher metamorphic grade rocks to the east from lower grade rocks to the west, suggesting a downthrow to the west and thus a normal sense of movement. The amount of throw appears to be variable, as exhalites are seen in the road section to the east of the fracture e.g. Y10 465, X764 095, indicating near stratigraphic continuity across the fault at this point. Thus a clockwise rotational component of movement is also present. From the variation in metamorphic grade observed across the fault, it would appear the maximum displacement is of the order of several hundred metres, though this is a very crude estimate.

This fault is not visibly deformed indicating it is D_3 , or post D_3 in age. The normal sense of displacement indicates σ_1 to have been approximately vertical, with σ_3 trending approximately W.N.W.-E.S.E. This orientation of principle stresses is consistent with that indicated by D_3 structures in the sedimentary rocks (Ch.4.3). Thus it appears that the temperature, pressure and stress conditions at the depth at which D_3 deformation of the presently exposed structural level occurred, were such as to allow plastic deformation in the less competent sedimentary rocks, but the more competent eruptive rocks deformed in a brittle manner. Thus precluding the formation of D_3 folds in the eruptive rocks.

Minor sets of conjugate, undeformed, slickensided fractures, with a normal sense of displacement and little or no rotation, consistent with the D_3 stress system are seen around the outcrop of the "Gjersvik Orebody" Fig. 4.4-1. Similar sets of conjugate fractures infilled by ferroan calcite occur locally in the sediments Fig. 4.4-1. The presence of these fractures is believed to support the interpretation made above.

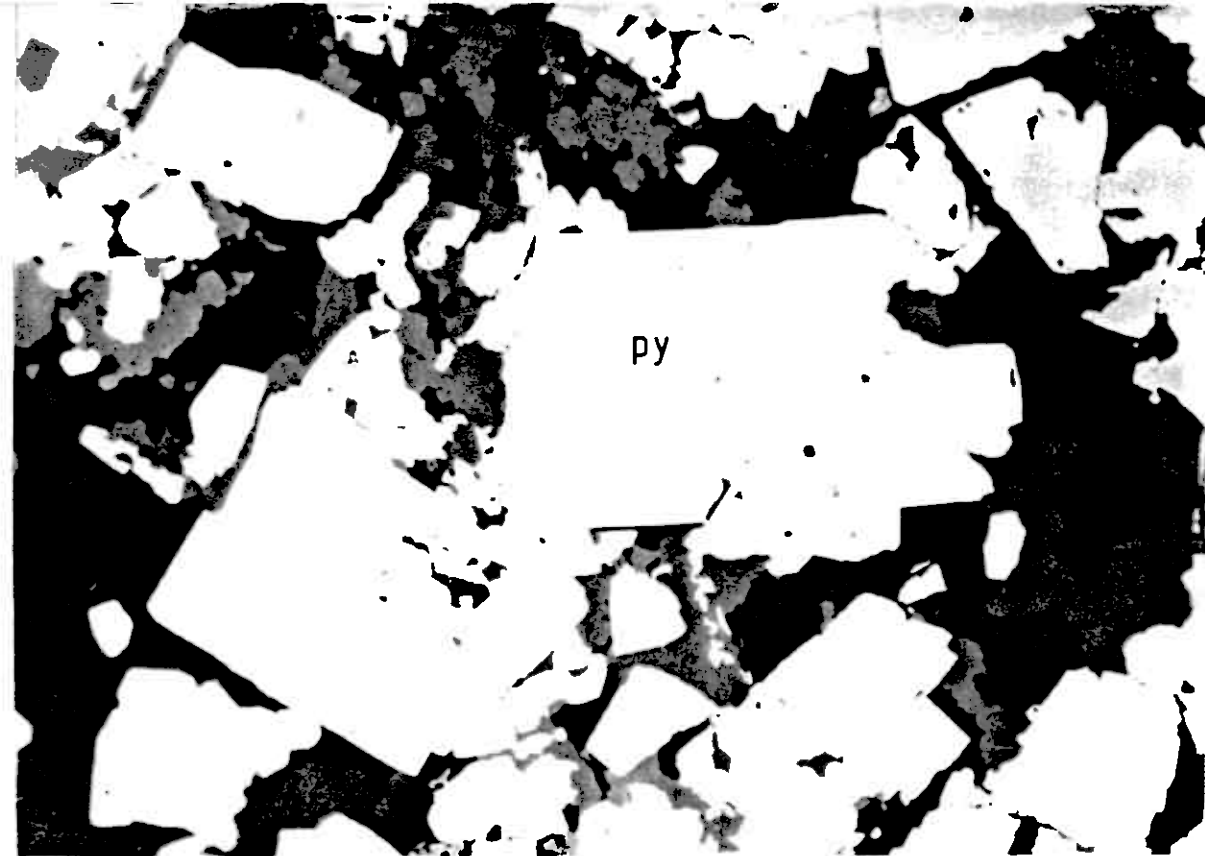
The 'Gjersvik Orebody' underwent development work during the early part of the 20th Century, primarily for the recovery of sulphur. It was abandoned soon after due to being uneconomic. It is now possible to view the massive sulphide mineralisation of the 'Gjersvik Orebody' in its regional context with regard to related mineralisation in the area.

5.1 MASSIVE SULPHIDE MINERALISATION - THE 'GJERSVIK OREBODY'

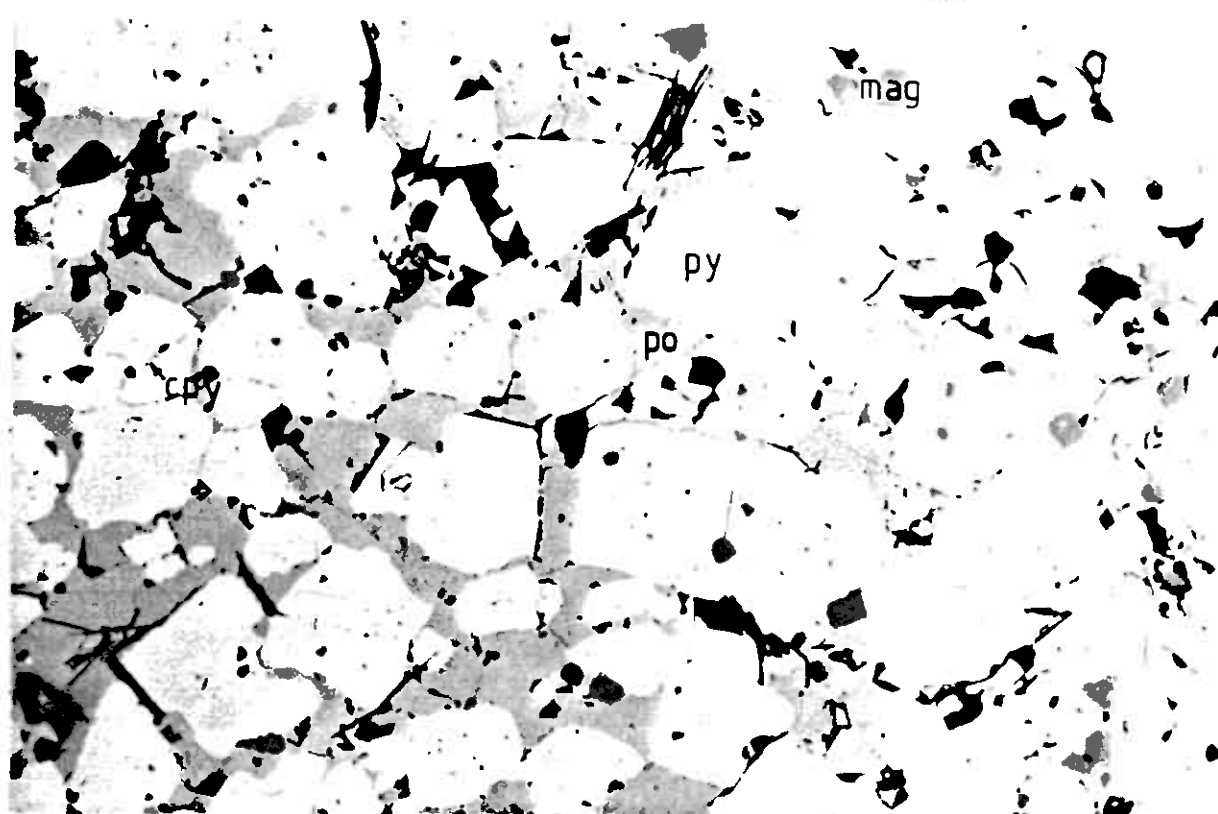
The present outcrop of the 'Gjersvik Orebody' has an irregular pseudo rectangular pattern (see accompanying map), mainly due to post depositional folding. The horizon itself is generally 1-3 m thick, the dominant mineralogy being pyrite, pyrrhotite, magnetite and chalcopyrite, with odd grains of sphalerite and a carbonate plus chert gangue.

Two distinct facies are seen within the massive sulphides (e.g. Y10 550, X764 010):

1. A pyritic facies, consisting of >95% compact pyrite, with some fine grained chalcopyrite (grain size c. 50 μ m), with a carbonate plus some chlorite gangue, Fig. 5.1-1(a).
2. A pyrite, pyrrhotite, magnetite facies, consisting of 50-60% euhedral-subhedral pyrite 0.4-1.2 mm in size, in a matrix of 25-30% anhedral monoclinic pyrrhotite, and 5-15% magnetite porphyroblasts 0.01 - 0.1 mm in size with 2-3% anhedral, intergranular chalcopyrite, grain size 0.01 - 0.2 mm. The gangue is predominantly carbonate (c. 10%), Fig. 5.1-1(b).



A.



B.

Fig. 5.1-1. A. Cataclastically deformed highly pyritic facies of Giersvik Orebody.

B. Typical pyrite(py) euhedra in matrix of pyrrhotite(po), chalcopyrite(cpy), magnetite(mag), with some carbonate + quartz gangue.

815 Ground
level
to 100m
100m

The origin of these distinct facies is not clear, but their nature and location suggests they are probably primary variations reflecting varying composition of the mineralising fluids and variable conditions in the environment of precipitation.

More siliceous facies occur in the lateral extensions of the mineralised horizon e.g. Y10 295 X764 100, which are often noticeably banded, Fig. 5.1-2. The bands consist of:

1. Anhedral pyrite 0.05 - 0.3 mm in size, with some large euhedra up to 1 mm in size, some anhedral chalcopryite 0.01 - 0.1 mm in size, odd fine grains of magnetite 0.05 - 0.1 mm in size and predominantly carbonate plus chert gangue.
2. Pyrite, magnetite bands; up to 50% magnetite as large anhedra 0.5 - 1 mm in size and also as finer anhedra 0.05 - 0.1 mm in size, some chalcopryite and sphalerite 0.01 - 0.1 mm in size and carbonate plus chert gangue.
3. Fine grained recrystalised chert with carbonate, fine grained sericite and odd pyrite euhedra.

These bands have been tectonically modified, but probably represent original stratification. Another facies recognised consists of recrystalised granular quartz with large pyrite euhedra up to 4 mm in size and a fine grained sericitic matrix, e.g. Y10 375, X764 150.

A pyrite cemented, dacite breccia is seen immediately beneath the mineralised horizon in some exposures e.g. Y10 412, X763 902, Fig. 5.1-3. The fragments of acidic material are highly siliceous varying in size from c.0.5 - 15 cm, generally sub-angular though



Fig. 5.1-2. Banded pyrite, chert facies of Gjersvik Orebody horizon.
Banding is probably original, though tectonically modified.

- △ F2 FOLD AXIS - PLUNGE
- ▲ F3 " " "
- F3 CONJUGATE FRACTURES - π POLES (VOLCANICS)
- S SLICKENSIDES ON FRACTURES - PLUNGE
- F3 CONJUGATE FRACTURES - π POLES (SEDIMENTS)
- ◆ F3 DILATANT FRACTURES - POLES

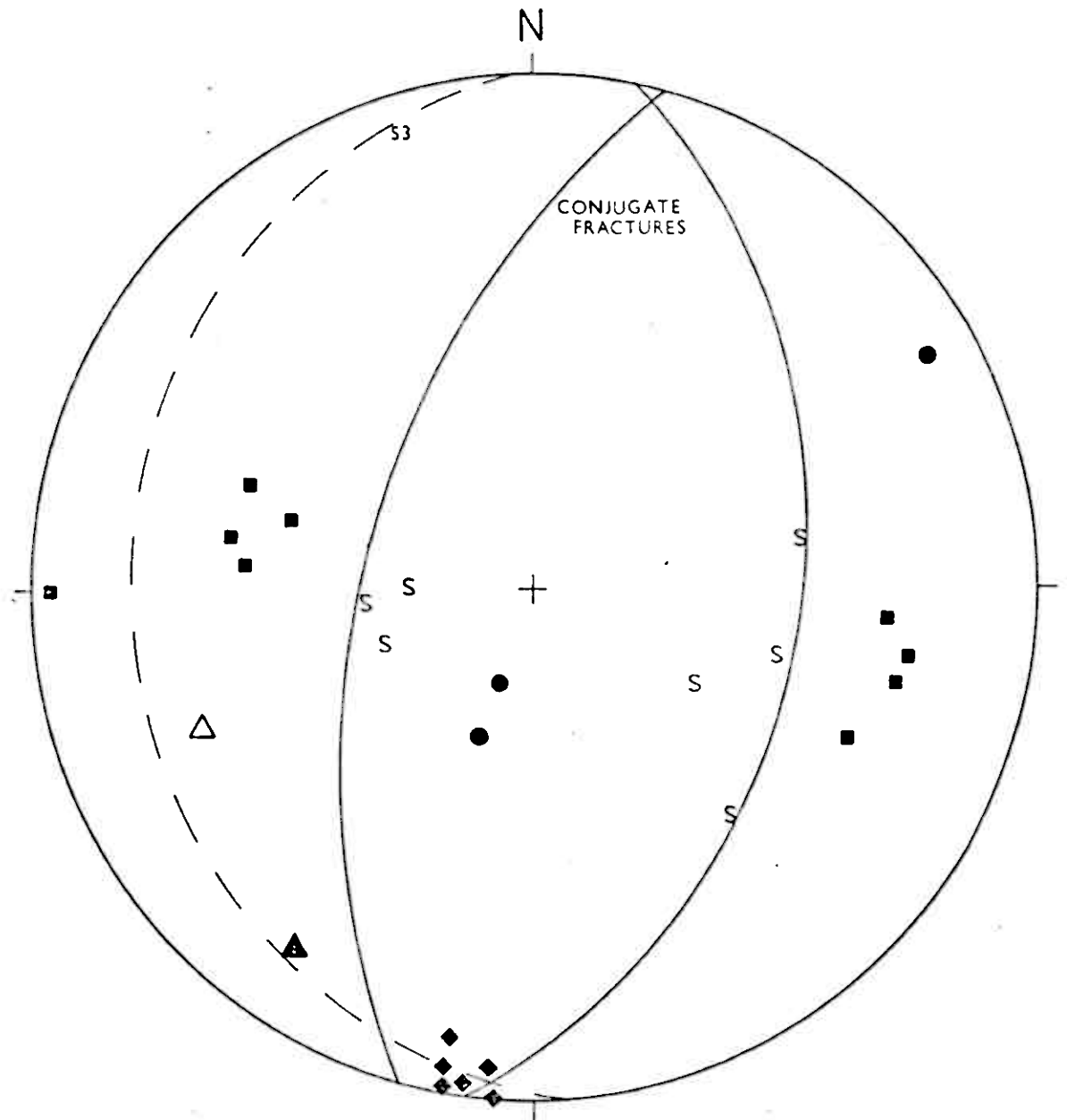


Fig.4.4-1. Geometrical Relationships between
F3 Fractures and Folds.

Lower hemisphere, equal area projection

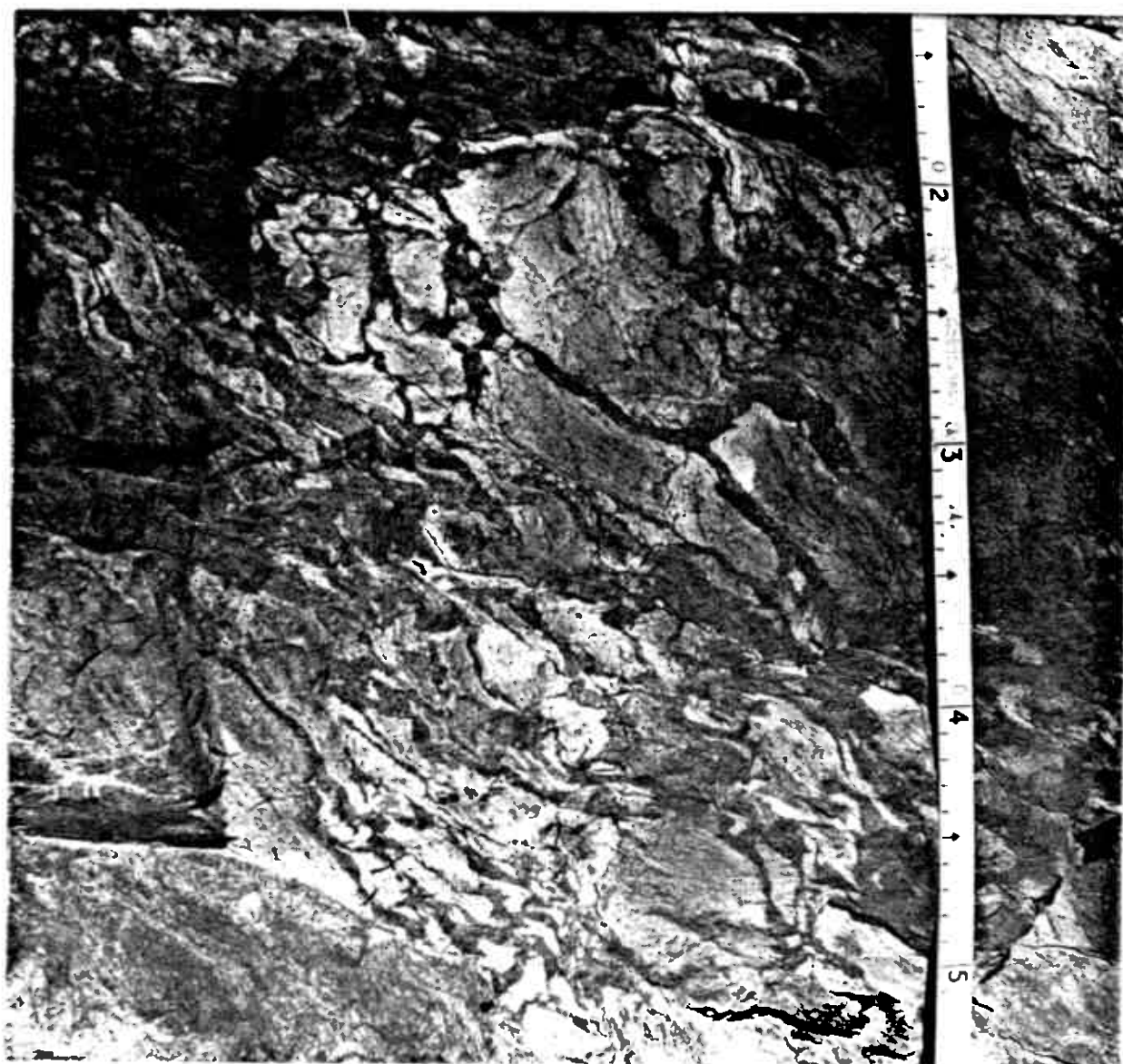


Fig.5.1-3. Angular pyrite cemented acidic breccia developed probably directly beneath the level of the massive sulphide mineralisation.



Fig. 5.1-4. Rounded fragments of pyroclastic dacite, cemented by pyrite, (same facies as fig. 5.1-3).

some fragments show more rounding Fig. 5.1-4. This breccia probably represents the path of mineralising solutions through the fragmented top of a pyroclastic dacitic flow unit.

The mineralised horizon is intimately associated with extrusive, pyroclastic acidic material, the presence of the mineralised acidic breccia suggesting the mineralised horizon immediately overlies the rhyo-dacitic pyroclastics Fig. 5.1-5. The mineralising episode also involved pervasive silicification of the immediately adjacent basalt and basaltic-andesite wall rocks. The effects are noticeable over 15 - 30 m, often with large pyritic euhedra associated with the granular quartz, but are only intense over approximately 2 m immediately adjacent to the mineralised horizon. Tectonic mobilisation of silica probably contributes to the alteration seen, but is considered, by comparison with the hydrothermal processes, to have been of minor significance.

STRUCTURE OF THE 'GJERSVIK OREBODY'

The detailed structure of the 'orebody' is very complex (see 1:200 sections), though the major structures affecting the outcrop pattern are more easily defined.

The body as a whole is contained in the lower limb of the major F_1 synformal anticline described in Ch.4.1. The interpreted structure of the 'orebody' is shown in Fig. 5.1-4, and consists of second order F_1 isoclinal closures, plunging approximately 10° to 195° , which have been refolded into an open, north-south trending, F_2 , periclinal synform, plunging gently to the south, Fig. 5.1-6. This structure effectively confines the mineralised horizon to the outcrop seen, with any immediate continuation having been eroded away. There is possibly a southerly continuation of the lower limb under the Limingen Lake, which is verified by

INTERPRETED MAJOR STRUCTURES CONTAINING THE GJERSVSK OREBODY

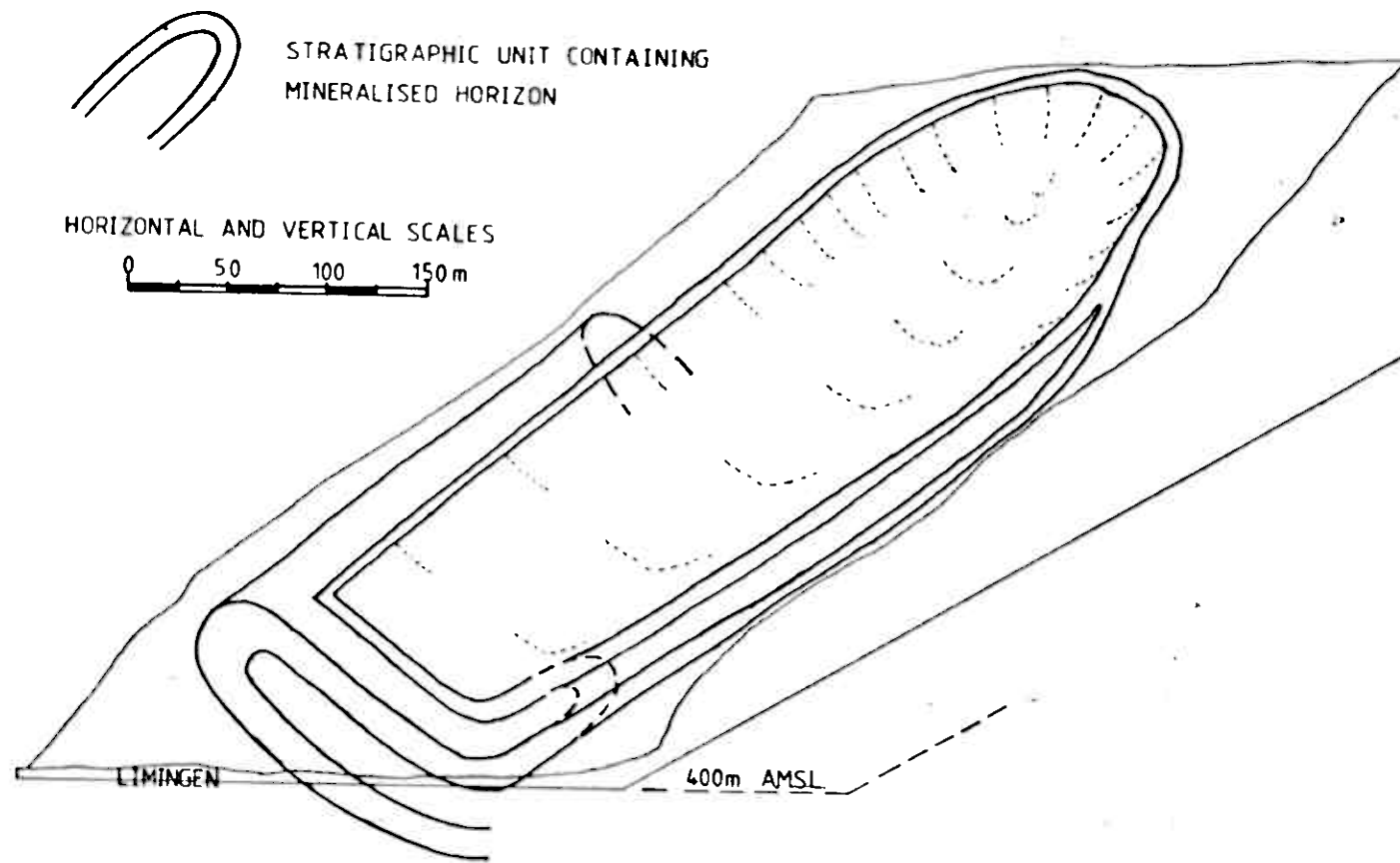


Fig51-5.

- S1 SHISTOSITY - π POLES
- △ F2 FOLD AXIS - PLUNGE
- △ " " " - □ POLE TO π CIRCLE
- S2 SHISTOSITY - π POLES

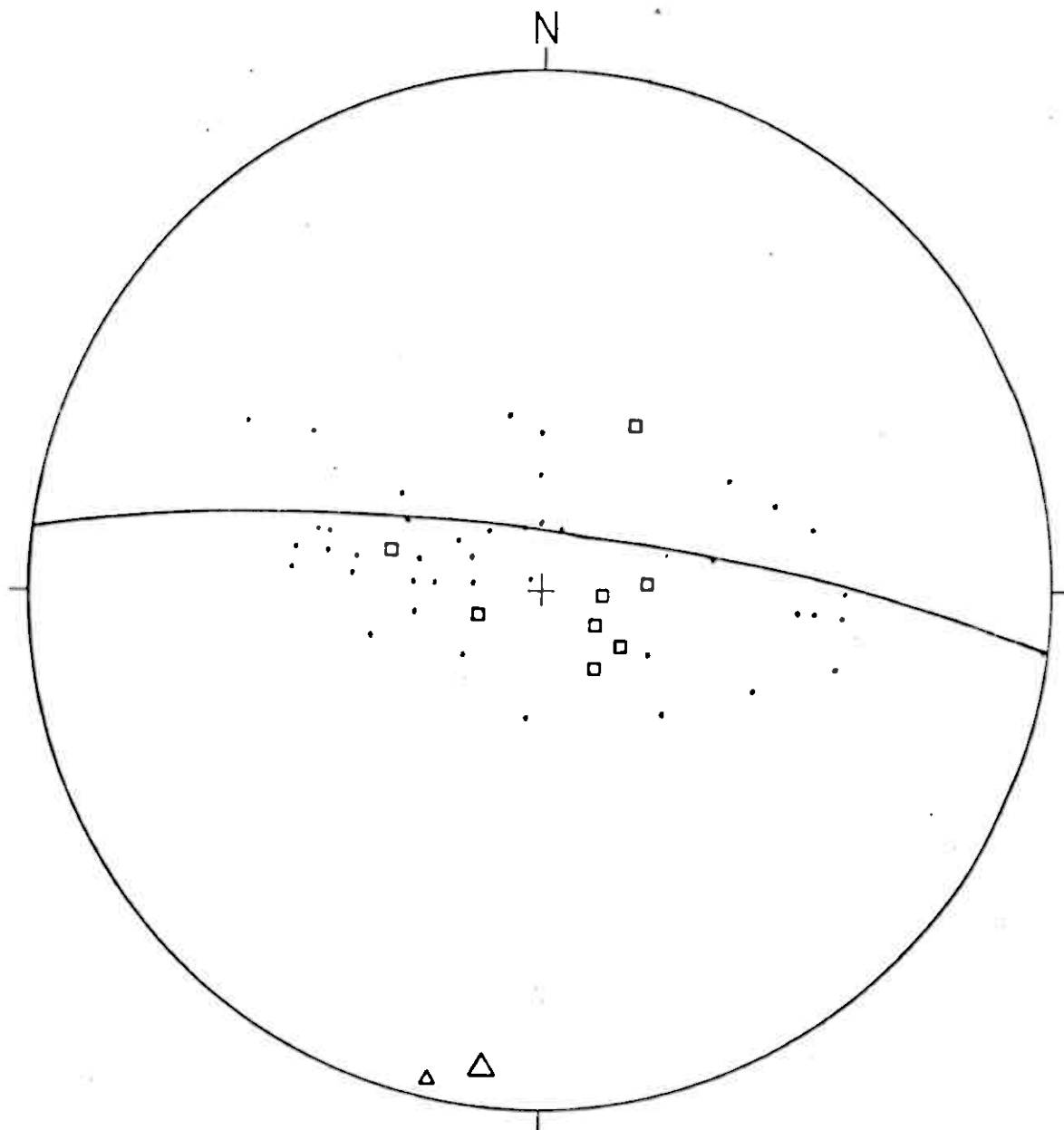


Fig.5.1-6. Structural data from area of
the "Gjersvik Orebody"
Lower hemisphere, equal area projection

the 'Turam' anomaly map of the 'orebody' area, Fig. 5.1-7.

The relatively incompetent pyrrhotitic massive sulphides may begin to deform before the more competent wall rock, thus initiating embryonic folds in these areas, which then develop into isoclinal fold closures with progressive deformation e.g. Y10 550, X764 010. The massive pyrite facies tend to deform cataclastically and probably form relatively competent bodies which become disrupted and boudinaged to form the irregular lenses and pods observed e.g. Y10 550, X764 010 (see 1:200 section).

5.2 DISSEMINATED MINERALISATION

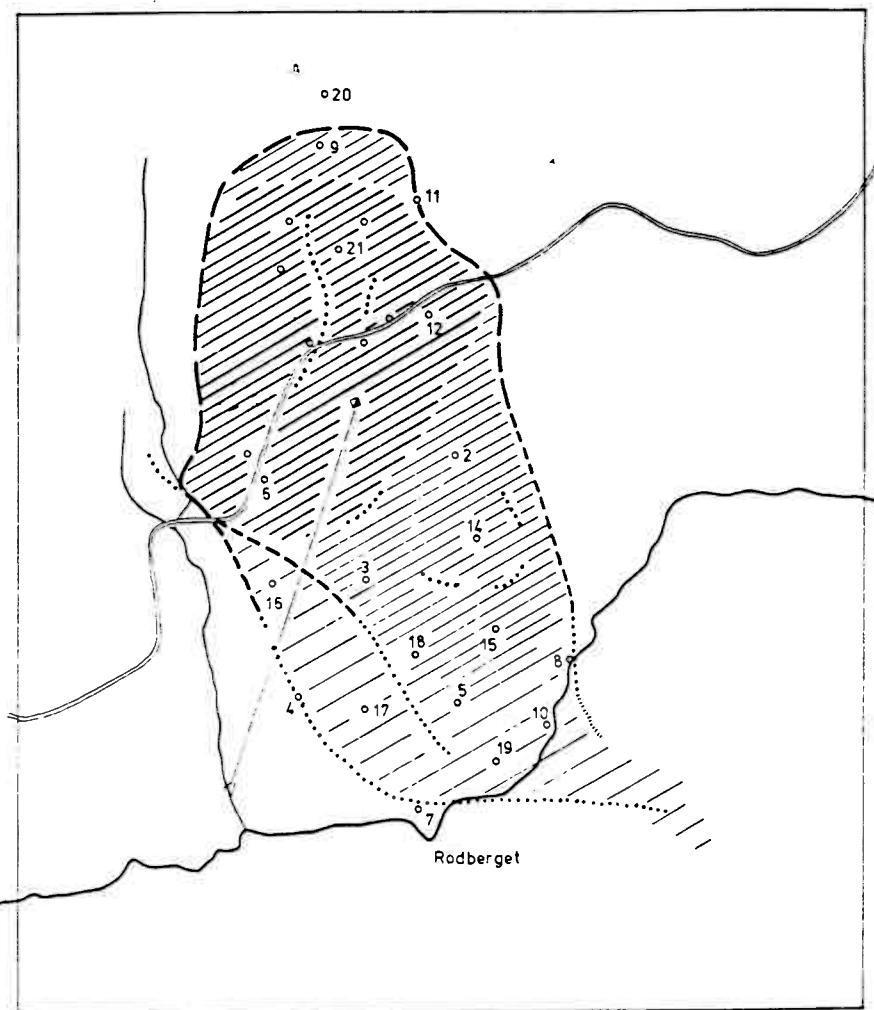
Disseminated sulphide mineralisation occurs associated with large numbers of dacitic dykes in the Lillefjell area. The acidic dykes in this area are feldspar porphyritic, and often contain biotite porphyroblasts. This suggests they are probably of sub-volcanic affinity (see Ch 3.2). No pyroclastic acidic material was recognised in this area thus supporting this interpretation. The acidic dykes cut basic stilpnomelane "greenstones", often containing magnetite and occasionally showing recognisable pillow structures.

The potentially economic mineralisation occurs mainly in the acidic dykes, though the adjacent basic "greenstones" contain similar amounts of sulphides but dominantly pyrite. The sulphide are present as fine veinlets approximately 1 - 5 mm wide, disseminated flattened irregular accumulations 1 - 30 mm in maximum dimension and dispersed euhedra of pyrite. Quartz is usually associated with the sulphides, with epidote and chlorite less commonly associated. Chalcopyrite occurs as anhedral grains 0.01 - 0.3 mm

GJERSVIK TURAM SURVEY 1:2500

GM REPORT 201

N 800



N 100

W 5300

W 4700

Fig. 5.1-7.

in size usually associated with pyrite or pyrrhotite, and less commonly as discrete grains and tends to be more concentrated in the acidic rocks where the iron sulphide is dominantly pyrrhotite, Fig. 5.2-1. This is probably due to less available iron within the acidic rocks causing the iron sulphide to crystallise as ferrimagnetic monoclinic pyrrhotite.

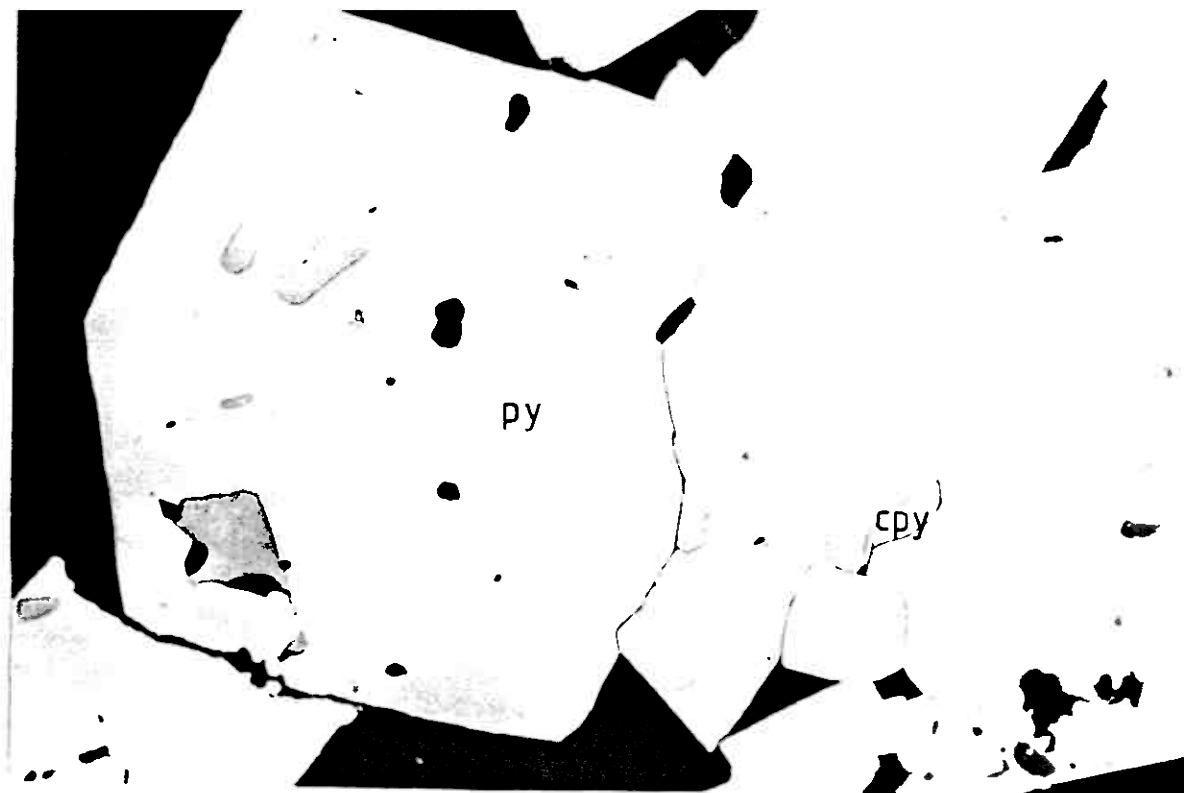
Trenches, approximately 1 m wide, blasted within this mineralisation, revealed a maximum grade of 0.1% Cu over a 5 m section which is sub-economic for this type of deposit under the present economic constraints.

5.3 PERIPHERAL EXHALITIVE MINERALISATION

Exhalites were recognised in the area to the east of the 'Gjersvik Orebody' e.g. Y10 465, X764 095 and to the north west e.g. Y11 017, X764 755. They form relatively thin horizons 5 - 15 cm thick, with sharp contacts against adjacent lithologies.

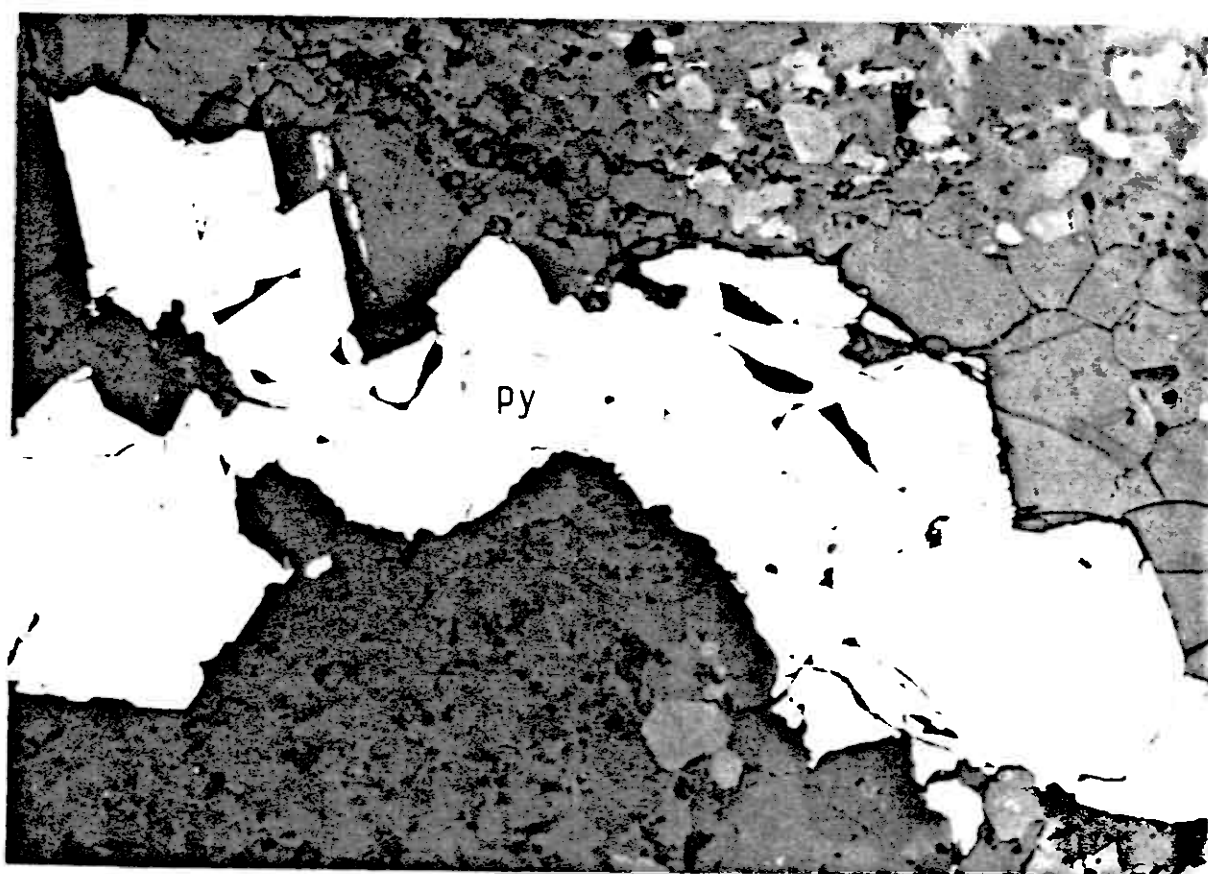
Three main facies of exhalites can be recognised:

1. Pyritic exhalites - consisting of bands of pyrite euhedra up to 3 cm in size in a dominantly recrystallised chert matrix with minor carbonate and chlorite, Fig. 5.3-1. Magnetite occurs associated with the pyrite and in magnetite rich bands, sphalerite is occasionally present. This banding probably reflects the episodic nature of emission of hydrothermal fluids onto the sea floor. In many exposures this banding is not visibly developed and the pyrite, magnetite assemblage forms as elongate 'pods' within basic greenstones.
2. Magnetite exhalites, consisting of predominantly magnetite and recrystallised chert, which form bands of lensoid 'pods' approximately 0.5 - 1 m in length.



A.

1mm



B.

0.5mm

Fig. 5.2-1. Typical pyrite(py), chalcopyrite(cpy), assemblage of disseminated mineralisation in the Lillefjell area.

A. In veinlets with calcite + quartz gangue.

B. In flattened disseminations within acidic dyke.

3. Sideritic exhalites, dominantly siderite with lesser recrystallised chert, Fig. 5.3-2, which form relatively extensive horizons 5 - 30 cm thick, continuous over up to 100 - 150 m.

The pyritic facies obviously reflects reducing conditions in the environment of precipitation. The pyritic 'pods' occur within basic lavas, suggesting this may reflect infiltration of the top of the lava pile by the hydrothermal solutions, or irregular 'niches' of reducing conditions in the lavas exposed on the sea floor. The magnetite facies form a continuum with the pyritic facies and represent more oxidising conditions in the area of deposition. The sideritic facies must have formed in an environment of high CO_2 fugacity, precipitating iron as the carbonate, probably reflecting shallow open marine conditions. The sideritic facies immediately overlies stratigraphically, extrusive pyroclastic acidic flows e.g. Y11 017, X764 755, Fig. 5.3 - 2 . Thus one may reasonably assume this represents the stratigraphic continuation of the 'Gjersvik Orebody'. Large amounts of siderite are remobilised during deformation and infill small fractures within the acidic material, Fig. 5.3-2 . It is also mobilised into late cross-cutting fractures (probably D_3 in age), where it forms linear zones of limonitic weathering e.g. Y10 840, X765 350.

Reticular networks of hydrothermal silica and pyrite are often seen in the basic lavas in the proximity of some exhalites e.g. Y10 830, X764 835 and also adjacent to the massive sulphide mineralisation e.g. Y10 570, X764 045, Fig. 5.3-3. These veins are cut by the penetrative S_1 shistosity indicating they are pre tectonic and probably associated with the period of mineralisation.

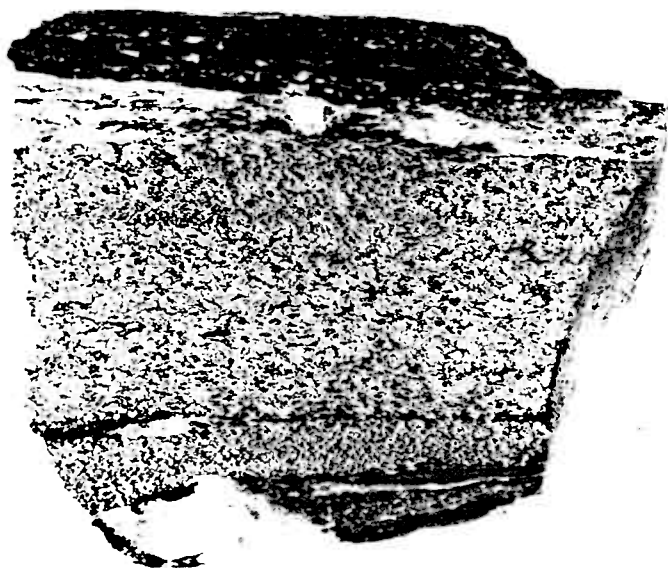


Fig. 5.3-1. Banded pyritic exhalite . Bands of pyrite and pyrite + magnetite euhedra in dominantly calcite + quartz gangue.



Fig.5.3-2. Highly leucocratic band of cherty sideritic exhalite lying structurally beneath acidic pyroclastics containing iron oxides mobilised from the sideritic horizon.



Fig. 5.3-3. Reticular network of rugose weathering, hydrothermal silica veins, developed in basic lavas near outcrop of Gjersvik Orebody.

5.4 RELATIONSHIPS BETWEEN INDIVIDUAL STYLES OF MINERALISATION

The evidence cited above suggests the massive sulphide mineralisation of the 'Gjersvik Orebody' probably formed from 'hydrothermal' solutions rich in base metals being discharged onto the sea floor and being contained by a trap, most likely a depression within the sea floor, thus confining the influence of the solutions to a relatively localised area. Reducing conditions prevailed, probably within the trap as a whole, thus giving the sulphide assemblage seen. The exhalites are probably formed from the same 'hydrothermal' solutions as the massive sulphides but as a thin dispersed 'blanket' deposit due to the lack of a containing trap for the dense solutions.

The unconfined solutions then crystallise under oxidising conditions in most cases, giving rise to the oxide and carbonate assemblages observed. The banded nature and variable composition of these extrusive bodies, suggest they are formed by accumulation over a short period of time from many pulses of 'hydrothermal' solution discharge.

The disseminated sulphide, probably sub-volcanic mineralisation of the Lillefjell area is interpreted as representing the upward path, taken by the mineralising fluids towards their point (or area) of discharge onto the sea floor. There is no evidence to suggest that the mineralising fluids responsible for the formation of the 'Gjersvik Orebody' and peripheral mineralisation emanated from the Lillefjell area, though this is a possibility.

The origin of the mineralising solutions is not clear from field relations, though several important features of the mineralisation must be borne in mind for any model postulated:

1. The exhalitive mineralisation is intimately associated with and probably immediately post dates, extrusion of rhyo-dacitic pyroclastics.
2. Disseminated sulphide mineralisation associated with large numbers of dacitic dykes probably represents the upward path taken by the mineralising fluids.
3. Pre tectonic deformation, 'hydrothermal' veinlets of quartz and pyrite in the vicinity of exhalitive mineralisation also suggests the mineralising solutions emanated from within the lava pile.

The primary sources of hot metaliferous solutions liable to produce the features described above may be envisaged:

1. Late stage hydrous volatile differentiates released from an inferred magma chamber at depth, migrating up along lines of structural weakness previously exploited by the acidic feeder dykes.
2. Hot circulating sea water within the volcanic pile, induced on a regional scale by the heat emitted from the inferred magma chamber at depth, leaching base metals from the mafic volcanic pile at depth. The base metal enriched solutions are then concentrated and circulated on a more local scale by convective systems set up by the intrusion of acidic dykes and the flow of magma along them. The metasomatic solutions migrating upwards in these areas of relatively high heat flow ultimately discharge onto the sea floor as dense metaliferous solutions.

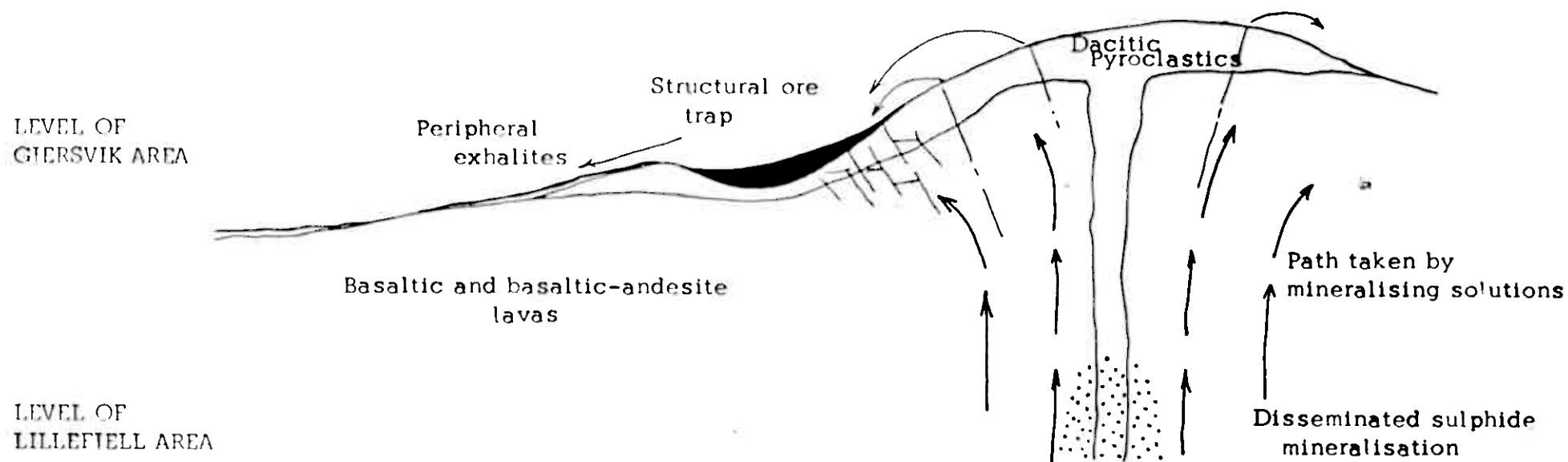


Fig 5 4-1. Diagrammatic representation of probable relationships between individual types of mineralisation in the Gjersvik and Lillefjell areas

A combination of these two sources may be the true origin of the mineralising fluids. However, it seems likely that stilpnomelane forms as a result of iron metasomatism (see Section B) and metaliferous sediments forming near the Mid-Atlantic Ridge, and the oceanic island arc environment of the East Pacific Rise are interpreted as resulting from hot circulating sea water within the volcanic pile, leaching base metals at depth, which are ultimately emitted onto the sea floor as dense metaliferous brines.^{1, 4, 4a.} Thus the second alternative is favoured as the dominant source of the mineralising solutions, though no factual evidence substantiating this interpretation can be offered.

It seems likely that the disseminated sulphide mineralisation of the Lillefjell area represents the sub-volcanic equivalent of the exhalative massive sulphide mineralisation of the 'Gjersvik Orebody'. Whether there is a direct connection between the two areas of mineralisation is difficult to ascertain, though it is possible. It is possible to trace the major D_1 synformal anticline in the Gjersvik area northwards towards the Lillefjell area. Combinations of D_2 and D_3 faulting in the area immediately south of Lillefjell Varde and D_1 thrusting, D_2 and D_3 faulting north of Lillefjell Varde destroys structural and stratigraphic continuity between the Gjersvik and Lillefjell areas.

The open D_2 periclinal synform containing the Gjersvik Orebody, plunges to the south at an angle greater than the slope of the hillside. Thus there is no immediate sub-outcrop continuation of the 'Gjersvik Orebody' outside the irregular rectangular pattern defined by the extremities of the outcropping mineralisation. There is probably a limited southerly continuation of the lower limb under the Limingen lake. There is an intimate relationship between rhyo dacitic pyroclastics and the massive sulphide mineralisation, which probably immediately post date extrusion of the pyroclastics. This association is also seen to the north of the Gjersvik Orebody where the association is between rhyo dacitic pyroclastics and sideritic exhalites. Thus a continuation of the mineralised horizon is seen on the northern limb of the major D_1 synformal anticline in the form of relatively thin exhalite horizons.

REFERENCES

1. Bignell R.D. , Cronan D.S. , Tooms J.S. (1976); Red Sea metalliferous brine precipitates.
Spec. Pap. geol. assoc. Can., no.14
2. Cann J.R. (1969); Spilites from the Carlsberg Ridge, Indian Ocean.
J. Petrol., 10, part 1, 1-19.
3. Carmichael I.S.E. , Turner F.J. , and Verhoogen J. (1974); Igneous Petrology.
Mcgraw-Hill; New York. 739p.
4. Cronan D.S. (1975); Manganese nodules and other ferro-manganese oxide deposits from the Atlantic Ocean.
J. Geophys. Res. , 80, No.27, 3831-3837.
- 4a. Frauchetau J. , Needham H.D. , Choukroune P. , Juteau T. , Seugret M. , Ballard R.D. , Fox P.J. , Normark W. , Carranza A. , Cordoba D. , Guerrero J. , Rangin C. , Boughault H. , Cambon P. , Hekinian R. (1979);
Massive deep-sea sulphide deposits discovered on the East Pacific Rise.
Nature, 277, 523-528.
5. Halls C. , Reinsbakken A. , Ferriday I. , Haugen A. , Rankin A. (1977);
Geological setting of the Skorovass orebody within the allochthonous metavolcanic stratigraphy of the Giersvik Nappe, central Norway: In volcanic processes and ore genesis.
London: Inst. Min. Metall. and Geol. Soc. , 128-151.
6. Hatch F.H. , Wells A.K. , Wells M.K. (1972); Petrology of the Igneous rocks.
Allen & Unwin; London. 551p.
7. Holtedahl O. (1920); Paleogeography and diastrophism in the Atlantic - Arctic region during Paleozoic time.
Am. J. Sci. , 49, 1-25.
8. Jones J.G. (1968); Pillow lava and pahoehoe.
J. Geol. , 76, 485-488.
9. Melson W.G. , Van Handel T.H. (1966); Metamorphism in the Mid - Atlantic Ridge, 22°N latitude.
Mar. Geol. , 4, 165-186.

10. Myashiro A., Shido F., Ewing., (1971); Metamorphism in the
Mid-atlantic Ridge near 24° and 30° N.
Phil. Trans. R. Soc. London, Ser. A, 268, 589-603.
11. ——— (1973); Metamorphism and metamorphic belts.
Allen & Unwin: London. 492p.
12. Moore J.G. (1965); Petrology of deep-sea basalts near Hawaii.
Am. J. Sci., 263, 40-52.
13. Ramsay J.G. (1967); Folding and fracturing in rocks.
Mcgraw-Hill: New York. 568p.

SECTION B.

A CHEMICAL AND MINERALOGICAL STUDY OF THE
ERUPTIVE ROCKS IN THE GIERSVIK REGION

INTRODUCTION

Representative samples of the eruptive rocks from the Gjersvik and Lillefjell areas were selected for detailed chemical, petrographic and mineralogical study.

A total of 76 samples were analysed for 20 elements using the Direct reading, plasma source, spectrophotometer and the atomic absorption spectrophotometer. Thirty - two thin sections were examined using the polarising microscope and a further nine polished thin sections were used for the analysis of selected minerals using the electron microprobe.

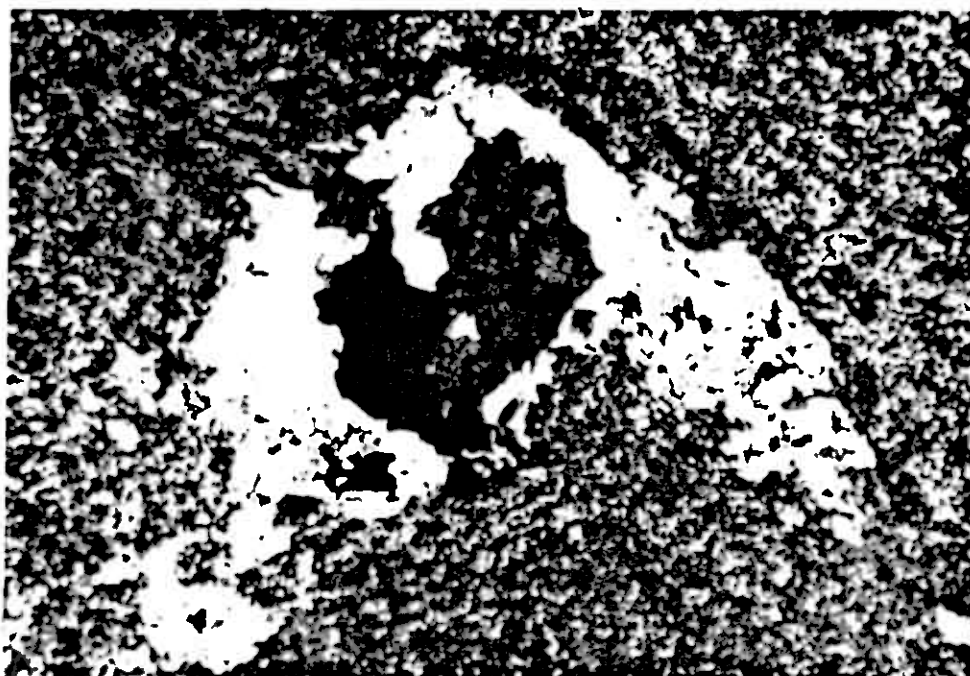
7.1 BASIC ERUPTIVES

The essential chlorite - epidote - albite - quartz mineral assemblage of the basic rocks has been described in Ch. 3.1. The content of both major and minor mineral phases is very variable and thus it is difficult to give representative modal compositions. Very fine grained albite and quartz 50-200 μm in size generally constitutes 60 - 70 % of the rock by volume, ususally as 55 - 65 % albite, 5 - 10 % quartz. Albite (almost pure, $\text{Ab} > 95\%$) probably results from the breakdown of original plagioclase feldspar, involving loss of calcium from the structure of the plagioclase which is unstable under greenschist facies metamorphic conditions. It seems likely that many of these rocks were originally of tholeiitic affinity (see below) and thus original quartz may be preserved. Quartz is also produced during many retrograde metamorphic reactions¹⁷, which probably results in the modal quartz content observed. The chlorite and epidote contents are highly variable, in both absolute and relative terms. The formation of highly chloritic 'hyalospilites' and epidote rich 'orthospilites'² has been described in Ch. 3.1. This usually results in a chemical variation, Table 7.1-1, with the orthospilites being noticeably enriched in calcium (HM159), whereas actual hyalospilites are usually more siliceous and slightly enriched in iron and magnesium. Although now totally recrystallised, chlorite is assumed to replace original ferro-magnesium phases, though it was never observed pseudomorphing an original phase. Thus the original identity of this phase is unknown but may reasonably be supposed to be a pyroxene. The more calcium rich rocks usually contain epidote as an essential component, though often ferroan calcite is the calcium phase. This obviously reflects differing physico-chemical conditions during metamorphism, probably varying $f\text{CO}_2$, $f\text{O}_2$, and/or $f\text{H}_2\text{O}$ and redistribution of calcium liberated from the breakdown of plagioclase feldspar.

The grain boundaries, particularly those between quartz and albite are irregular and grains sometimes appear to penetrate adjacent grains, suggesting a certain ammount of pressure solution along



A. PPL



B. PPL

Fig. 7.1-1. A. Folded quartz, epidote veinlet in pyroclastic dacite, with chlorite aligned along axial plane schistosity (S_1).
 B. Quartz, pyrite, epidote infilled vesicle in chloritic basic lavas, deformed by D_1 .

grain boundaries. Also, veinlets produced during alteration to greenschist facies, can be seen to be folded during D_1 , Fig. 7.1-1, suggesting the greenschist facies metamorphic mineral assemblage was formed prior to regional tectonic deformation and underwent refabrication during this episode. Thus it seems likely that the greenschist facies metamorphic mineral assemblage probably developed during the period of ocean floor metamorphism¹⁶ (O.F.M.) and was then tectonically modified during D_1 .

Representative analyses of the basic rocks are shown in Table 7.1-1. The accuracy of the analytical method employed is poor for major elements and thus many of the totals are significantly removed from 100%, even if one assumes up to 2% H_2O ¹³ and <1% P_2O_5 , CO_2 and S. However the presence of hydrated and carbonate phases may be reflected in abnormally high concentrations of dominantly CO_2 , H_2O , & S. As such absolute values must be used with some caution in any interpretation made.

Silica contents of these basic rocks are generally in the range 48 - 53 % i.e. basalts³, with some up to approximately 60 % suggesting they are basaltic andesites. However many such rocks occur near mineralised horizons and are also slightly depleted in iron, suggesting they are silicified basalts. This silicification of the wall rocks occurs immediately adjacent to mineralised horizons (e.g. HM33 - 80% SiO_2 , 10% FeO), with the more mobile iron causing iron enriched horizons 4 - 30m away from the mineralised horizon (e.g. HM34 - 46% SiO_2 , 21% FeO). Less marked enrichments in Mg, Ti and Mn also occur coupled with iron enrichment. Thus it is difficult to assess the relative importance of individual secondary processes in producing the compositions observed, particularly in the vicinity of mineralised horizons.

These basic rocks are noticeably enriched in sodium and depleted in calcium compared with 'typical' basalt analyses³ Table 7.1-1 and this confirms the spilitic affinity^{3,15,16,22} of these rocks suggested by petrographic study (Ch. 3.1). The plot of $Na_2O + K_2O$ against $(K_2O / Na_2O + K_2O) \times 100$, Fig. 7.1-2 shows that

	HM7	HM26	HM33	HM34	HM91	HM92	HM159	MH6	MH11	MH14	HM60	12
SiO ₂	50.70	49.80	75.90	46.20	58.30	62.20	49.80	56.90	58.10	54.10	54.30	50.42
TiO ₂	.91	.98	.14	.99	.54	.96	.80	1.07	.86	.92	.32	1.00
Al ₂ O ₃	11.72	12.16	5.40	13.81	11.41	11.06	12.61	13.13	12.05	12.08	11.21	13.7
FeO	12.22	14.58	10.03	20.80	13.02	8.44	9.24	12.39	12.21	14.81	11.05	12.77
MnO	.19	.26	.07	.20	.21	.14	.29	.37	.27	.19	.30	.30
MgO	4.11	4.39	3.20	5.94	3.79	2.53	3.71	3.52	3.74	3.66	4.94	5.10
CaO	4.99	2.74	.10	.11	.54	2.67	8.36	5.14	4.61	2.23	9.65	8.36
Na ₂ O	4.89	2.49	.01	.03	1.61	4.60	2.03	3.26	1.68	2.91	1.89	1.70
K ₂ O	.14	.13	.14	.59	.83	.11	.01	.52	.28	.10	.01	.40
Total	89.87	87.55	94.99	88.68	90.24	92.71	86.13	96.29	93.80	90.90	93.68	98.79
FeO:MgO	2.97	3.32	3.13	3.50	3.44	3.34	2.49	3.52	3.27	4.05	2.24	2.43

Table 7.1-1. Representative analyses of meta basalts and meta basaltic andesites from Giersvik and Lillefjell areas.

- HM7 -Stilpnomelane, biotite basalt.
HM26 -Highly pyritic basalt from near outcrop of Giersvik Orebody.
HM33 -Highly silicified, pyritic basalt from immediately adjacent to Giersvik Orebody.
HM34 -Highly chloritic, pyritic basalt from near outcrop of Giersvik Orebody.
HM91 -Highly chloritic, siliceous 'hyalospilite' with pyrite.
HM92 -Silicified basaltic andesite?, with pyrite and magnetite.
HM159 -Epidote, calcite rich 'orthospilite'.
MH6 -Stilpnomelane, pyritic basalt.
MH11 -Stilpnomelane, minor chalcopyrite and pyrrhotite bearing basalt.
MH14 -Stilpnomelane, chalcopyrite, pyrrhotite silicified basalt.
HM60 -Chloritic basalt with some pyrite.
12 -Representative modern island arc tholeiite ³ (p550, no. 4)

- - Basic rocks - Gjersvik area
- - Basic rocks - Lillefjell area
- ▲ - Acidic rocks - Gjersvik area
- - Acidic rocks east of main fracture - Gjersvik area
- △ - Acidic rocks - Lillefjell area

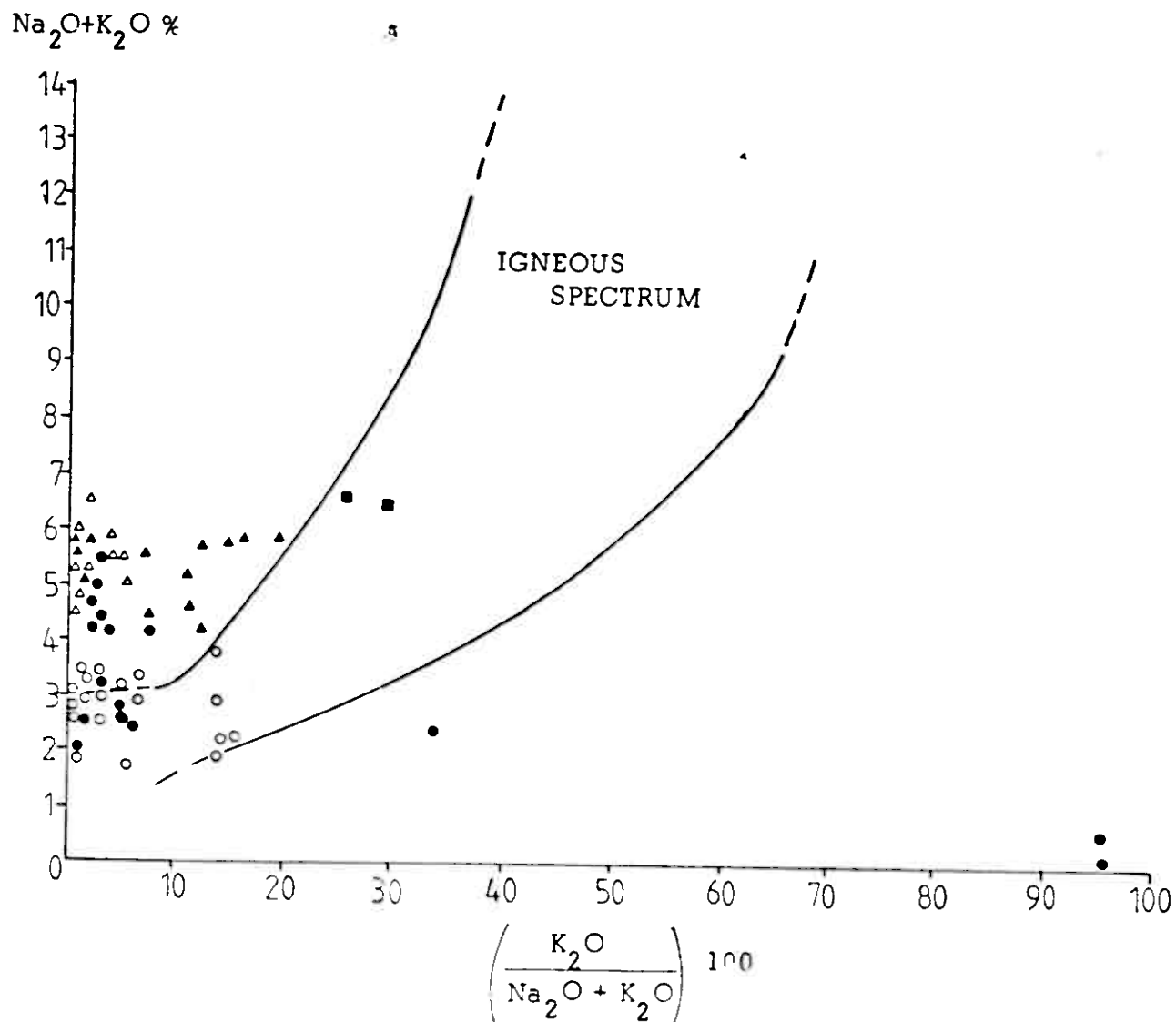


Fig 7.1-2. Plot of eruptive rocks of the Gjersvik and Lillefjell areas relative to the 'igneous spectrum' (After Hughes¹⁰)

most of the Gjersvik eruptives lie outside the 'igneous spectrum' defined by Hughes¹⁰. This also suggests the rocks have undergone post crystallisation alteration involving sodium enrichment. The basic rocks tend to plot near the region of tholeiitic basalts in this diagram, suggesting an original tholeiitic affinity.

The lack of rare earth element analyses precludes the use of incompatible element 'fingerprinting' for these rocks. Trace element data has been accumulated by Lutro¹³ from rocks in the Gjersvik area and suggests an island arc tholeiite affinity for the basic rocks of the Gjersvik Nappe as suggested above. The plot of TiO_2 against FeO/MgO , Fig. 7.1-3, for the basic rocks lie between the typical trends shown by modern island arc tholeiites and calc alkaline suites¹⁸. None of the data suggests ocean floor, continental or high alumina affinities for the basic rocks. Thus it seems likely that the original basaltic lavas developed from tholeiitic or possibly more calc alkaline magmas in an island arc environment.

7.2 ACIDIC ERUPTIVES

The major petrographic features of the acidic rocks are described in Ch. 3.2. The distinction between extrusive pyroclastic and intrusive acidic material is difficult to make from thin section examination due to the usually complete textural reconstitution which has occurred during metamorphism. Some ghost fragmentary textures are preserved and the macroscopically defined pyroclastics are often very fine grained, which, if this reflects original grain size, suggests they have cooled very rapidly. Chemically the extrusive material shows no marked difference from the intrusive material, Table 7.2-1 and thus it appears the most confident method of distinguishing intrusive from extrusive acidic material is from macroscopic textures observed in the field.

Representative analyses of the acidic rocks are given in Table 7.2-1.

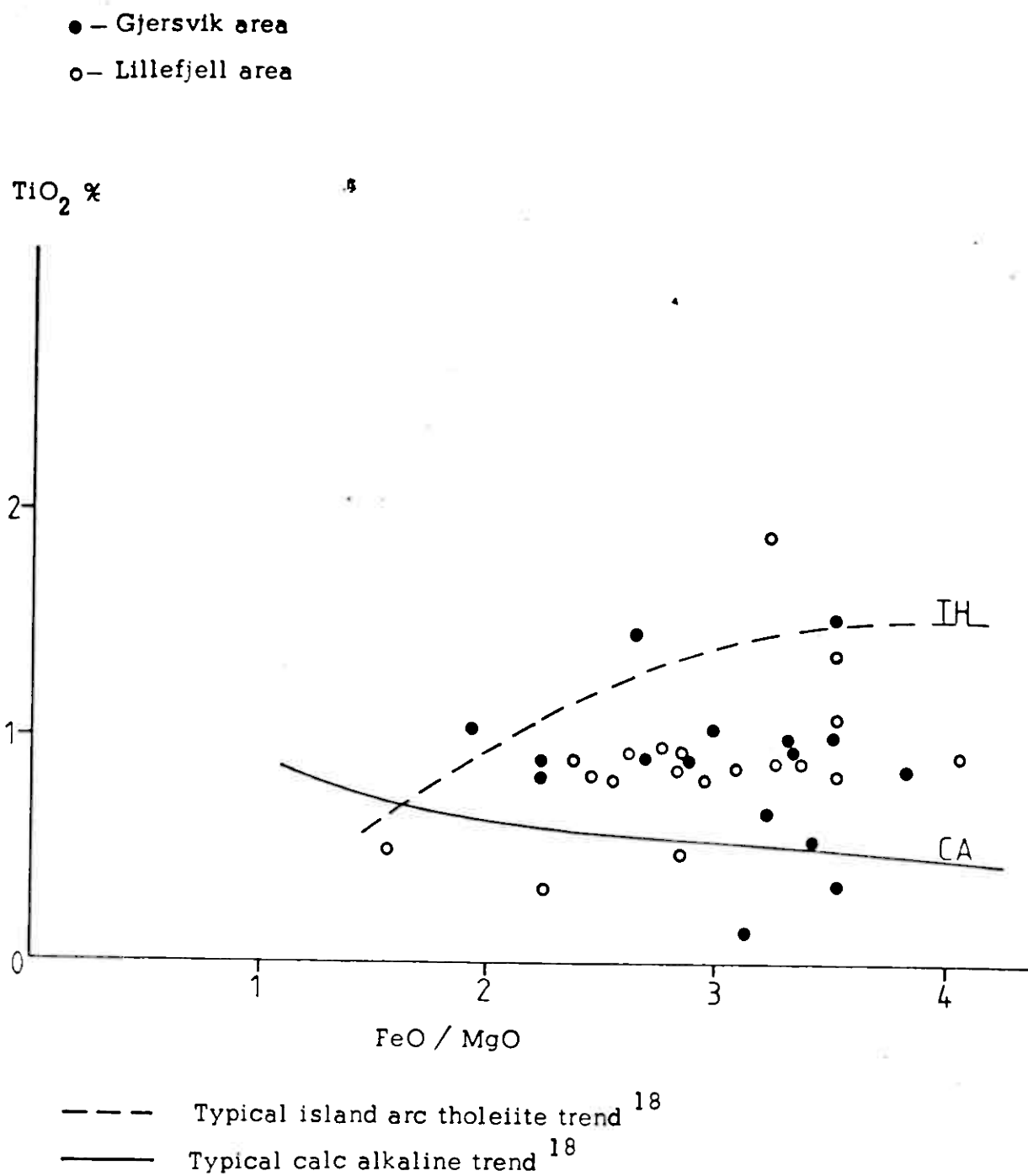


Fig 7.1-3. Trend of meta basalts and meta basaltic andesites from Gjersvik and Lillefjell areas relative to modern island arc suites (after Myashiro, 1974).

	HM9	HM75	HM102	HM105	HM110	HM150	MH3	MH5	MH10	HM61	11
SiO ₂	84.20	81.90	81.90	72.70	74.60	85.70	84.20	77.60	79.90	75.90	67.23
TiO ₂	.28	.25	.07	.41	.25	.24	.29	.25	.30	.33	.34
Al ₂ O ₃	9.01	9.12	9.22	8.89	9.93	9.68	7.86	10.10	7.43	9.39	15.12
FeO	3.81	4.41	4.69	5.91	3.93	3.92	3.51	4.51	4.81	5.56	3.5
MnO	.06	.15	.04	.14	.04	.05	.10	.10	.05	.05	.09
MgO	.78	.78	.85	2.09	.80	.62	.48	.60	.46	.87	2.02
CaO	1.57	.59	.50	.38	.21	1.23	1.90	2.11	.73	.80	4.25
Na ₂ O	4.89	4.56	4.09	4.18	4.40	4.97	5.26	5.30	5.20	4.83	3.55
K ₂ O	.98	.61	.54	.36	2.35	.08	.26	.25	.04	.29	2.20
Total	105.67	102.47	101.91	95.11	96.50	106.50	103.95	100.83	98.93	98.01	98.30
FeO:MgO	4.89	5.65	5.49	2.83	4.94	6.30	7.29	7.55	10.36	6.38	1.59

Table 7.2-1. Representative analyses of acidic rocks from Gjersvik and Lillefjell areas.

- HM9 -Silicified?, stilpnomelane rhyo-dacite pyroclastic.
- HM75 -Silicified?, stilpnomelane rhyo dacite pyroclastic - Gjersvik Orebody area
- HM102 -Pyrite, arsenopyrite rhyo dacite pyroclastic? - Gjersvik Orebody area.
- HM105 -Dacitic pyroclastic - Gjersvik Orebody area (hanging wall).
- HM110 -Biotite, feldspar porphyritic intrusive dacite - East of main fracture, Gjersvik area.
- HM150 -Stilpnomelane, intrusive dacite - Gjersvik area.
- MH3 -Silicified, stilpnomelane pyrrhotite, chalcoppyrite intrusive rhyo dacite? - Lillefjell area.
- MH5 -Pyritic intrusive rhyo dacite - Lillefjell area.
- MH10 -Pyritic, pyrrhotite, chalcoppyrite rhyo dacite - Lillefjell area
- HM61 -Biotite, pyrrhotite, chalcoppyrite dacite - Lillefjell area.
- 11 -Modern island arc dacite ³ (p554, no.4)

The silica analyses indicate dacitic, rhyo dacitic or rhyolitic³ compositions for these rocks. As in the basic rocks secondary silica may be introduced during mineralisation thus producing the apparently rhyolitic compositions of some of these rocks. The acidic rocks are enriched in Na_2O and impoverished in CaO and K_2O relative to modern island arc dacites and rhyo dacites³ Table 7.2-1, consistent with the basic rocks. This confirms the spilitic affinity suggested by previous observations. Myashiro et. al.¹⁶ suggested that spilitic suites produced during ocean floor metamorphism (O.F.M.) result from metasomatic replacement by circulating sea water within the volcanic pile. This is considered to be the most likely process from which the spilitic chemistry of these rocks resulted. Most of the acidic rocks lie outside the igneous spectrum¹⁰, Fig.7.1-2, also suggesting secondary sodium enrichment.

The acidic rocks to the East of the major N.N.E. - S.S.W. trending fault (e.g. Y10 760, X765 000) which are interpreted as being deeper in the volcanic pile than those to the West of the fracture, show an apparent substantial enrichment in K_2O , though the other major element chemistry is not significantly different. It is not clear whether this represents a primary enrichment, less intense mobilisation of potassium during O.F.M. or selective enrichment due to crystallisation of biotite at this level during O.F.M.. The similarity of the compositions of these rocks with unaltered dacites and rhyo dacites Table 7.2-1 and the fact that these rocks lie within the 'igneous spectrum'¹⁰ Fig.7.1-2, suggests that these rocks have undergone relatively little potassium leaching during O.F.M.. In the Lillefjell area which probably represents a similar structural level, the acidic rocks show very low K_2O contents (Table 7.2-1, Appendix 1). This would suggest that potassium has been leached from these rocks probably by hydrothermal - metasomatic solutions during mineralisation (Ch.8.5).

Stilpnomelane occurs in two forms: a ferrous iron rich variety :- ferrostilpnomelane and a ferric iron rich variety:- ferristilpnomelane¹. The use of the term stilpnomelane refers to the mineral group as a whole when a distinction between the two forms is unnecessary.

8.1 FIELD OCCURRENCE

Stilpnomelane occurs in both acidic and basic rocks, though it is more widespread and usually more abundant in the basic rocks. It forms large, light green, dark green or brown irregular brittle platy crystals 0.5 - 1.5 mm in maximum dimension, showing no obvious relationships with existing fabrics in the rock. Magnetite is commonly associated with stilpnomelane and also biotite when it occurs and very stilpnomelane rich horizons are often also strongly magnetic. The stilpnomelane bearing rocks tend to occur in areas with large numbers of acidic dykes and stilpnomelane concentrations can often be seen to decrease away from a particular intrusive body e.g. Y10 780, X765 400. This correlation with acidic dykes is very noticeable and is a major consideration when defining the genesis of the stilpnomelane. The occurrence of stilpnomelane in a particular area is often patchy on varying scales from centimetres to ten's of metres. This may be reflected by completely stilpnomelane free areas within otherwise stilpnomelane rich lavas, or just by areas which are relatively impoverished in comparison with the surrounding rocks. This local patchy development of stilpnomelane is not as common in the acidic rocks. Stilpnomelane bearing acidic rocks usually occur in areas where the basic rocks are fairly stilpnomelane rich. Though not all acidic dykes/sills within stilpnomelane bearing basic rocks contain stilpnomelane.

In the region around the outcrop of the 'Gjersvik Orebody' (see Ch.5.1) Y10 000-11 000, X764 000 - 764 500 stilpnomelane

is only present in isolated exposures well away from the mineralised horizon. In these areas pyrite is a common accessory mineral where it forms large euhedra up to 3mm in size. It occurs in the main body of the rock, associated with quartz, in veinlets and occasionally infilling vesicles. The pyrite content of the eruptives tends to decrease away from the mineralised horizon, but is still noticeable to a distance of 150m structurally. In the Lillefjell area stilpnomelane (and to a lesser extent biotite) occurs in mineralised rocks containing abundant pyrite, pyrrhotite and chalcopyrite, though it does not usually occur in very heavily mineralised areas.

Biotite occurs mainly in acidic rocks, but also in basic rocks to the East of the main N.N.E. - S.S.W. fracture in the Gjersvik area and to a limited extent in the Lillefjell area. It occurs as large green platy crystals 0.3 - 1 mm in maximum dimension dispersed throughout the rock. It is often difficult to distinguish biotite from stilpnomelane in hand specimen but is distinctive in thin section. Biotite bearing lithologies are not usually as rich in biotite as stilpnomelane in stilpnomelane bearing lithologies. As stated above magnetite is commonly associated with the biotite in these rocks. In the Lillefjell area, recognisable biotite bearing lithologies occur 100 - 200m to the east of the stilpnomelane bearing lithologies. Unfortunately the area was not studied in sufficient detail to ascertain the cause of this. The presence of biotite has been interpreted as representing higher metamorphic grade in the rocks (Ch.3.2) and it is probably unstable at the higher structural level where stilpnomelane occurs. Chlorite can be seen pseudomorphing biotite at Y10 850, X764 050 (HM 7) thus supporting this interpretation.

8.2 RELATIONSHIPS BETWEEN FERRO AND FERRI-STILPNOMELANE

In the field it is sometimes possible to see samples with a core of light green ferrostilpnomelane surrounded by dark green ferristilpnomelane, Fig.8.2-1. This would suggest that ferri-stilpnomelane forms from supergene oxidation of ferrostilpnomelane and this interpretation is supported by other workers ^{1,7,19}. In thin section the transition between green pleochroic ferrostilpnomelane and brown pleochroic ferristilpnomelane usually occurs over less than 10mm. In some samples (e.g. YH70B) a transition zone occurs between the two end members Fig.8.2-2. This transition zone has an intermediate composition (see Ch.8.4) and a dark irregular form. Ferristilpnomelane often occurs in what are otherwise unweathered rocks, suggesting that ferrostilpnomelane is very unstable in the supergene environment and readily oxidises to ferristilpnomelane.

8.3 TEXTURAL AND CRYSTALLOGRAPHIC FEATURES

Stilpnomelane occurs as lath like crystals c.0.3 - 1.5 mm in length and 0.01 - 0.05 mm wide, Fig.8.3-1, occasionally showing a platy habit when cut parallel to 001. The crystals do not show well - developed crystallographic faces, but are somewhat irregular, obviously influenced by adjacent grains. Stilpnomelane also occurs in fine veinlets up to 2mm wide. The veinlets consist predominantly of stilpnomelane and epidote with minor quartz and chlorite, Fig.8.3-2. These veinlets can be seen to cut pure epidote veinlets in some exposures and thus post - date them. The stilpnomelane crystals tend to grow with their long axes perpendicular to the veinlet walls, though towards the centre of wider veinlets the orientation becomes more random. The stilpnomelane laths in the body of the rock tend to show no preferred orientation and cut all existing textures and fabrics. This suggests that the growth of stilpnomelane post dated the formation of the tectonic fabrics and has strong crystalloblastic tendencies, Fig.8.3-3. Stilpnomelane commonly forms radiating crystal aggregates, Fig.8.3-4. This radiating form

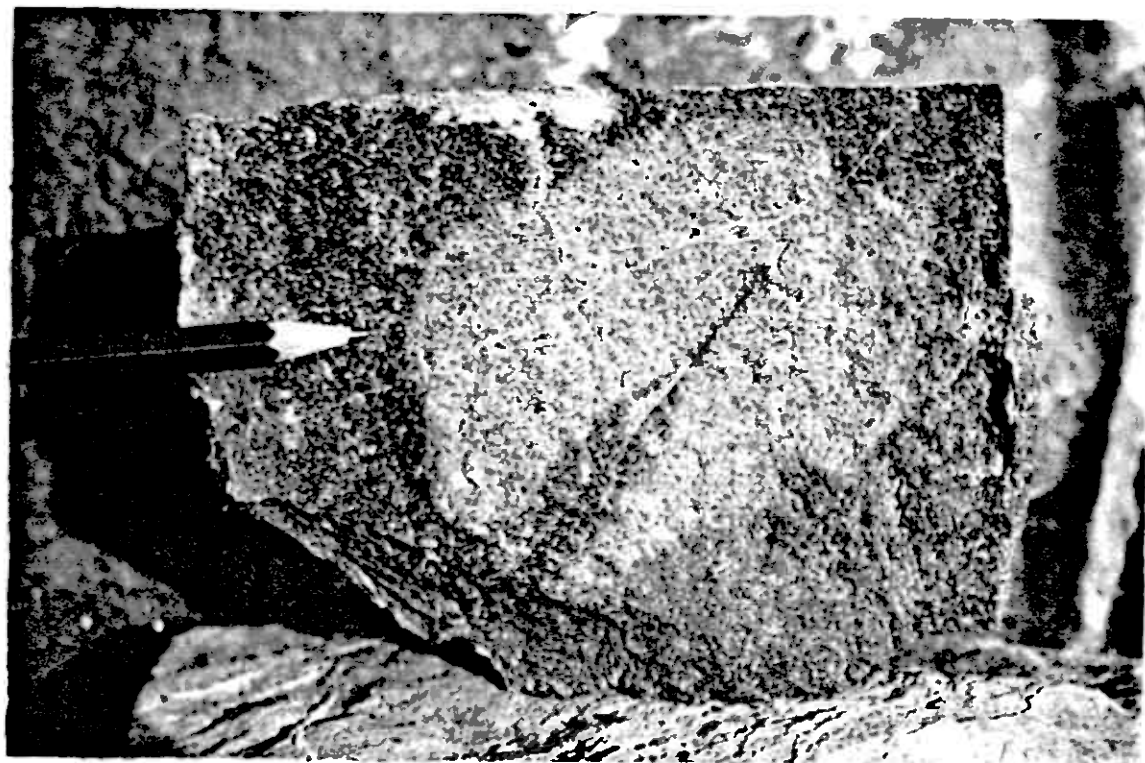
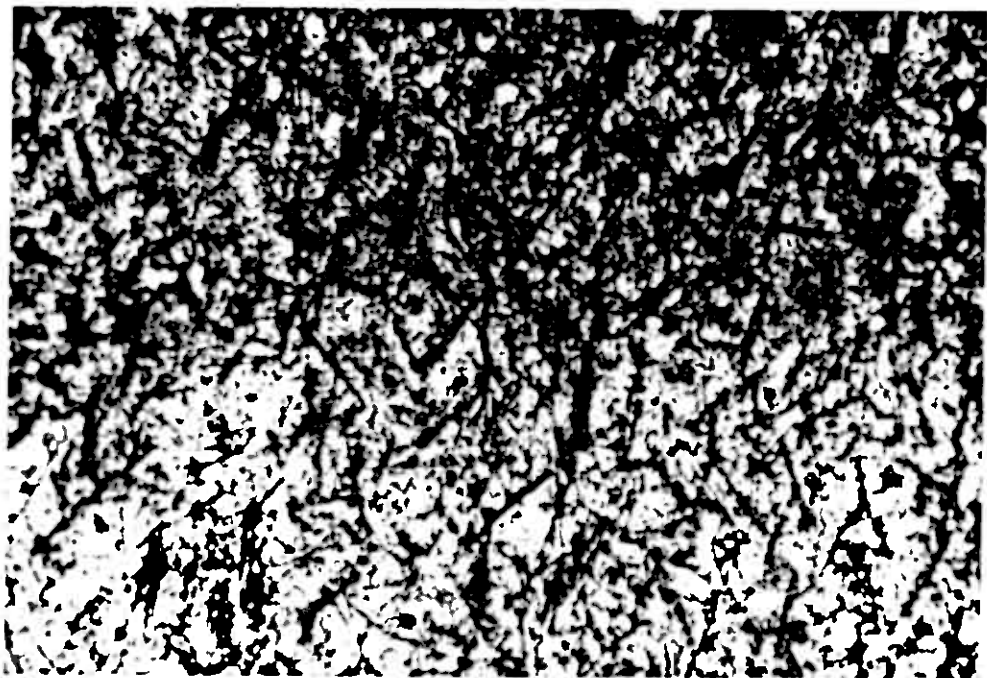
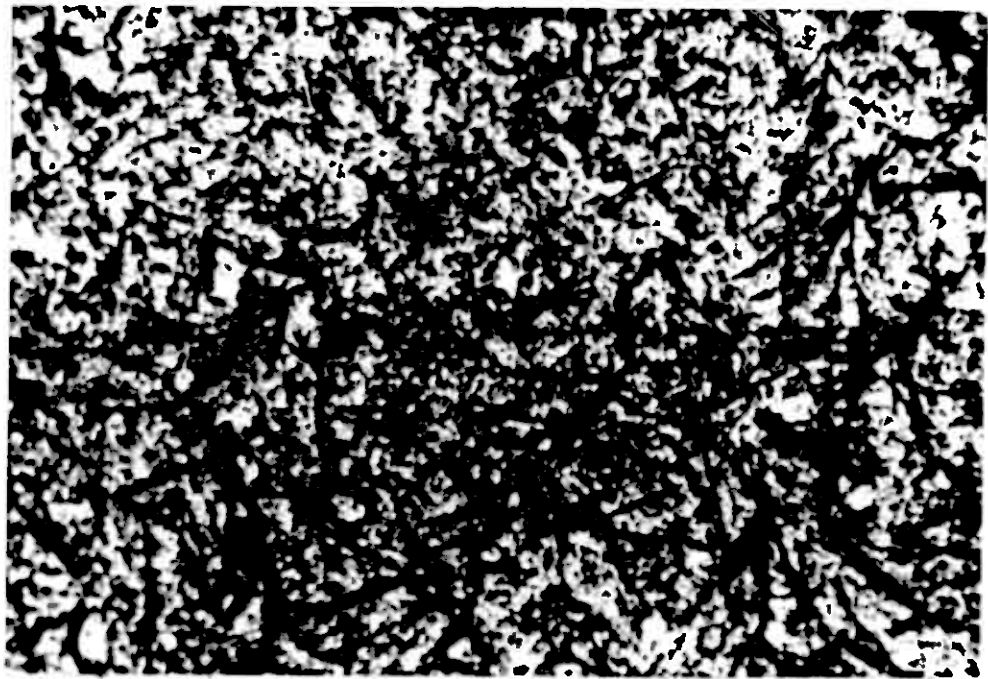


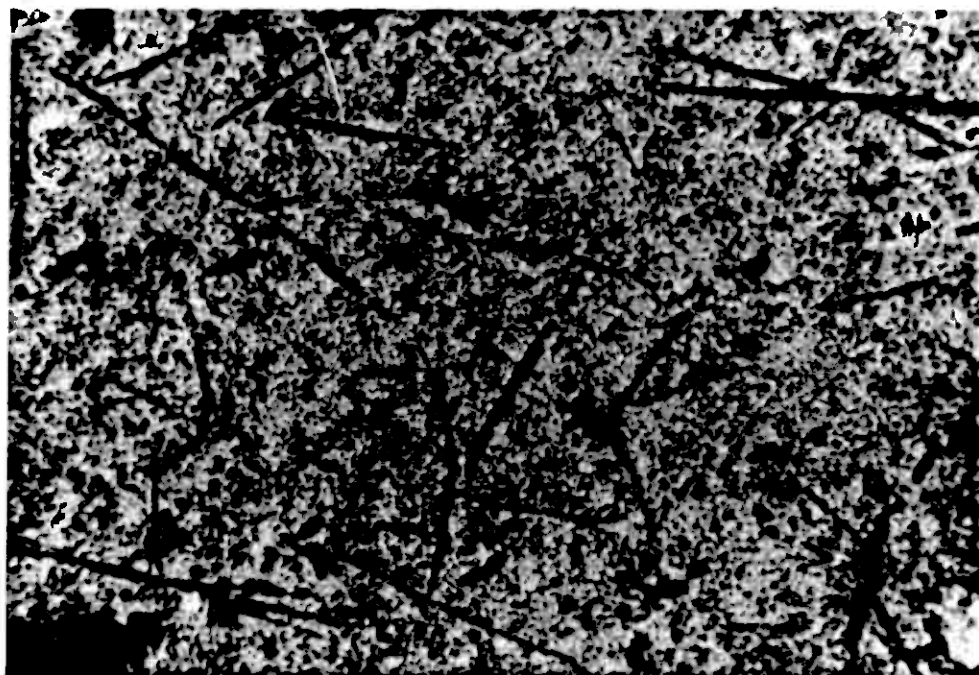
Fig8.2-1. Core of green ferrostilpnomelane surrounded by weathered ferristilpnomelane developed in meta basalt from the Lillefjell area.



PPL

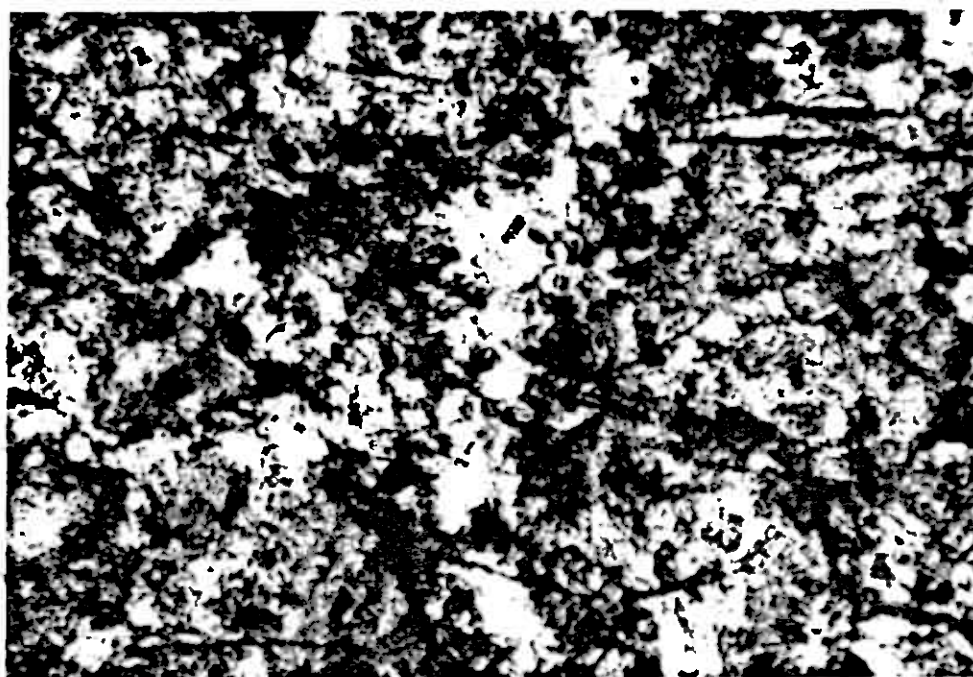
1mm

Fig.8.2-2. Transition from green ferrostilpnomelane (top) to a transitional phase (middle), to brown ferristilpnomelane (bottom). (specimen YH70B).



A. PPL

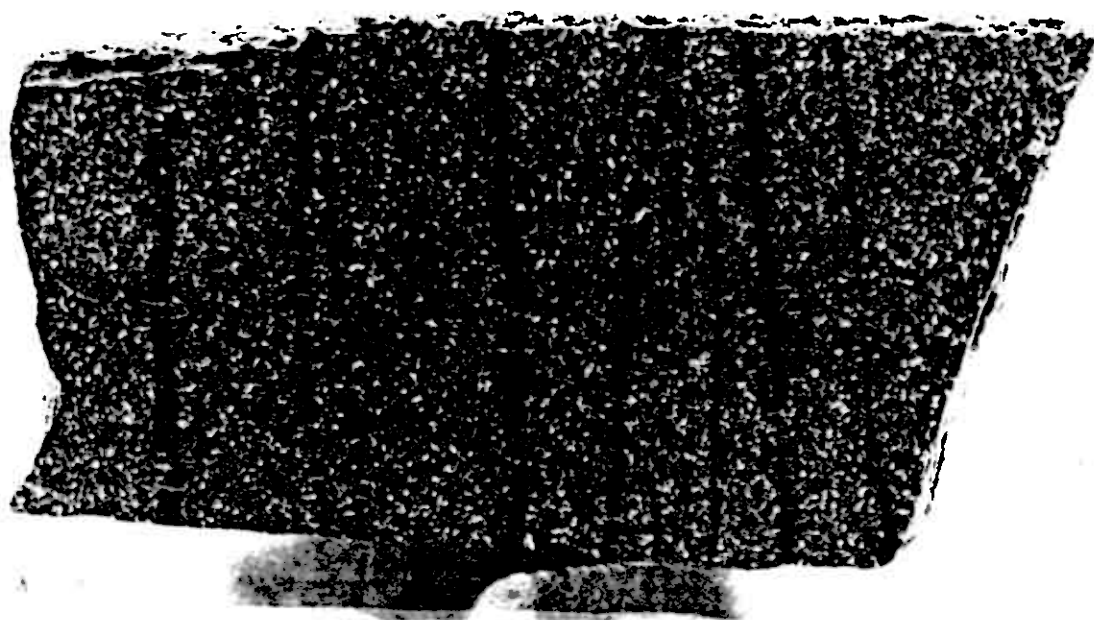
1mm



B. PPL

250 μ m

Fig. 8.3-1. A. Needles of green ferrostilpnomelane in intrusive meta dacite. (specimen HM150).
B. Brown ferristilpnomelane in typical meta basalt from the Gjersvik area. (specimen HM122).



A.

1cm



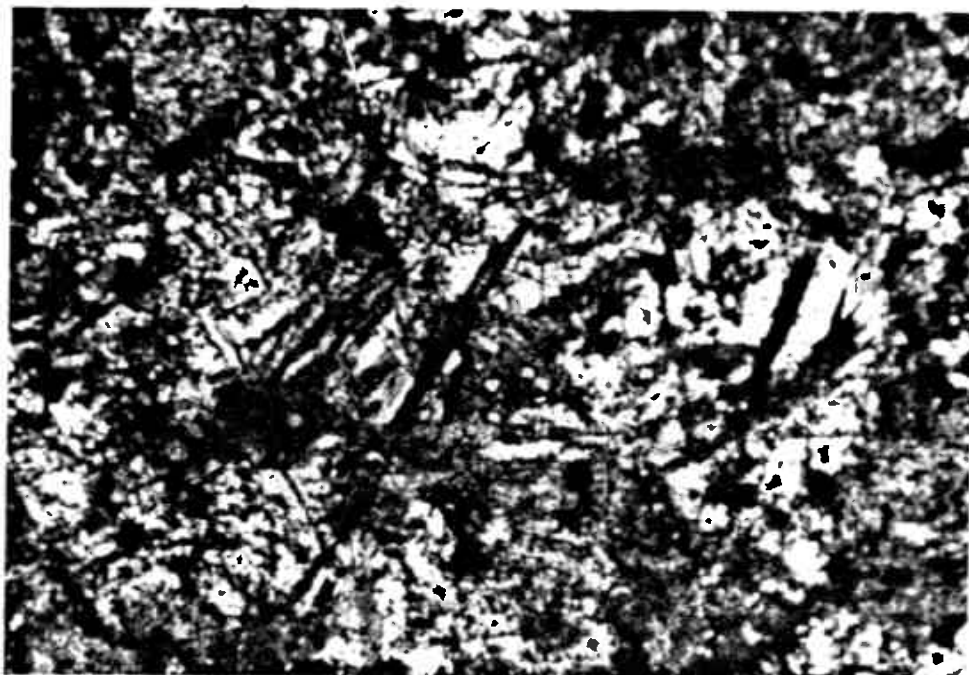
B. PPL

1mm

Fig. 8.3-2. Veinlets of brown ferristilpnomelane and epidote cutting basic lavas - Lillefjell area (specimen YH18B).

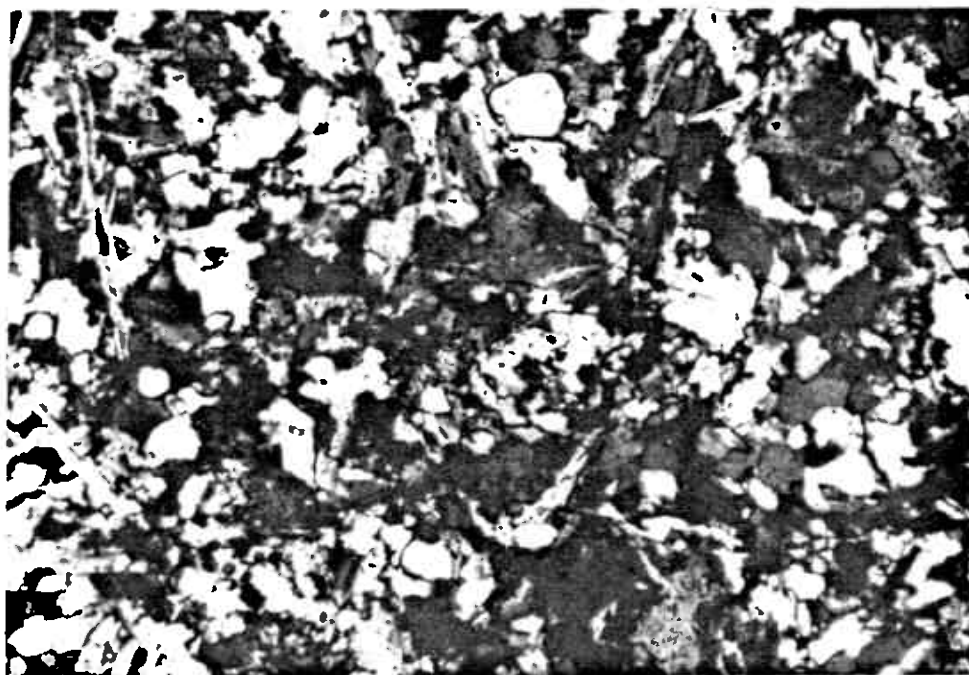
A. In hand specimen.

B. In thin section.



A. PPL

250μm



B. XN

250μm

Fig.8.3-3. Needles of stilpnomelane cutting pre existing textures and fabrics.

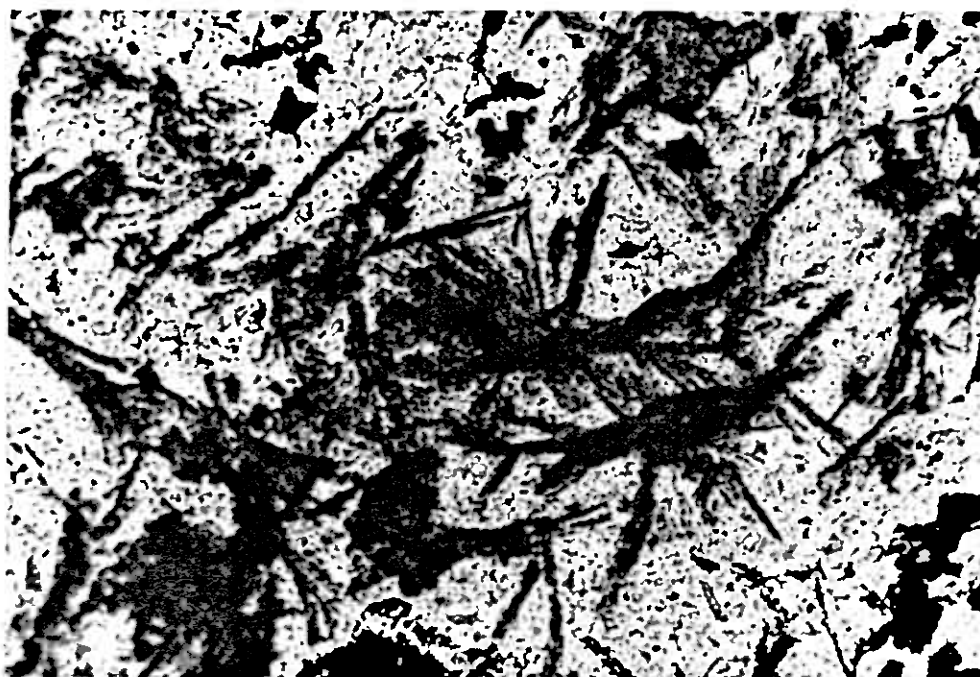
A. In meta basalt (specimen HM37).

B. In meta dacite (specimen HM39).



A. PPL

100 μ m



B. PPL

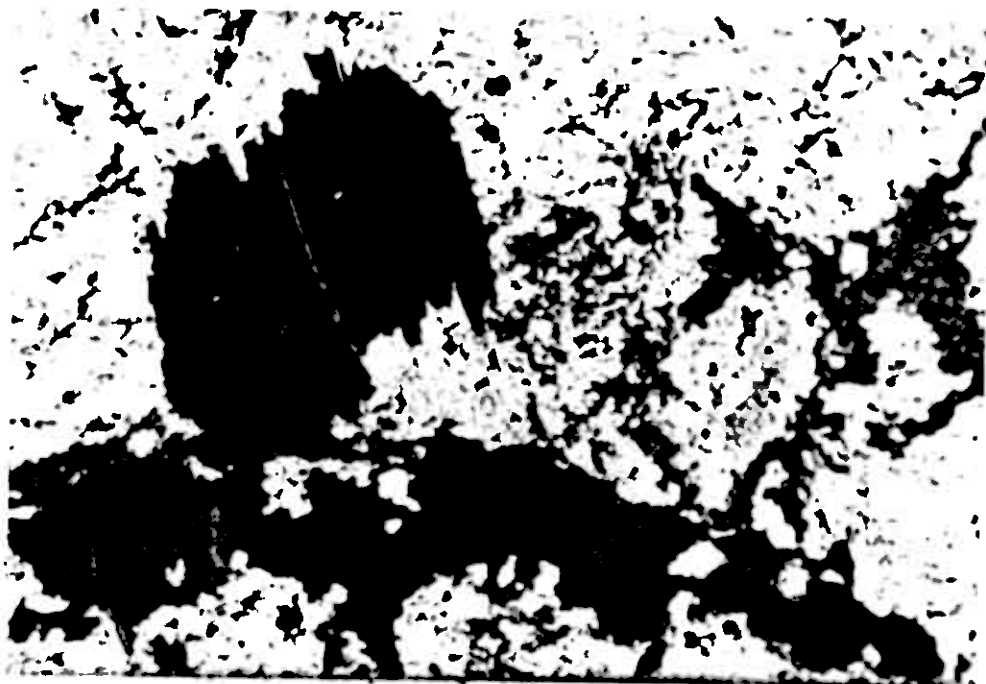
250 μ m

Fig. 8.3-4. Radiating crystal accumulations of (ferri) stilpnomelane developed in meta dacite from the Gjersvik area.

consists of two or more crystals, sometimes cutting at a common point or sometimes displaying multiple intersections. The acute angle between the two extreme crystals of the aggregate rarely exceeds 60° and is commonly less. The reason for this is not known but it is frequently observed in stilpnomelane bearing rocks.

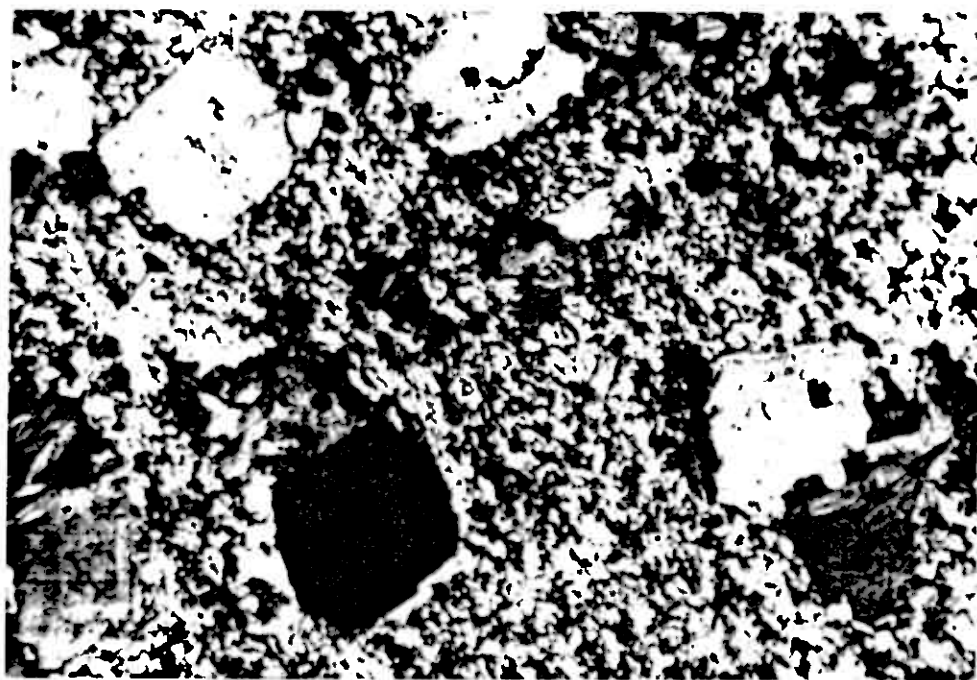
Biotite forms as large platy crystals 0.5 - 1.5 mm in size occasionally with a pseudo - hexagonal morphology, but usually it displays a more 'ragged' morphology, Fig.8.3-5. A light brown - dark brown pleochroic variety, Fig.8.3-5 a. occurs in the probably slightly higher metamorphic grade rocks, whereas a light brown - dark green pleochroic variety often showing partial or complete alteration to chlorite along 001 occurs in the slightly lower grade rocks, Fig.8.3-5 b. As with stilpnomelane, the biotite when elongate shows no preferred orientation and cuts all existing textures and fabrics within the rock, Fig.8.3-6, 8.3-5 b. This again suggests that biotite was the last phase to crystallise in these biotite bearing rocks.

Magnetite porphyroblasts are commonly associated with both biotite and stilpnomelane, Fig.8.3-5, though in stilpnomelane bearing rocks the magnetite tends to be finer grained. This generation of magnetite is much larger and more euhedral than the very fine grained, anhedral accessory magnetite found in the groundmass of many of these rocks and appears to be linked with the formation of both stilpnomelane and biotite where it occurs. Biotite and stilpnomelane have only been seen to coexist in one locality (Y10 850, X764 050, HM7) and here the biotite is pseudomorphed by chlorite. No cross - cutting textures were observed between these two phases and they appear to have formed concurrently and to have existed in equilibrium.



A. PPL

1mm



B. PPL

1mm

Fig. 8.3-5. A. Irregular crystals of light brown - dark brown pleochroic biotite in porphyritic meta dacite from the Lillefjell area. Note the presence of secondary magnetite (opaque).
B. Light brown - dark green pleochroic biotite from the Giersvik area (again with magnetite porphyroblasts).



XN

1mm

Fig.8.3-6. Elongate brown pleochroic crystals of biotite cutting all pre existing textures within intrusive meta dacite - Lillefjell area (specimen HM61).

No obvious systematic chemical enrichment or depletion in absolute terms, is seen in analyses of stilpnomelane or biotite bearing rocks (Table 7.1-1, 7.2-1, Appendix 1) which distinguishes them from similar non - stilpnomelane or biotite bearing lithologies. The biotite bearing rocks in the Gjersvik area do show a very marked enrichment in K_2O (see Ch.7.2) containing 1.7 - 2.3 % K_2O , compared with e.g. 0.5% K_2O in non - biotite bearing lithologies. However in the Lillefjell area biotite bearing rocks show no such enrichment, containing a maximum of 0.3% K_2O (HM61). Stilpnomelane bearing basic rocks show a higher FeO:MgO ratio compared with purely chloritic basic rocks. The stilpnomelane bearing rocks generally have an FeO:MgO ratio of 2.9 - 3.5 whereas the chloritic rocks have FeO:MgO ratios of c. 2.2 - 2.7. Lithologies rich in pyrite and/or magnetite also show FeO:MgO ratios in the same range as the stilpnomelane bearing rocks, e.g. pyrite bearing basic rocks from the area of the 'Gjersvik Orebody'. The iron enrichment with respect to magnesium is thus not a unique feature of stilpnomelane bearing rocks, but does appear to be coupled with the crystallisation of an iron rich phase. The acidic rocks do not show any obvious correlation between FeO:MgO ratios and the crystallisation of stilpnomelane or biotite. However all the acidic rocks have very high FeO:MgO ratios compared with modern island arc dacites and rhyo dacites ³ Table 7.2-1.

The presence of relatively high FeO:MgO ratios in the basic rocks containing secondary stilpnomelane (or biotite) and/or magnetite and/or pyrite seems to suggest iron enrichment in areas where these minerals occur. The irregular distribution of these enriched horizons and their strong correlation with acidic dykes (see Ch.8.1) would suggest that this iron enrichment is not a primary feature and is more likely to be linked to a secondary introduction of iron or alternatively removal of magnesium, though the former seems more likely. Chemical enrichment is obviously

not the only factor governing the formation of stilpnomelane and ultimately other physico - chemical parameters must govern the nucleation and crystallisation of stilpnomelane and biotite, pyrite and magnetite. These parameters are not obvious from the present studies, though the nature of the phases which apparently nucleate in preference to stilpnomelane i.e. magnetite and pyrite, would suggest that the relative fugacities of O_2 and S are probably the major controls.

8.5 CHEMISTRY OF STILPNOMELANE AND BIOTITE

Electron microprobe analyses of stilpnomelanes, biotites and chlorites were obtained using a Cambridge Geoscan 5 instrument coupled to an energy dispersive analysis system. Standards similar in composition to the minerals analysed were used for calibration, with regular checks for current drift of the electron beam during operation. The complete set of analyses are given in Appendix 2. Total iron is calculated as FeO except in analyses of ferristilpnomelanes where it is calculated as $Fe_2O_3 \cdot H_2O$. H_2O cannot be analysed with the electron microprobe and to a first approximation the H_2O content can be assumed to equal: 100% - Total Oxide analysis.

Representative analyses of stilpnomelanes and biotites are given in Tables 8.5-1 a and b respectively. It can be seen from Table 8.5-1 a, that the transition from ferro to ferristilpnomelane does not only involve oxidation of the ferrous iron to the ferric state. Most of the potassium is lost from the lattice and there is an apparent increase in hydration, though there is no apparent decrease in total iron. Otherwise the chemistry does not change within the limits of statistical and analytical error. The loss of potassium ions, presumably from inter-layer sites, is probably due to the increased positive charge caused by oxidation of Fe^{2+} to Fe^{3+} in octahedral sites causing an excess positive charge in the octahedral sheet and an overall charge imbalance.

	YH70B		HM45A		HM7	101
	Ferro	Trans.	Ferri	Ferro	Ferro	Ferri
SiO ₂	44.19	47.34	44.96	45.48	48.29	46.40
TiO ₂	tr	tr	tr	tr	tr	tr
Al ₂ O ₃	6.50	6.43	6.45	6.45	7.52	6.01
FeO ^a	25.21	24.82	—	25.41	23.78	—
Fe ₂ O ₃ ^b	—	—	28.49	—	—	24.74
MnO	1.27	1.33	1.35	1.21	.99	4.69
MgO	6.57	6.52	6.24	6.19	6.72	6.44
CaO	tr	tr	.14	tr	.23	.33
Na ₂ O	.25	.20	.27	.40	3.00	.26
K ₂ O	6.18	2.53	.47	4.45	2.71	.31
Total	90.32	89.28	89.37	90.19	93.24	89.18
FeO/MgO	3.84	3.81	4.10	3.74	3.54	3.84

Number of ions on basis of 8 Si						
Si	8.00	8.00	8.00	8.00	8.00	8.00
Al	1.39	1.28	1.35	1.33	1.47	1.22
Ti	—	—	—	—	—	—
Fe	3.57	3.51	3.82	3.74	3.30	3.21
Mn	.19	.19	.20	.18	.14	.69
Mg	1.79	1.64	1.65	1.78	1.66	1.65
Ca	—	—	.03	—	.04	.06
Na	.09	.07	.09	.14	.97	.09
K	1.43	.55	.11	1.00	.57	.07
O	24.72	23.63	25.73	24.26	24.11	25.11

Table 8.5-1.a. Representative analyses of stilpnomelane.

HM45a, YH70b in meta basalt from Lillefjell area.

HM7 in stilpnomelane + chlorite after original biotite meta basalt from the Gjersvik area.

101 in exhalite from Skorovass area.

a total iron as FeO

b total iron as Fe₂O₃

tr trace

	HM61 Biotite	HM113 Biotite	HM7 Chlorite	Number of ions on the basis of 24(O,OH,F)			
SiO ₂	35.55	36.52	25.28				
TiO ₂	2.13	1.45	tr				
Al ₂ O ₃	15.68	14.45	18.50				
FeO ^a	26.33	21.25	28.53				
MnO	.26	.31	.45				
MgO	7.17	10.15	14.03				
CaO	tr	0.00	tr				
Na ₂ O	tr	.14	.31				
K ₂ O	8.83	9.76	0.00				
Total	94.95	94.02	87.10				
FeO/MgO	3.67	2.09	2.03				
				Si 6.24	6.25		
				Al 1.76	1.75	8.0	8.0
				Al 1.48	1.16		
				Ti .28	.18		
				Fe 3.86	3.04	7.53	7.01
				Mn .04	.04		
				Mg 1.87	2.59		
				Ca —	—		
				Na —	.04	1.98	2.17
				K 1.98	2.13		
				O 24.00	24.00		

Table 8.5-1.b). Representative analyses of biotite and chlorite after biotite.

HM61 Biotite in mineralised meta rhyo dacite Lillefjell area.

HM113 Biotite in meta basalt east of main fracture Gjersvik area

HM7 Chlorite pseudomorphing biotite in stilpnomelane meta basalt Gjersvik area.

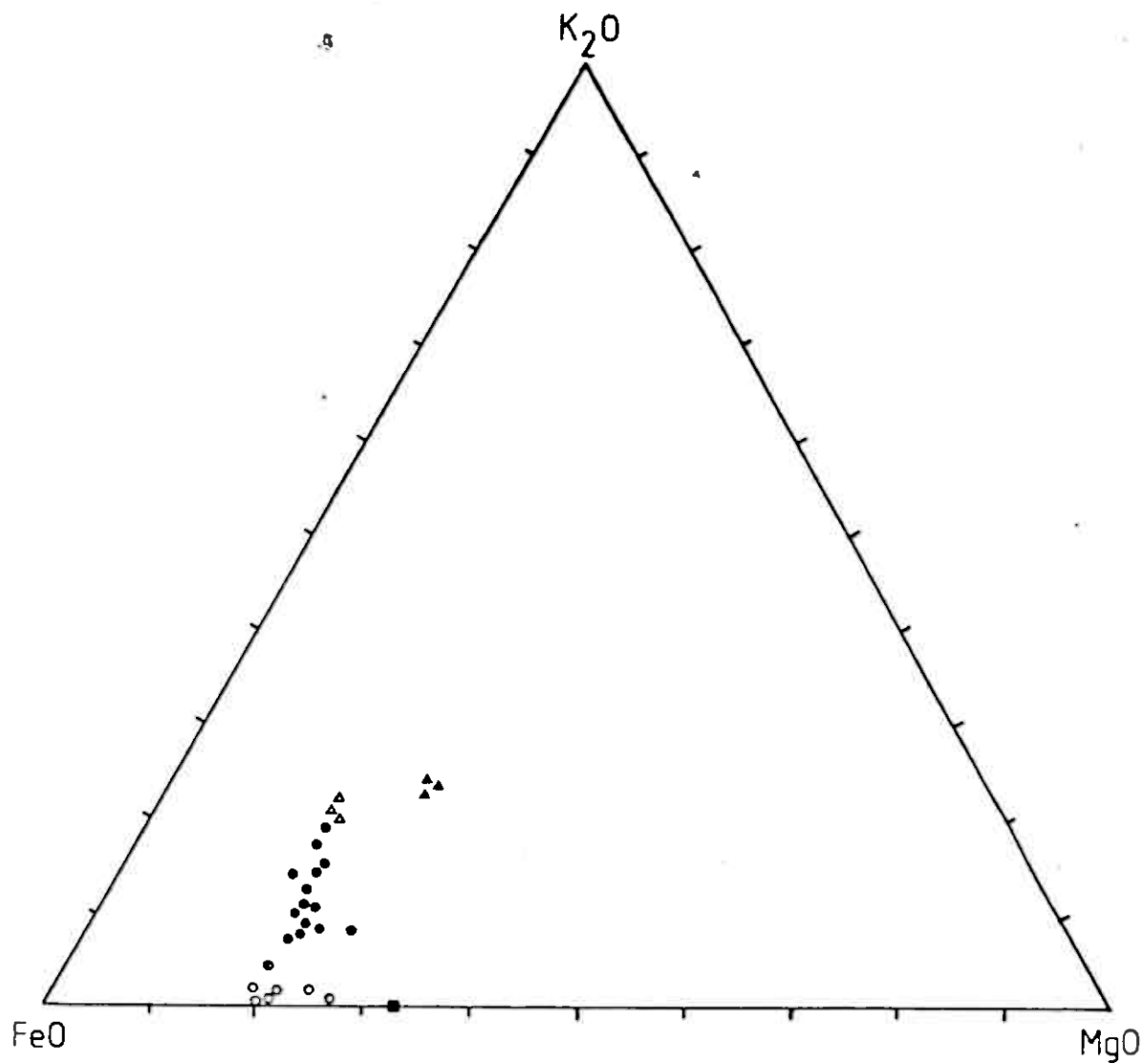
a- total iron as FeO

tr-trace

Both ferro and ferri-stilpnomelane show fairly constant compositions with slight variations in major elements probably reflecting varying chemical conditions in the environment of crystallisation. Potassium is somewhat variable in ferro-stilpnomelane and this is probably partly due to partial oxidation to ferristilpnomelane in some samples. The FeO:MgO ratios show quite a wide variation and this is presumably due to coupled substitution of Fe^{2+} , Fe^{3+} , Mg^{2+} , Al^{4+} (+Mn) in octahedral sites. The ferristilpnomelane in specimen 101 contains up to 5.10% MnO, predominantly substituting for iron in the octahedral sites. This specimen is taken from an exhalite horizon in the Skorovass area which also contains nearly pure spessartine garnet. The MnO content of the ferristilpnomelanes in specimen 101 is substantially greater than any published analyses encountered by the author.

The range of major element compositions can be seen in the KFM diagram, Fig.8.5-1 and the AFM diagram, Fig.8.5-2. From the KFM diagram it can be seen that the stilpnomelane analyses show relatively constant FeO:MgO ratios but vary considerably in their K_2O content. As suggested above this variation in K_2O content of ferrostilpnomelanes may be partially primary, but probably also reflects partial oxidation to ferristilpnomelane. The presence of biotite from the Lillefjell area plotting at the high K_2O end of this trend in stilpnomelane compositions, suggests that the biotite has formed under the same chemical conditions as the stilpnomelane. The biotites analysed from the Gjersvik area (HM113) show a significant variation in composition, Table 8.5-1 b. They contain significantly less iron and more magnesium, thus giving much lower FeO:MgO ratios, and are slightly richer in K_2O . Chlorite after biotite in HM7 plots very close to specimen HM113 in the AFM diagram. This suggests that the composition of the original biotite in HM7 was similar to that of the biotite further to the north in the Gjersvik area.

The textural evidence presented in Chapter 8.3 shows no significant variation between the two areas. However there



- - Ferrostilpnomelane(16 analyses)
- - Recognisable transitional ferro to ferri-stilpnomelane(2 analyses)
- - Ferristilpnomelane(12 analyses)
- ▲ - Biotite - Gjernsvik area(9 analyses)
- - Chlorite after biotite - Gjernsvik area(2 analyses)
- △ - Biotite - Lillefjell area

Fig 8.5-1. KFM diagram showing individual analyses of stilpnomelane biotite and chlorite from Gjernsvik, Lillefjell and Skorovass areas

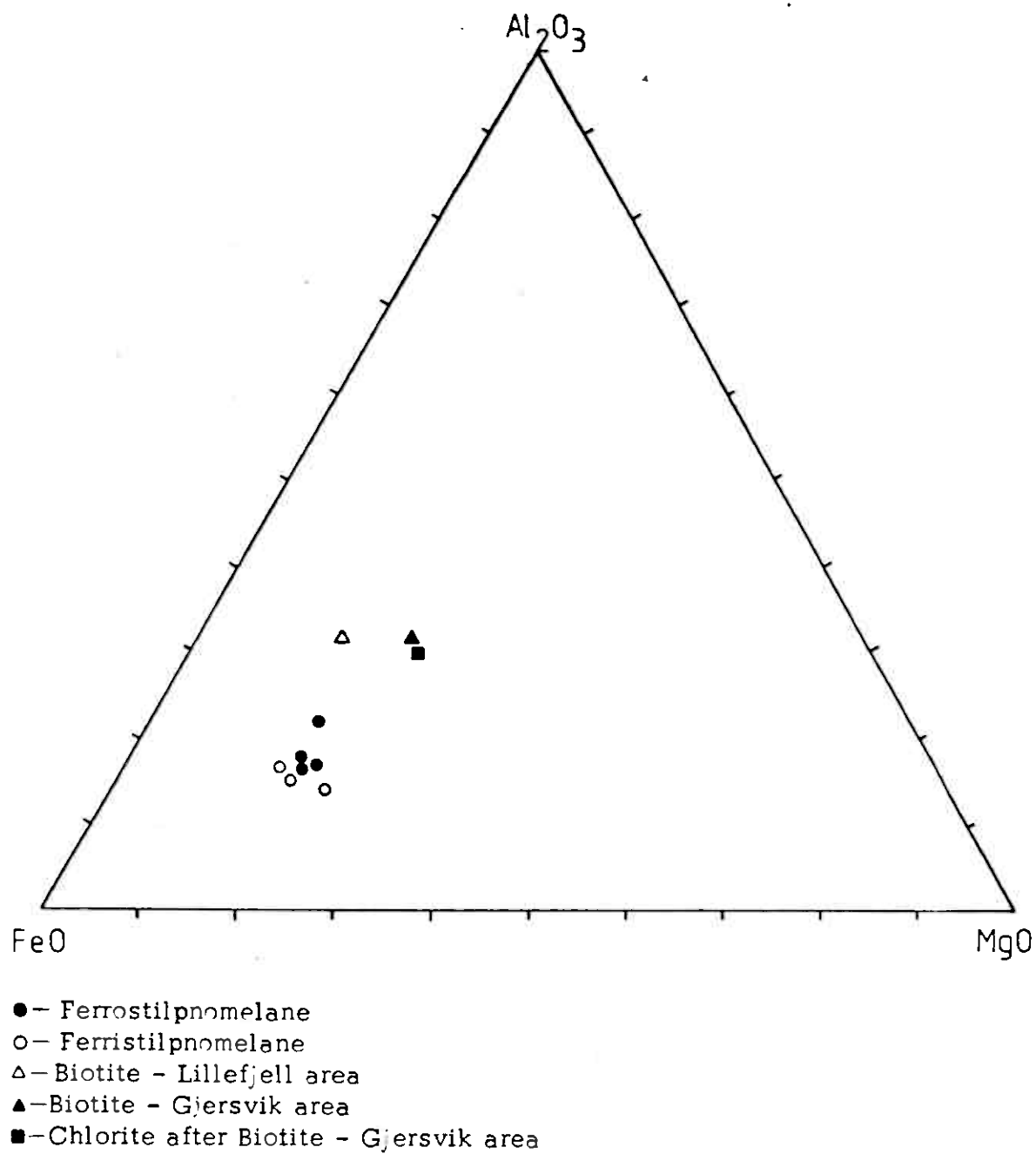


Fig 8.5-2. AFM diagram showing mean compositions of stilpnomelane, biotite and chlorite of individual specimens.

is an obvious chemical variation between the analysed biotites in the two areas, though the explanation for this is not clear. The formation of biotite in the Lillefjell area appears to be linked to the secondary processes giving rise to the formation of stilpnomelane (see Ch. 8.3). The textural evidence would seem to suggest that biotite in the Gjersvik area formed in the same manner as that in the Lillefjell area. This would suggest that the chemical variation is due to differing chemical conditions in the Gjersvik area during this secondary alteration. Alternatively the biotite in the Gjersvik area is of a different generation to that in the Lillefjell area (probably primary) which has undergone recrystallisation during secondary alteration to produce the consistent textural features observed.

8.6 GENESIS OF STILPNOMELANE AND BIOTITE

The strong correlation with acidic dykes, the iron enrichment shown by stilpnomelane bearing lithologies and the patchy development of stilpnomelane within these rocks suggests that stilpnomelane has formed in response to a secondary process in some way related to the intrusion of acidic dykes and is not due to a primary chemical enrichment. The above observations would seem to suggest introduction of iron, with probably other elements by solutions moving out from the acidic dykes and pervasively altering the 'wall rocks'. Two sources of such solutions may be envisaged:

1. Late stage hydrous differentiates released from the inferred main magma chamber at depth, passing up along the lines of the acidic dykes as hydrothermal solutions which then pervade the wall rocks at the higher structural level
2. Iron rich hydrothermal metasomatic solutions which are induced to circulate within the volcanic pile by the heat released by the cooling acidic intrusives, pervasively altering the rocks through which they pass at the higher structural level.

It has been suggested ¹⁴ that stilpnomelane crystallises under low hydrostatic pressures. This supports the interpretation of formation from pervading solutions but gives no indication as to whether they are magmatic hydrothermal or metasomatic hydrothermal in origin. The fact that the solutions are dominantly iron rich with minor silica and the generally low energy pervasive action of the hydrothermal solutions, suggest that they are hot circulating, metal enriched, sea water and this interpretation is made here. If one accepts a hydrothermal metasomatic origin for both the stilpnomelane (and biotite in the Lillefjell area) and the sulphide mineralisation of the Gjersvik and Lillefjell areas (Ch. 5.4) it would seem likely that the two processes are related. It seems likely that pyrite and stilpnomelane would form under the same physico - chemical conditions and that crystallisation of the two phases was not concurrent. This leads the author to suppose that pyrite and stilpnomelane formed from different generations of hydrothermal metasomatic solutions. The most likely explanation being that stilpnomelane (and biotite in the Lillefjell area) formed from late stage, cooler and less iron (and generally base metal) enriched solutions. It is difficult to find textural evidence to support this hypothesis as it is unlikely that the stilpnomelane would cut pyrite and it seems likely that the stilpnomelane has recrystallised during later deformation (see below).

Textural evidence (Ch. 8.3) suggests that both stilpnomelane and biotite crystallised after the last phase of texturally reconstructive tectonic deformation. In the light of it's interpreted hydrothermal metasomatic origin this could mean one of two things:

1. The original metasomatic chemical enrichment caused an unknown mineral phase to crystallise, which during the last phase of regional metamorphism underwent mineralogical change or metamorphic reaction with other mineral phases to produce stilpnomelane and/or biotite.
2. Stilpnomelane recrystallised during the last phase of deformation with the textures produced mimetic after the

original random orientation of stilpnomelane formed during metasomatism.

Brown¹ noted the mimetic recrystallisation of stilpnomelane in rocks from Western Otago, New Zealand. This together with the evidence presented above suggests that mimetic recrystallisation of stilpnomelane and biotite is the most likely explanation for the textures observed and is the interpretation favoured here. Stilpnomelane and biotite pseudomorphs of original phases was never observed, though this is thought to reflect total recrystallisation of these phases. The cause of of the chemical variation of the biotites in the Gjersvik area and it's influence on the interpretation of genesis remains unresolved due to a lack of convincing evidence to support either of the two interpretations proposed in Chapter 8.5.

The chemistry and petrography of the eruptive rocks in the Gjersvik region shows them to be of basaltic, basaltic andesite and dacitic or rhyo dacitic composition. It has been shown that these rocks most likely developed in an island arc environment of probably tholeiitic affinity. The rocks have undergone considerable secondary chemical involving introduction of base metals, particularly iron, during metasomatism by hydrothermal solutions. Also loss of calcium and potassium, with introduction of sodium during ocean floor metamorphism, producing rocks of spilitic affinity.

Stilpnomelane appears to have formed during late stage iron metasomatism and then recrystallised during the late stages of regional metamorphism as mimetic crystals showing no correlation with tectonic fabrics. Biotite in the Lillefjell area appears to have formed from the same hydrothermal metasomatic solutions as the stilpnomelane, though it is not known whether it originally crystallised as biotite, or as stilpnomelane which subsequently altered to biotite during prograde regional metamorphism. The origin of biotite in the Gjersvik area is not clear and further work is required to resolve the question of genesis.

Many of the interpretations made here are somewhat tentative and further data from other areas is required to substantiate and further refine them. Total mineralogical reconstitution during metamorphism limits the interpretations which can be made on the basis of petrographic study. Further chemical study, in particular of incompatible elements, would allow a greater understanding of the magmatic affinity and deformational history of these rocks.

ACKNOWLEDGEMENTS

The author wishes to thank Grong Gruber A/S, particularly Ing. A. Haugen, for their help and support, both material and financial for the duration of the field work. Also Dr. Chris Halls for help and encouragement during both field and laboratory work and for a critical reading of the manuscript and Mr. I. Ferriday for helpful discussion and use of specimens for analytical work.

I would also like to thank members of the academic and technical staff of Imperial College; in particular Mr. P Suddaby and Mr. N. Wilkinson for help with microprobe analyses, Dr. M. Thompson and Dr. S. Wood for help with chemical analyses and Mr. B. Foster, Miss Liz. Morris and Mr. A. Hill for help with obtaining thin and polished sections. I am also indebted to Miss S. Puddephatt for her help and support in the preparation of this manuscript.

REFERENCES

1. Brown E.H.(1971); Phase relations of biotite and stilpnomelane in the greenschist facies.
Contr. Mineral. and Petrol., 31, 275-299.
2. Cann J.R.(1969); Spilites from the Carlsberg Ridge, Indian Ocean.
J. Petrol., 10, part 1, 1-19.
3. Carmichael I.S.E., Turner F.J., and Verhoogen J.(1974); Igneous Petrology.
Mcgraw-Hill; New York. 739p.
4. Deer W.A., Howie R.A., Zussman J.(1962); Rock forming minerals, Volume 3 (Sheet silicates).
Longman.
5. ————, ————, ———— (1966); An introduction to the rock - forming minerals.
Longman.
6. Eggleton R.A.(1972); Stilpnomelane as a guide to oxidation state.
Int. cong. proc. geol. int., 24, p191.
7. ———— (1972 b); The crystal structure of stilpnomelane. Part II. The full cell.
Mineral. Mag., 38, 693-711.
8. Halls c., Reinsbakken A., Ferriday I., Haugen A., Rankin A.(1977); Geological setting of the Skorovass orebody within the allochthonous metavolcanic stratigraphy of the Gjersvik Nappe, central Norway. In Volcanic processes in ore genesis.
London: Inst. Min. Metall. and Geol. Soc., 128-151.
9. Hashimoto M.(1969); A note on stilpnomelane mineralogy.
Contr. Mineral. and Petrol., 23, 86-87.
10. Hughes C. J.(1972); Spilites, keratophyres and the igneous spectrum.
Geol. Mag., 109(6), 513-527.
11. Hutton C.O.(1938); The stilpnomelane group of minerals.
Mineral. Mag., 25, 172-206.
12. ———— (1956); Further data on the stilpnomelane group of minerals.
Am. Mineralogist, 41, 608-615.

13. Lutro O. (1979); The geology of the Gjersvik area, Nord Trondelag, central Norway.
In the press. May 1979.
14. Matthews D.W. and Scoon J.H. (1963); Notes on a new occurrence of stilpnomelane from North Wales.
Min. Mag., 33, p1032.
15. Melson W.G., Van Handel T.H. (1966); Metamorphism in the Mid - Atlantic Ridge, 22°N Latitude.
Mar. Geol., 4, 165-186.
16. Myashiro A., Shido F., Ewing M. (1971); Metamorphism in the Mid - Atlantic Ridge near 24° and 30°N.
17. ——— (1973); Metamorphism and metamorphic belts.
Allen & Unwin; London. 492p.
18. ——— (1974); Volcanic rock series in island arcs and active continental margins.
Am. J. Sci., 274, 321-355.
19. Robinson P. (1969); Weathering of ferrostilpnomelane to ferristilpnomelane in the Otago schist, East Otago, New Zealand.
Geol. Soc. Amer. Abstr. part 7, (Ann. Meet), 288-289.
20. Smith R.E. (1968); Redistribution of major elements in the alteration of some basic lavas during burial metamorphism.
Jour. Petrol., 9, part 2, 191-219.
21. Streckeisen A. (1968); Stilpnomelan im Kristallin der Ostkarpathen.
Sonderdruck aus, Schweiz. Min. Petr. Mitt., 48, Heft 3.
22. Vallance T.G. (1974); Spilitic degradation of a tholeiitic basalt.
Journ. Petrol., 15, part 1, 79-96.
23. Zen E-an. (1960); Metamorphism of Lower Paleozoic rocks in the vicinity of the Taconic Range in West-Central Vermont.
Am. Mineralogist, 45, 129-175.

APPENDIX

APPENDIX 1: Whole rock analyses

APPENDIX 2: Electron microprobe analyses

APPENDIX 1

Meta basalt analyses - Gjersvik and Lillefjell areas

	SiO ₂	TiO ₂	Al ₂ O ₃	FeO	MnO	MgO	CaO	Na ₂ O	K ₂ O	Total
HM7	50.7	.91	11.72	12.22	.19	4.11	4.99	4.89	.14	89.86
HM26	49.8	.98	12.16	14.58	.26	4.39	2.74	2.49	.13	87.52
HM28	46.5	1.03	14.31	11.99	.22	6.23	2.90	3.86	.32	87.37
HM33	82.0	.14	5.40	10.03	.07	3.20	.10	.01	.14	101.09
HM34	46.2	.99	13.81	20.80	.20	5.94	.11	.03	.59	88.68
HM69	52.4	1.23	11.95	11.14	.18	3.18	4.92	2.49	.03	87.53
HM79	55.1	.89	12.07	13.74	.22	4.83	1.03	2.35	.15	90.37
HM91	58.3	.54	11.41	13.02	.21	3.79	.54	1.61	.83	90.24
HM92	62.2	.96	11.06	8.44	.14	2.53	2.67	4.60	.11	92.71
HM92	67.3	1.03	12.21	8.92	.15	2.74	2.13	5.32	.16	99.95
HM98	58.1	.89	12.28	8.89	.22	4.00	3.61	4.07	.11	92.27
HM98	----	.83	11.34	8.21	.20	3.71	3.04	4.02	.16	89.60
HM157	82.5	.34	7.65	6.88	.16	1.95	.36	2.67	.14	102.66
HM159	49.8	.80	12.61	9.24	.29	3.71	8.36	2.03	.01	86.85
HM27	48.7	1.00	11.70	12.29	.24	4.68	4.87	4.22	.01	87.71
MH2	48.8	1.36	12.64	13.11	.35	3.73	6.02	1.96	.37	88.34
MH4	48.9	1.88	11.47	13.26	.38	4.12	5.17	2.52	.41	88.11
MH6	56.9	1.07	13.13	12.39	.37	3.52	5.14	3.26	.52	96.29
MH7	60.1	.82	12.07	10.38	.31	4.06	4.42	2.78	.01	94.97
MH7	----	.83	12.50	10.29	.31	4.15	4.38	2.93	.05	95.54
HM48	53.2	.49	12.52	10.25	.26	3.60	5.30	3.42	.03	89.06
HM51	57.1	.88	13.00	11.14	.30	3.94	4.70	1.65	.10	92.81
HM51	----	.91	12.98	11.09	.18	3.90	5.81	3.15	.22	95.35
MH9	49.4	.91	14.35	11.13	.31	4.24	7.00	3.07	.01	90.43
MH11	58.1	.86	12.05	12.21	.27	3.74	4.61	1.68	.28	93.80
HM52	54.7	.88	12.33	12.60	.32	4.08	4.74	1.91	.33	91.87
MH13	50.21	.92	12.05	10.58	.18	3.68	5.77	3.01	.15	86.54

Appendix 1 - Meta basalt analyses cont.

	SiO ₂	TiO ₂	Al ₂ O ₃	FeO	MnO	MgO	CaO	Na ₂ O	K ₂ O	Total
HM56	50.9	.83	11.63	10.58	.17	3.57	5.52	2.74	.19	86.14
MH14	54.1	.92	12.08	14.81	.19	3.66	2.23	2.81	.10	90.90
MH15	48.1	.49	12.36	12.66	.30	5.99	5.81	2.66	.01	88.37
HM60	54.3	.32	11.21	11.05	.30	4.94	9.65	1.89	.01	93.68
MH16	76.7	.85	10.74	11.37	.20	2.98	2.57	2.51	.08	108.98
MH17	53.7	.88	12.16	10.56	.20	4.46	4.02	3.26	.04	89.29
HM42	57.7	.97	13.15	11.15	.19	4.00	4.41	3.34	.10	95.02
MH20	53.7	.90	12.28	13.30	.18	3.94	1.83	3.00	.11	89.24

Specimen MH2 onwards - Lillefjell area

Meta dacite and rhyo dacite analyses - Gjersvik
and Lillefjell areas

HM9	84.2	.29	8.71	4.04	.06	.80	1.70	4.87	.98	105.65
HM9	----	.28	9.01	3.81	.06	.78	1.57	4.89	.87	105.47
HM18	82.5	.20	7.44	3.86	.06	1.29	.50	4.68	1.17	101.71
HM24	80.2	.29	9.31	5.07	.03	.79	1.13	5.72	.13	102.67
HM68	82.9	.20	8.33	3.29	.11	.96	.70	5.14	.42	102.05
HM75	81.9	.29	10.70	5.29	.18	.90	.76	4.97	.73	105.73
HM75	----	.25	9.12	4.41	.15	.78	.59	4.56	.61	102.47
HM80	65.4	.67	10.84	9.37	.13	2.90	2.35	3.10	.11	94.87
HM83	66.7	.39	10.19	7.28	.11	1.21	1.11	4.28	.15	91.42
HM94	85.7	.27	8.63	3.34	.02	.38	.31	5.72	.03	104.40
HM102	81.9	.07	9.22	4.69	.04	.85	.50	4.09	.54	101.91
HM104	79.9	.05	10.47	4.51	.15	2.36	.12	3.72	.56	101.83
HM105	72.7	.41	8.89	5.91	.14	2.09	.38	4.18	.36	95.15
HM108	78.4	.21	11.93	3.78	.05	.71	.12	4.92	1.69	101.80
HM110	74.6	.25	9.93	3.93	.04	.80	.21	4.40	2.35	96.50
HM134	84.9	.27	10.10	4.17	.02	.33	1.23	5.90	.08	107.09

Appendix 1 - Meta dacite and rhyo dacite analyses cont.

	SiO ₂	TiO ₂	Al ₂ O ₃	FeO	MnO	MgO	CaO	Na ₂ O	K ₂ O	Total
HM134	84.9	.25	8.84	3.72	.01	.30	1.06	5.54	.07	104.79
HM150	85.7	.24	9.68	3.92	.05	.62	1.23	4.97	.08	106.50
HM151	85.3	.23	11.34 ₅	4.51	.08	1.08	1.10	4.49	1.84	109.96
HM158	94.5?	.21	8.91	2.56	.01	.36	.39	5.86	.10	112.91
MH1	88.5	.28	8.30	5.22	.06	.38	.43	5.27	.05	108.59
MH3	84.2	.29	7.86	3.51	.10	.48	1.90	5.26	.26	103.96
MH5	77.6	.25	10.10	4.51	.10	.60	2.11	5.30	.26	100.83
HM46	80.4	.21	9.96	3.89	.10	.58	1.43	5.22	.30	102.18
MH8	85.7	.27	8.87	5.09	.05	.35	.51	6.36	.14	107.34
HM50	84.0	.23	9.08	3.75	.05	.36	.44	5.69	.14	103.74
MH10	82.5	.30	7.43	4.81	.05	.46	.73	5.20	.04	101.53
MH10	79.9	.29	11.03	4.99	.05	.51	.86	5.36	.10	103.10
HM53	87.4	.26	9.71	4.27	.05	.49	.59	5.47	.04	107.29
MH12	81.4	.32	7.65	4.60	.07	.70	1.03	4.77	.07	100.61
HM54	82.5	.25	10.14	4.90	.07	.75	.91	4.50	.03	104.05
MH18	87.4	.24	8.13	3.71	.07	.50	1.26	5.16	.10	106.56
MH19	80.8	.28	7.79	3.54	.02	.41	.48	5.37	.17	98.87
HM61	75.9	.33	9.39	5.56	.05	.87	.80	4.83	.29	98.01
MH21	73.3	.55	9.49	6.41	.08	1.70	1.13	5.22	.04	97.91

Specimen MH1 onwards - Lillefjell area

(Specimens HM80, HM83 are possibly silicified basalts)

APPENDIX 2

Electron microprobe analyses of stilpnomelanes (St), Biotites (Bi), and Chlorites (Cl)

	HM7-St			HM149-St				HM45A-St						
	Ferro	Ferro	Ferro	Ferro	Ferro	Ferro	Ferro	Ferro	Ferro	Ferro	Ferro	Ferro	Ferro	Ferro
SiO ₂	49.82	46.75	52.01	46.07	48.48	44.89	45.83	44.44	45.26	45.68	47.02	44.84	45.65	44.94
TiO ₂	.10	.04	.11	.14	.15	.13	.29	.03	.11	.10	.09	.05	.04	.00
Al ₂ O ₃	8.49	6.54	9.60	6.53	6.40	7.10	6.37	6.80	6.19	6.64	6.47	6.27	6.31	6.43
FeO ^a	21.56	25.99	20.24	24.35	23.24	24.06	24.28	26.12	25.15	24.78	26.39	24.99	25.04	24.84
MnO	.92	1.05	.85	1.67	1.63	1.39	1.59	1.41	1.05	1.16	1.28	1.24	1.12	1.14
MgO	6.10	7.33	5.70	7.62	7.32	8.14	7.59	6.85	7.13	6.37	6.97	6.42	7.02	6.45
CaO	.26	.19	.19	.49	.30	.21	.47	.04	.11	.07	.10	.10	.20	.15
Na ₂ O	3.00	.73	3.09	.83	.37	.53	.55	.55	.33	.77	.17	.31	.26	.47
K ₂ O	2.30	3.11	2.24	2.69	2.68	2.40	2.90	3.58	5.65	4.73	2.44	6.43	3.87	2.22
Total	92.56	91.73	94.04	90.44	90.64	88.91	89.95	89.82	91.04	90.34	91.06	90.79	89.51	86.68

a - Total iron as FeO

Appendix 2 - Microprobe analyses cont.

	101-St					YH18B-St(veinlets)					YH70B-St				
	Ferri	Ferri	Ferri	Ferri	Ferri	Ferri	Ferri	Ferri	Ferri	Ferro	Ferro	Ferro	Ferri	Ferri	Ferri
SiO ₂	48.53	45.80	45.68	45.60	48.03	46.34	46.78	46.73	47.10	45.16	42.49	44.92	44.43	45.01	45.43
TiO ₂	.08	.13	.19	.00	.00	.00	.00	.08	.04	.05	.04	.05	.09	.00	.07
Al ₂ O ₃	5.87	6.14	6.03	6.00	5.55	5.45	5.75	5.43	5.89	6.52	6.63	6.35	6.40	6.50	6.44
FeO ^a										26.15	24.68	24.80			
Fe ₂ O ₃ ^b	26.62	26.15	23.16	23.01	27.01	27.05	28.15	26.26	28.15				28.80	28.66	27.99
MnO	3.92	4.78	4.94	5.10	.65	.70	.80	.96	.96	1.32	1.29	1.20	1.33	1.37	1.35
MgO	6.59	6.49	6.38	6.31	8.92	7.87	8.18	8.55	8.34	6.24	6.74	6.72	6.07	6.25	6.41
CaO	.24	.38	.42	.28	.93	.14	.10	.93	.07	.08	.11	.08	.15	.14	.12
Na ₂ O	.30	.15	.34	.24	.15	.21	.24	.43	.07	.26	.13	.36	.28	.26	.26
K ₂ O	.39	.28	.39	.17	.23	.46	.69	.38	.30	5.30	7.91	5.34	.57	.52	.32
Total	88.87	87.56	87.57	86.74	88.79	85.53	87.91	87.13	88.11	91.07	90.01	89.81	85.21	85.85	85.62

a-Total iron as FeO

b-Total iron as Fe₂O₃

Appendix 2 - Microprobe analyses cont.

	YH7OB-St		HM7-C1		HM61-B1		HM113-B1								
	Trans.	Trans.													
SiO ₂	49.67	45.01	25.15	25.41	34.68	34.78	34.19	36.06	36.60	36.02	36.57	36.52	36.74	36.35	36.69
TiO ₂	.09	.04	.06	.12	2.12	2.08	2.19	1.56	1.27	1.37	1.42	1.42	1.49	1.31	1.41
Al ₂ O ₃	6.37	6.48	18.73	18.28	15.95	15.34	15.76	14.15	14.91	14.10	14.35	14.43	14.35	14.45	14.60
FeO ^a	24.76	24.93	28.83	28.23	26.72	25.79	26.48	21.35	20.66	21.26	21.34	21.01	20.83	21.32	21.64
MnO	1.35	1.31	.46	.43	.21	.30	.28	.30	.26	.29	.30	.30	.35	.33	.32
MgO	6.15	6.89	13.83	14.22	7.34	7.08	7.09	10.15	10.03	10.21	9.93	10.14	10.09	10.01	10.29
CaO	.04	.05	.05	.02	.13	.08	.02	.00	.00	.09	.00	.00	.00	.00	.02
Na ₂ O	.23	.16	.37	.25	.28	.00	.10	.23	.07	.15	.01	.04	.09	.21	.23
K ₂ O	1.22	3.84	.00	.00	8.59	9.12	8.78	9.72	9.79	9.56	9.89	9.70	9.63	9.88	9.94
Total	89.90	88.68	87.50	86.96	96.01	94.61	94.93	93.93	93.96	93.58	94.34	93.86	94.34	93.95	95.22

a - Total iron as FeO